Performance evaluation of cascaded latent heat storage systems for domestic medium temperature applications

Chidiebere Samson Ekwomadu

orcid.org/0000-0001-7057-2256

Dissertation accepted in fulfilment of the requirements for the degree Master of Science in Physics at the

North West University

Supervisor: Prof. A. Mawire

Co-Supervisor: Dr. A.B. Shobo

Graduation ceremony: October 2020

Student number: 31493173

Table of Contents

Table of Contents i

Declaration iv

Dedication v

Acknowledgements vi

List of Figures vii

List of Tables xi

List of acronyms xii

List of symbols xiii

List of publications xiv

Abstract xv

1 INTRODUCTION 1

1.1 Background of the study 1

1.1.1 Thermal Energy Storage 3

1.2 Problem statement 10

1.3 Aim and objectives 11

1.4 Outline of the dissertation 11

1.5 Summary of the chapter 12

1.6 References 12

2 LITERATURE REVIEW 17

2.1 Latent heat storage system using PCMs 17

2.1.1 Low temperature latent heat storage (LHS) applications 18

2.1.2 Medium temperature latent heat storage (LHS) applications 23

2.1.3 High temperature latent heat storage (LHS) applications 25

2.2 Packed bed latent heat thermal energy storage (LHTES) systems 26
2.2.1 Low temperature packed bed LHTES systems 27
2.2.2 Medium temperature packed bed LHTES systems 29
2.2.3 High temperature packed bed LHTES systems 31
2.3 Cascaded latent heat thermal energy storage (CLHTES) system 32
2.4 Summary of the chapter 35
2.5 References 36
3. EXPERIMENTAL METHOD AND ANALYSES 46
3.1 Experimental setup and method 46
3.1.1 Encapsulation of PCM spherical capsules and thermophysical properties 50
3.1.2 Single PCM packed bed latent heat storage system 53
3.1.3 Cascaded latent heat storage system 1 54
3.1.4 Cascaded latent heat storage system 2 55
3.2 Experimental thermal analysis 57
3.3 Experimental uncertainty 59
3.4 Summary of the chapter 59
3.5 References 60
4 RESULTS AND DISCUSSION 62
4.1 Charging results 62
4.1.1 Effect of the flow rate 62
4.1.2 Effect of the temperature 74
4.2 Discharging results 83
4.2.1 Effect of flow rate 83
4.2.2 Effect of temperature 93
4.3 Energy and exergy storage efficiencies 100
4.3.1 The effect of flow rate on energy and exergy efficiencies 100

4.3.2 The effect of temperature on energy and exergy efficiencies 104
4.4 Summary of the chapter 107
4.5 References 107
5. CONCLUSIONS AND RECOMMENDATIONS FOR FUTURE WORK 109
5.1 Conclusions 109
5.2 Recommendations for possible future work 111

Declaration

I, Chidiebere Samson Ekwomadu, declare that this dissertation titled “Performance evaluation of cascaded latent heat storage systems for domestic medium temperature applications", and the work presented in it are my own. I confirm that:

- This work was carried out wholly while I was a candidate for the Master of Science degree in Physics ~~a~~t North-West University.
- I have clearly stated that no part of this dissertation has been previously submitted for a degree or any other qualification at this University or any other institution.
- I have given sources of quotations from the work of others in this dissertation.
- I have acknowledged all the main sources used in this dissertation.
- I have made clear any contributions from any other person apart from myself in this work.

Signed: _____

Date: _____

Dedication

"I dedicate this dissertation to every member of the Ekwomadu family for their combined effort towards my academic career. I will always be grateful for the financial and spiritual support, encouragement and love you gave me during my academic journey."

Acknowledgements

- Firstly, I would like to show gratitude to the Almighty God for his mercy and grace during my academic journey.
- I am grateful to my supervisors; Prof. Ashmore Mawire and Dr. B.A Shobo for their fruitful discussions related to my research work and choosing to believe in me as I pursued my degree. Their professional guidance during this research is greatly appreciated.
- I would like to offer my deepest gratitude to Dr Theodora Ekwomadu and her family for their financial support and care throughout my MSc programme.
- I also acknowledge the Deeper-Life campus fellowship and the Watchman Catholic Charismatic Renewal Movement (Mafikeng Parish) for their spiritual guidance in some challenging days.
- I would like to appreciate Dr Dzivhuluwani Ndiitwani and Prof. Amare Abebe for their support as Departmental heads during my academic programme.
- I also acknowledge the support of my friends and colleagues who made pursuing my degree worthwhile.
- I also greatly appreciate the support from the Physics Department.

List of Figures

Figure 1.1: A chart showing the power consumption by different sectors in Bangladesh [1]. 1

Figure 1.2: A map obtained from NREL data showing the average daily direct normal irradiation (DNI) for South Africa annually [10].....2

Figure 1.3: Behaviour of LHTES and SHTES systems during storing and releasing energy with respect to temperature [16]. 5

Figure 1.4: Some sensible heat materials; (a) pebbles, (b) sand and (c) water [25-26]. 8

Figure 1.5: A combined sensible and latent heat thermal energy storage consisting of a small layer of PCM on the top of a packed bed of pebbles [32]. 9

Figure 1.6: Schematic diagram of the adsorption and desorption processes [38]. 10

Figure 2.1: Plane and finned shell and tube configurations investigated in [39]. 20

Figure 2.2: A solar cooker integrated with a TES system for off-sunshine cooking [19]. 21

Figure 2.3: A schematic view of a packed bed LHTES unit [51]. 27

Figure 2.4: A schematic view of a cascaded LHTES unit [69]. 33

Figure 3.1: Schematic diagram of the experimental setup [5]. 47

Figure 3.2: Photograph of the experimental setup [4]. 49

Figure 3.3: (a) Aluminium PCM capsule with a screw cap, (b) aluminium PCM capsule with a thermocouple screw cap [5]. 51

Figure 3.4: Photographs showing (a) adipic acid, (b)erythritol and (c) eutectic solder used as PCMs in the spherical aluminium capsules [6]. 52

Figure 3.5: The schematic diagram of storage system (a) which was the single PCM TES system. It shows forty PCM capsules in the storage tank with four capsules having thermocouples (red).....54

Figure 3.6: The schematic diagram of storage system (b) which was a 2-PCM cascaded TES system. It shows twenty eutectic solder PCM capsules at the top and twenty erythritol PCM

capsules at the bottom of the storage tank with four capsules having thermocouples (red and green). 55

Figure 3.7: The schematic diagram of storage system (c) which was a 2- PCM cascaded TES system. It shows twenty eutectic solder PCM capsules at the top and twenty adipic acid PCM capsules at the bottom of the storage tank with four capsules having thermocouples (red and blue). 56

Figure 3.8: The schematic diagram of storage system (d) which was a 3-PCM cascaded TES system. It shows fourteen eutectic solder PCM capsules at the top, fourteen adipic acid PCM capsules at the middle and fourteen erythritol PCM capsules at the bottom of the storage tank with six capsules having thermocouples (red, blue and green). 57

Figure 4.1: Average charging temperature profiles at a heater set temperature of 280 ^{o}C using a low flow rate of 4 ml/s for (a) the single PCM system, (b) cascaded system 1, (c) cascaded system 2 and (d) cascaded system 3. 63

Figure 4.2: Average charging temperature profiles at a heater set temperature of 280 ^{o}C using a medium flow rate of 6 ml/s for (a) the single PCM system, (b) cascaded system 1, (c) cascaded system 2 and (d) cascaded system 3. 67

Figure 4.3: Average charging temperature profiles at a heater set temperature of 280 ^{o}C using a high flow rate of 8 ml/s for (a) the single PCM system, (b) cascaded system 1, (c) cascaded system 2 and (d) cascaded system 3. 68

Figure 4.4: Charging energy rate profiles at (a) low, (b) medium and (c) high flow rates for the four storage systems. 69

Figure 4.5: Charging exergy rate profiles at (a) low, (b) medium and (c) high flow rates for the four storage systems. 72

Figure 4.6: Average charging temperature profiles at a low set heater temperature of 260 ^{o}C with a flow rate of 6 ml/s for (a) the single PCM system, (b) cascaded system 1, (c) a cascaded system 2 and (d) cascaded system 3. 75

Figure 4.7: Average charging temperature profiles at a medium set heater temperature of 280 ^{o}C with a flow rate of 6 ml/s for (a) the single PCM system, (b) cascaded system 1, (c) cascaded system 2 and (d) cascaded system 3. 76

Figure 4.8: Average charging temperature profiles at a high set heater temperature of 300 ^{o}C with a flow rate of 6 ml/s for (a) the single PCM system, (b) cascaded system 1, (c) a cascaded system 2 and (d) cascaded system 3. 78

Figure 4.9: Charging energy rate profiles at (a) low, (b) medium and (c) high set heater temperatures for the four storage systems. 79

Figure 4.10: Charging exergy rate profiles at (a) low, (b) medium and (c) high set heater temperatures for the four storage systems. 82

Figure 4.11: Average discharging temperature profiles at a low flow rate of 4 ml/s for (a) the single PCM system, (b) cascaded system 1, (c) cascaded system 2 and, (d) cascaded system 3. 84

Figure 4.12: Average discharging temperature profiles at a medium flow rate of 6 ml/s for (a) the single PCM system, (b) cascaded system 1, (c) cascaded system 2 and (d) cascaded system 3. 87

Figure 4.13: Average discharging temperature profiles at a high flow rate of 8 ml/s for (a) the single PCM system, (b) cascaded system 1, (c) cascaded system 2 and (d) cascaded system 3. 88

Figure 4.14: Discharging energy rate profiles at (a) low, (b) medium and (c) high flow rates for the four storage systems. 90

Figure 4.15: Discharging exergy rate profiles at (a) low, (b) medium and (c) high flow rates for the four storage systems. 92

Figure 4.16: Average discharging temperature profiles after charging with at a low set temperature for (a) the single PCM system, (b) cascaded system 1 (c), cascaded system 2 and (d) cascaded system 3. 94

Figure 4.17: Average discharging temperature profiles after charging with at a medium set temperature for (a) the single PCM system, (b) cascaded system 1, (c) cascaded system 2 and (d) cascaded system 3. 95

Figure 4.18: Average discharging temperature profiles after charging with at a high set temperature for (a) the single PCM system, (b) cascaded system 1, (c) cascaded system 2 (d) and cascaded system 3 97

Figure 4.19: Discharging energy rate profiles after charging with (a) low, (b) medium and (c) high set temperatures for the four storage systems. 98

Figure 4.20: Discharging exergy rate profiles after charging with (a) low, (b) medium and (c) high set temperatures for the four storage systems. 100

Figure 4.21: The effect of the flow rate on the energy storage efficiencies for the four storage systems. 101

Figure 4.22: The effect of the flow rate on the exergy storage efficiencies for the four storage systems. 103

Figure 4.23: The effect of the temperature on the energy storage efficiencies for the four storage systems. 104

Figure 4.24: The effect of the temperature on the exergy storage efficiencies for the four storage systems. 106

List of Tables

Table 1.1: Comparison of properties of PCM families for TES system [17]. 6

Table 1.2: Thermal properties of some solid sensible heat storage materials [27]. 8

Table 3.1: The thermophysical properties of the three PCMs. 53

List of acronyms

CLHTES	Cascaded Latent Heat Thermal Energy Storage
CTES	Combined Thermal Energy Storage
DC	Direct Current
D-C	Disperation-Concentric
HTF	Heat Transfer Fluid
LHTES	Latent Heat Thermal Energy Storage
NEPCM	Nano- Enhanced Phase Change Material
NTU	Number of heat Transfer Unit
MF-CTES	Metal Foam enhanced Cascaded Thermal Energy Storage
MNHH	Magnesium Nitrate HexaHydrate
PCM	Phase Change Material
PVC	Photovoltaic Cell
SHTES	Sensible Heat Thermal Energy Storage
SSPCM	Solid-Solid Phase Change Material
TTES	Thermochemical Thermal Energy Storage
TES	Thermal Energy Storage

List of symbols

C_{av}	Average specific heat capacity of liquid	$JKg^{-1}K^{-1}$
$\dot{E}_{CH}$	Charging energy rate	W
E_{DIST}	Total energy discharged	J
E_{ST}	Total energy stored	J
$\dot{E}_{Xch}$	Charging exergy rate	W
$\dot{E}_{xdis}$	Discharging exergy rate	W
$\dot{E}_{dis}$	Discharging energy rate	W
E_{XDIST}	Total exergy discharged	J
E_{XCHT}	Total exergy charged	J
T_{disout}	Discharging outlet temperature	^oC
T_{disin}	Discharging inlet temperature	^oC
T_{chin}	Charging inlet temperature	^oC
T_{out}	Charging outlet temperature	^oC
T_{amb}	Ambient temperature	^oC
T_{disin}	Discharging inlet temperature	^oC
t_f	Final charging time	mins
t_{ini}	Initial charging time	mins
$\dot{Vch}$	Volumetric charging flow rate	mls^{-1}
$\dot{V_{dis}}$	Volumetric discharging flow rate	mls^{-1}
η_{ex}	Exergy efficiency	(-)
η_e	Energy efficiency	(-)
ρ_{av}	Temperature dependent density of the HTF	(Kgm^{-3})

List of publications

- 2020, Mawire A, Lefenya TM, **Ekwomadu CS**, Shobo AB. Performance of a medium temperature eutectic solder packed bed latent heat storage system for domestic applications. *Journal of Energy Storage* 28, 101294.
- 2020, Mawire A, Lefenya TM, **Ekwomadu CS**, Lentswe KA, Shobo AB. Performance comparison of medium temperature domestic packed bed latent heat storage systems. *Renewable Energy* 146, 1897-1906.
- 2020, Mawire, A, **Ekwomadu, CS,** Lefenya, TM, and Shobo, A. Performance comparison of two metallic eutectic solder based medium-temperature domestic thermal energy storage systems. *Energy* 194, 116828.
- 2019**, Ekwomadu CS**, Mawire A, Lefenya TM, Shobo AB. Comparison of the thermal behaviour of two eutectic solder cascaded latent heat thermal energy storage systems during charging. Presented at the Southern African Solar Energy Conference, 2019, SASEC 2019, East London, South Africa, November 25-27, 2019.
- 2019, Lefenya TM, Mawire A, **Ekwomadu CS,** Shobo AB. Charging characteristics of packed bed latent heat storage systems for medium temperature solar applications. Presented at Southern African Solar Energy Conference, 2019, SASEC 2019, East London, South Africa, November 25-27, 2019.
- 2019, Mawire A, **Ekwomadu C,** Lefenya TM, Shobo AB. Performance comparison of two medium temperature packed bed latent heat storage systems during charging. Presented at the Solar World Congress 2019, SWC 2019, Santiago, Chile, November 04-07, 2019.
- 2019, Mawire A, **Ekwomadu CS**, Lefenya T, Shobo AB. Performance of a small domestic eutectic solar medium temperature latent heat storage system during charging. Presented at the 18th International Conference on Sustainable Energy Technologies, SET 2019, Kuala Lumpur, Malaysia, August 20-22, 2019.
- 2019, Mawire A, **Ekwomadu CS**, Lefenya TM, Shobo AB. Performance comparison of two eutectic solder based latent heat storage systems during discharging. Presented at the International Conference on Sustainable Energy and Green Technology 2019 SEGT 2019, Bangkok, Thailand, December 11-14, 2019.

Abstract

The charging and discharging thermal performances of three packed bed cascaded latent heat thermal energy storage (LHTES) systems for medium temperature applications are experimentally evaluated and compared to a single PCM packed bed LHTES of eutectic solder capsules. Cascaded system 1 comprises of eutectic solder PCM capsules at the top, and erythritol PCM capsules at the bottom in equal storage volumes. Cascaded system 2 consists of eutectic solder PCM capsules at the top and adipic acid PCM capsules at the bottom in equal storage volumes. Cascaded system 3 consists of three PCM capsule layers of eutectic solder at the top, adipic acid in the middle, and erythritol at the bottom in equal storage volumes. The charging thermal performance characteristics of the four systems are evaluated in terms of the charging temperature profiles, charging energy rates and charging exergy rates. The effects of the flow rate and the heater set charging temperature are investigated in the experiments. Three different charging flow rates (4 ml/s, 6 ml/s, 8 ml/s), and three different heater set temperatures (260 ^{o}C, 280 ^{o}C and 300 ^{o}C) are used in the experimental tests. The effect of flow rate on the charging performance is more pronounced than the effect of the heater set charging temperature. Cascaded system 3, with 3 PCMs shows the best overall thermal performance as it possesses higher energy and exergy rates for most of the experimental conditions due to the 3 phase change transitions. The single PCM system shows the worst thermal performance, but its performance becomes better with an increase in the charging flow rate. The discharging thermal performance characteristics are also presented in terms of discharging temperature profiles, discharging energy and exergy rates. The effect of flow rate and the influence of the charging heater set temperatures is also investigated. To investigate the effect of the flow rate, three different flow rates (4 ml/s, 6 ml/s and 8 ml/s) are used during the discharging cycles. To investigate the effect of the final charging temperature on the discharging characteristics, discharging is carried out with a flow rate of 6 ml/s after charging with set temperatures of 260 ^{o}C, 280 ^{o}C and 300 ^{o}C. The final charging temperature shows an insignificant influence on the discharging performance. The increase in flow rate increases the rate of heat transfer which causes the energy rate, exergy rate and discharging inlet temperature peak values to occur earlier with increasing peak values. The single PCM system shows the best discharging characteristics with the least widening of the

thermal gradient as compared to other systems. This is an evidence of good heat transfer in the single PCM system. Cascaded system 2 and cascaded system 3 show comparable thermal performances during discharging, while cascaded system 1 shows a slightly worse thermal performance with greater temperature reversals in the storage tank. The overall storage performance is evaluated in terms of the energy and exergy storage efficiencies. Cascaded system 2 shows the highest energy and exergy storage efficiencies, which seem to increase with an increase in flow rate. However, the energy and exergy storage efficiencies of cascaded system 3 and cascaded system 2 are comparable. The energy and exergy efficiency of the single PCM is the worst, possibly due to the longer charging time. The higher energy and exergy efficiencies of cascaded system 2 in almost all the experiments when compared to cascaded system 3 is due to a greater volume of adipic acid in cascaded system 2. Adipic acid has a slightly higher thermal conductivity and a higher melting temperature as compared to erythritol at the bottom of cascaded system 2. The results also suggest that the performance of a cascaded system may depend on the PCM properties irrespective of the number of stages since a two PCM system with a higher bottom melting temperature shows better overall performance than the three PCM system. Cascaded system 1 shows lower energy and exergy storage efficiencies as compared to the other two cascaded systems.

Keywords; Phase change materials, Energy and exergy rate, Cascaded system, Latent heat thermal energy storage

1 INTRODUCTION

1.1 Background of the study

Energy is an essential need for the survival of humans since it is needed for daily activities such as washing, lighting and cooking. The rapid increase in the demand for energy is a result of an increase in economic development, population and civilization. The major energy consumption sectors in developed or developing countries are industrial and domestic sectors [1]. For instance, Bangladesh is one of the fastest developing countries in the world [2], and its energy analysis is illustrated in Figure 1.1. The rate of energy demand or energy consumption in a country determines the development rate of that country, and countries with high energy demand rates tend to develop at much faster rates as compared to those with a low demand for energy [3-4]. The rate of energy demand can never be satisfied with one energy source such that different sources are needed to meet the energy demand for a country whether developing or developed [5-6].

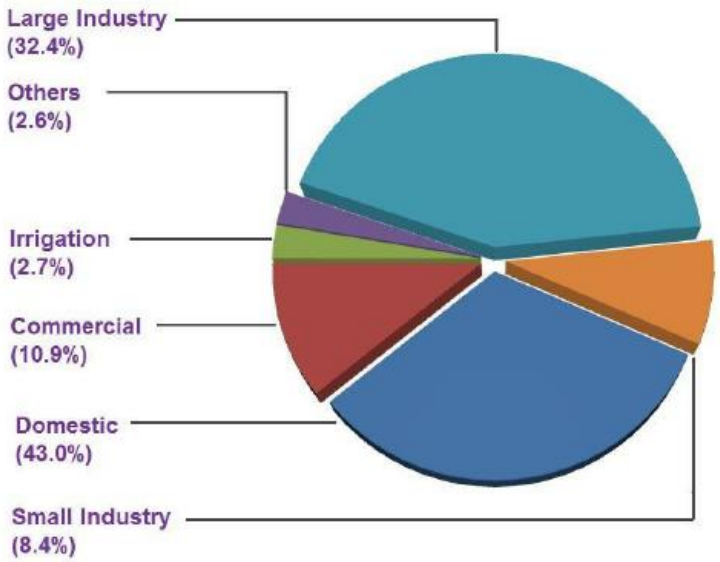

Figure 1.1: *A chart showing the power consumption by different sectors in Bangladesh [1].*

Energy sources are categorized into renewable and non-renewable sources. Renewable energy sources are sometimes referred to as sustainable energy sources, and these sources replenish naturally within a short time. The sources include; solar energy, wind energy, tidal energy, and geothermal energy. Non-renewable energy sources collectively known as fossil

fuels are combustible carbon-based sources for example; coal, crude oil, natural gas or heavy oil that were formed in the earth's crust over hundreds of millions of years ago. Although fossil fuels are the cheapest and most readily available energy sources, they are considered unsustainable since they get depleted and have harmful environmental effects.

Renewable energy has an important role to play in meeting up with the present and future energy demand in both rural and urban areas to minimize the dependency on carbon-based energy sources. This helps to eliminate the environmental effects and health issues associated with carbon-based fossil fuels [7-8]. Solar energy is one of the renewable energy resources that is clean and environmentally friendly. It has been reported that solar energy provides 120000 TW of energy to the earth annually [9]. The average sunshine duration in most provinces of South Africa is more than 2500 hours annually. This makes the daily average solar-radiation of South Africa to be within the range of 4.5 to 6.5 kWh/m^2 [10]. Figure 1.2 is a map obtained from the National Renewable Energy Laboratory (NREL), which shows the average daily direct normal irradiation (DNI) of South Africa. The South African average 24-hour global solar radiation is about 220 W/m^2, while in parts of USA and Europe it is 150 W/m^2 and 100 W/m^2, respectively. This makes South Africa one of the regions with the highest level of solar radiation in the world [11]. Despite the abundance of solar energy resources in South Africa, it is underutilized for domestic purposes due to the cost of installation equipment, insufficiency of the skilled workers and lack of sufficient promotion of its use [12].

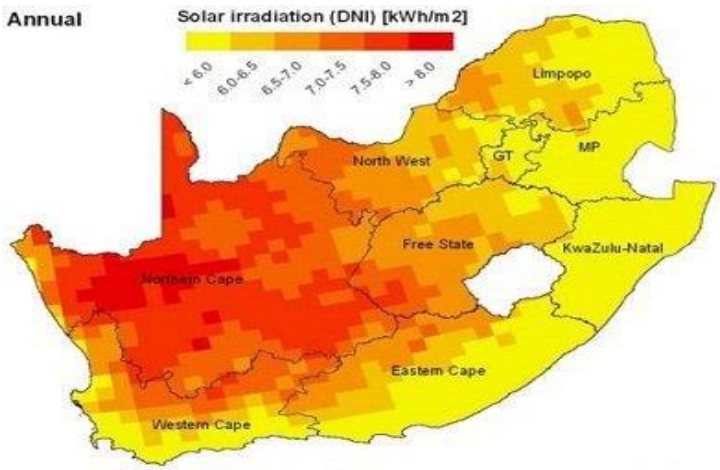

Figure 1.2: *A map obtained from NREL data showing the average daily direct normal irradiation (DNI) for South Africa annually [10].*

The major problem with the use of the solar energy resource is its intermittent nature, which can be partially solved with the use of a thermal energy storage (TES) system. In a TES system,

thermal energy can be stored during non-peak demand periods or hours when it is available. The stored energy can be used when the solar energy resource is not available (e.g., at night or during cloudy periods). Domestically, solar energy can be used for solar cooking, solar water heating, and space heating applications. Solar energy technology applications are categorized into three temperature ranges which are; low temperature (less than 100 ^{o}C), medium temperature (greater than 100 ^{o}C and less than 400 ^{o}C) and high temperature (greater than 400 ^{O}C) applications.

1.1.1 Thermal Energy Storage

Thermal energy storage (TES) is a technology of storing thermal energy by cooling and heating of a storage medium or by using thermochemical reactions for later usage. The energy stored in the TES system can be used later for either heating or cooling applications and power generation. Some of the benefits associated with the use of thermal energy storage include; improvement of the cost effectiveness, energy efficiency improvement and catering for intermittent energy resources such as solar energy. The three major classifications of thermal energy storage systems are; latent heat thermal energy storage (LHTES), sensible heat thermal energy storage (SHTES) and thermochemical thermal energy storage (TTES) system.

1.1.1.1 Latent Heat Thermal Energy Storage (LHTES) system

Latent heat thermal energy storage (LHTES) is based on the absorption or release of heat when the storage materials undergo a change in phase during heating or cooling. This system is made up of materials that can change phase when raised to a particular temperature. These storage materials are called phase change materials (PCMs). The phase change processes can be from the solid to the liquid phase, liquid to the gas phase, solid to the solid phase or from the solid to the gas phase or vice versa. However, the only two applicable phase change processes in a LHTES system are solid to liquid and solid to solid phase change transitions because the rise in volume is within a controllable range (<10%) as compared to solid to gas and liquid to gas transitions [13-14]. The PCMs that undergo solid to liquid phase change transitions are considered to be more economically viable for the LHTES system due to their higher latent heat released as compared to solid to solid transitions [15].

LHTES is more efficient in the storage of thermal energy as compared to SHTES due to its high-energy storage density and nearly isothermal behaviour during storing and releasing energy. A solid to liquid phase change LHTES system stores energy when charged up to the phase change temperature (melting temperature), and it releases the heat while cooling during discharging as the PCM solidifies. The equation for the heat stored during charging is given by;

$$Q = \int_{T_i}^{T_m} mC_l \, dT + fm\Delta h_f + \int_{T_m}^{T_f} mC_s \, dT \quad (1.1)$$

, where Q is the quantity of heat storage, C_l and C_s are specific heat capacities of liquid and the solid phases of the PCM used, Δh_f is the latent heat of fusion,T_m is the melting temperature, T_i initial temperature of the storage system and T_f is the final temperature.

The disadvantages of a LHTES system include; large volumetric changes during phase change, high cost of the PCMs, low thermal conductivity of the PCMs, supercooling of most of the PCMs and phase segregation of the PCMs after several cycles.

1.1.1.2 Phase Change materials

Phase change materials are materials used in LHTES systems due to their ability to change from one phase to another when a specific amount of heat is applied or removed. These materials are used for high density TES. During TES with PCMs, the PCMs will initially behave as sensible heat storage materials until the melting temperatures are reached as illustrated in Figure 1.3. The melting (endothermic) process requires heat from a source for bond breaking making the PCM temperature to be almost constant until the phase change transition process is completed releasing large amounts of energy. The heat absorbed or released during the period of phase change is called latent heat.

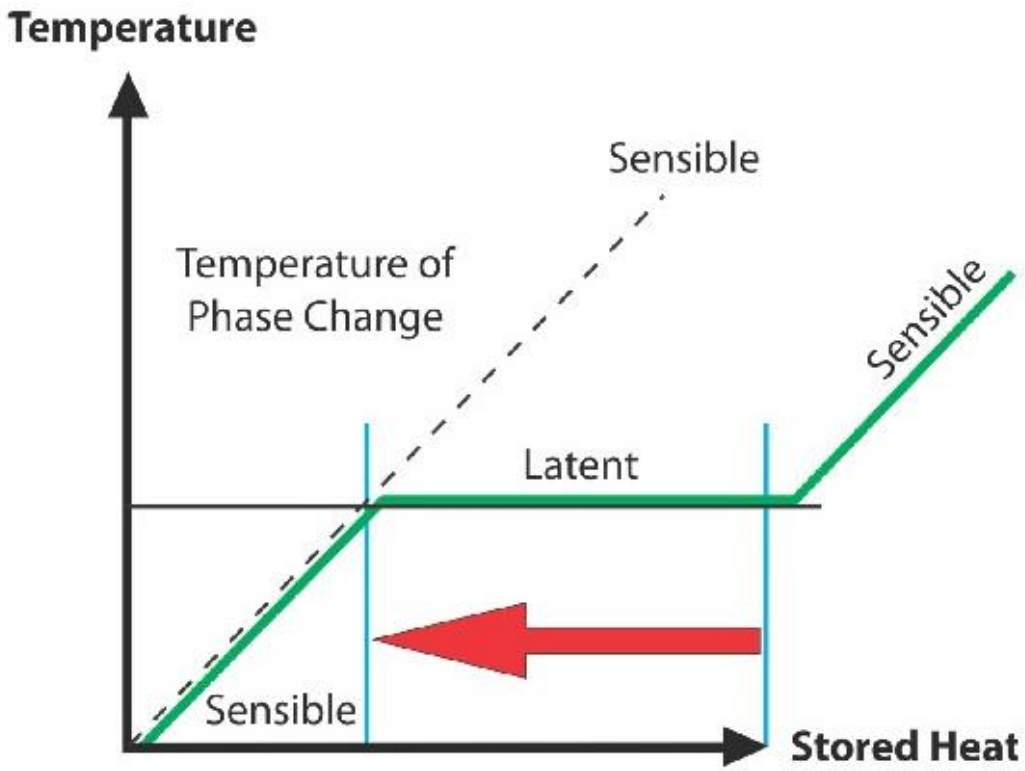

Figure 1.3: *Behaviour of LHTES and SHTES systems during storing and releasing energy with respect to temperature [16].*

The melting temperature is the basic criterion for categorizing a PCM for a particular application for energy storage. PCMs are classified as organic, inorganic and eutectic PCMs as shown in Table 1.1. The advantages and disadvantages of different types of PCMs are also shown in Table 1.1. The desirable properties of an ideal PCM for LHTES include:

- Chemical stability;
- High thermal conductivity of both solid and liquid phases;
- Non-corrosiveness to either the encapsulation material or the storage tank;
- High nucleation rate to avoid supercoiling;
- High specific heat;
- A small rise in volume during phase change;
- Availability at low cost;
- Melting temperature within the desired operating temperature range;
- High latent heat of fusion per unit volume;
- No degradation after several cycles;
- Ability to return to the initial state after a freezing/melting cycle;

Table 1.1: *Comparison of properties of PCM families for TES system [17].*

Types of PCM	Advantages	Disadvantages
Organic	• Available in a large temperature range; • Chemically inert; • Do not undergo phase segregation; • Thermally stable for repeated freeze/melt cycles; • Low vapor pressure in the melt form; • Relatively small melting heat; • Non-corrosive, or mildly corrosive (fatty acids); • Compatible with construction materials; • Small volume changes during phase transitions; • Little or no supercooling effect during freezing; • Innocuous (usually non-toxic and non-irritant; non-paraffin type may have various levels of toxicity); • Stable below 500 ^{o}C (non-paraffin type shows instability at high temperatures; • Recyclable.	• Low thermal conductivity (around 0.2 W/mK); • Moderately flammable; • Non-compatible with plastic containers.
Inorganic	• High volumetric storage heat; • High melting heat; • High thermal conductivity (0.5 W/m K); • Cheap and readily available; • Nonflammable; • Compatible with plastic containers; • Sharp phase change; • Low environmental impact; • Potentially recyclable.	• Supercooling during freezing; • Phase segregation during transitions; • Corrosive to metals; • Irritant; • High vapor pressure (inducing water loss and progressive changes in thermal behavior during thermal cycles); • Low durability (possible long term degradation when exposed to environmental agents); • Moderate chemical stability; • High volume change.
Eutectic	• Sharp melting temperature; • High volumetric thermal storage capability (slightly lower than organic PCMs).	• Limited data available on their thermophysical properties.

1.1.1.3 Packed bed (single PCM) LHTES system

The single PCM packed bed LHTES system is one of the most common configurations of LHTES. This system is made up of encapsulated PCM capsules of the same material. The capsules are usually cylindrical or spherical, although other shapes are also possible. In a packed bed

configuration, the PCM capsules will have direct contact with the heat transfer fluid (HTF) unlike in the tube and shell and other configurations where heat transfer is usually through the pipe wall. The common problem of this configuration is the long charging and discharging times while other drawbacks such as low thermal conductivity, low energy storage density, and low heat capacity are a direct result of the PCM properties. The problem of the long charging time can be alleviated with the use of a cascaded configuration [18], while other enhancement techniques such as the addition of fins and the addition of nucleating agents can help to increase the heat transfer rate [19-21].

1.1.1.4 Cascaded latent heat thermal energy storage (CLHTES) system

This is an advanced technique of an LHTES system for performance enhancement purposes. CLHTES is a configuration of multiple latent heat storage materials (PCMs) in a storage system arranged in a cascade depending on their melting temperatures. CLHTES can be in different configurations such as the shell and tube, planar slabs and cylindrical or spherical capsules in a packed bed configuration. The employment of a multiple PCM system can assist in reducing long charging and discharging durations associated with single PCM systems [18, 22-23]. The selection of a suitable PCM for a CLHTES is an important factor that can reduce the efficiency of the system if proper care is not taken.

1.1.1.5 Sensible heat thermal energy storage (SHTES) system

This system stores thermal energy by raising the temperature of the storage medium without a change in the phase. A SHTES system uses sensible heat materials (usually liquids or solids) that are heated up to store energy when their temperature is raised as a result of their specific heat capacities. Examples of SHTES materials are clay, bricks, sandstone, wood, concrete, glass and water. Figure 1.4 rock pebbles, sand, and water which are examples of SHTES materials. The selection of a sensible heat storage material for the SHTES system is governed by the thermal properties of the material and also depends on the application. Table 1.2 also shows the thermal properties of some solid sensible heat storage materials. The amount of heat energy stored is dependent on the specific heat of the medium, the temperature change, and the amount of storage material [24]. The quantity of energy stored by a SHTES material is given as;

$$Q_s = \int_{T_i}^{T_f} m\, C_p dT \qquad (1.2)$$

, where Q_s is the quantity of energy stored, m is the mass of the heat storage medium, C_p is the specific heat capacity, and the dT is change in temperature.

(a) (b) (c)

Figure 1.4: *Some sensible heat materials; (a) pebbles, (b) sand and (c) water [25-26].*

A SHTES system is mostly used due to its cheapness, availability and chemical stability. The limitations of this system are its low energy density and large space requirements.

Table 1.2: *Thermal properties of some solid sensible heat storage materials [27].*

Storage Materials	Working Temperature (°C)	Density (kg/m^3)	Thermal Conductivity (W/(m·K))	Specific Heat (kJ/(kg·°C))
Sand-rock minerals	200–300	1700	1.0	1.30
Reinforced concrete	200–400	2200	1.5	0.85
Cast iron	200–400	7200	37.0	0.56
NaCl	200–500	2160	7.0	0.85
Cast steel	200–700	7800	40.0	0.60
Silica fire bricks	200–700	1820	1.5	1.00
Magnesia fire bricks	200–1200	3000	5.0	1.15

1.1.1.6 Combined thermal energy storage (CTES) system

A combined thermal energy storage (CTES) system is a combination of sensible and latent heat storage materials in a single storage system. This combination technique does not only help in reducing the issue of the large volume requirements of SHTES, but it also reduces the cost associated with LHTES. CTES thus compensates for the drawbacks of the individual

systems. However, one of the major benefits of this combination technique is that it helps to establish temperature stability at the outlet especially when PCM is added at the top of the storage tank [28-31], as illustrated in Figure 1.5.

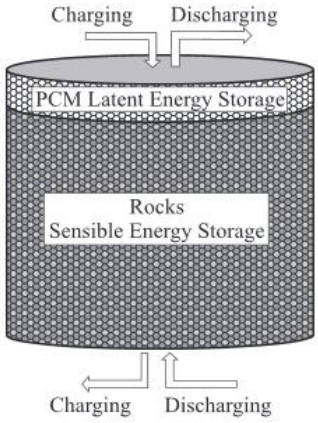

Figure 1.5: *A combined sensible and latent heat thermal energy storage consisting of a small layer of PCM on the top of a packed bed of pebbles [32].*

1.1.1.7 Thermochemical thermal energy storage (TTES) system

TTES is the process of storing energy using reversible thermochemical reactions. Thermochemical energy generation depends on adsorption and desorption processes. During the adsorption process, gas (adsorbate) binds to the liquid (adsorbent) to form a product at the same time liberating energy. The energy released is recovered during the desorption process. The illustration of this process is presented in Figure 1.6. Thermochemical energy is obtained through a reversible chemical reaction, and energy recovery is during the reverse cycle. This type of energy storage sometimes requires a catalyst for heat liberation and reaction control. Although TTES systems generally have a high energy density, different chemical reactions have different energy densities. This storage system has a high enthalpy of reaction compared to SHTES and LHTES due to its greater energy storage density [33]. Another advantage of this system is that thermal insulation is not required. Factors that affect the behaviour of the adsorbent bed and the ideal adsorbent characteristics have been reported in [34-37].

The disadvantages of a TTES system are the high cost of the installation or storage materials and the technical complexity in its operation.

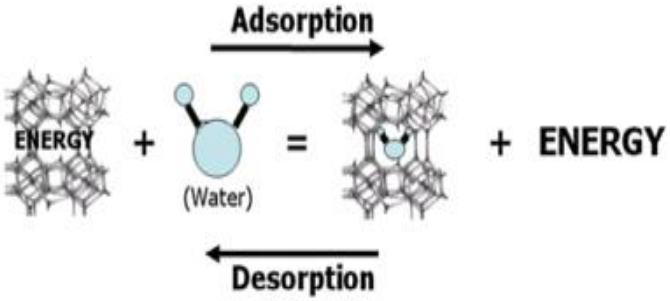

Figure 1.6: *Schematic diagram of the adsorption and desorption processes [38].*

1.2 Problem statement

Solar energy is one of the renewable energy resource that is clean and environmentally friendly. Solar energy is plentiful in South Africa, however, it is underutilized for domestic purposes due to its cost of installation and lack of sufficient promotion of its use. Solar energy is an intermittent resource that is not always available. To cater for this intermittency, a thermal energy storage (TES) system can be utilized. Solar energy can be stored during non-peak demand periods using a TES system. TES can be used during periods when the solar energy resource is not available, for example at night and during cloudy periods.

SHTES system is the most commonly used TES system due to its low cost of installation, availability of the storage materials and its simplicity of operation. Although LHTES system is relatively costly, its energy storage density is higher resulting in more compact storage. The major drawback of a SHTES system is its low energy storage density as compared to a LHTES system. Most work has focused on LHTES using single PCMs in a storage. Recent work has shown that cascaded latent heat storage systems are more thermodynamically efficient when compared to a single PCM system [19, 23- 24]. There have been limited experimental studies on CLTES for medium temperature applications like cooking of food using liquid heat transfer fluids [22-23, 39-43]. Sunflower oil has been studied recently [44-48] as a suitable SHTES medium and heat transfer fluid (HTF) for medium temperature domestic applications. However, there has been no application using sunflower oil as a heat transfer oil in a CLHTES system. The use of sunflower oil is justified since it is cheap, readily available, non-toxic and has properties comparable to other commercially available heat transfer oils.

Energy and exergy analyses will be used to evaluate the LHTES systems. Energy analysis is based on the first law of thermodynamics, and it evaluates the quantity of energy stored. To evaluate the quality of TES, exergy analysis based on the second law of thermodynamics accounts for irreversible changes such as heat losses in the storage of thermal energy, and it gives a more realistic picture of the stored heat with reference to the ambient surrounding conditions. Thermal energy storage losses will be accounted for in exergy analysis by subtracting the thermal losses from the energy analysis evaluations thus giving a more realistic picture of the available thermal energy for storage.

1.3 Aim and objectives

The aim of this research is to compare three different cascaded LHTES systems for use in domestic medium temperature applications using sunflower oil as the heat transfer fluid.

The specific objectives are to:

- Evaluate and compare the performance of 2-stage and 3-stage PCM cascaded TES systems using both energy and exergy analyses.
- Compare a single PCM system with the cascaded PCM systems using both energy and exergy analyses.
- Evaluate the performances of different PCMs combinations in the cascaded systems during charging and discharging processes.

1.4 Outline of the dissertation

This dissertation begins with Chapter 1, the introduction which contains the background of the study, the problem statement and the objectives of the study. Chapter 2 presents a comprehensive review of related literature on packed bed LHTES systems. Experimental methods and analyses are presented in Chapter 3. The results, and a critical discussion of these results are presented in Chapter 4. Chapter 5 presents conclusions drawn up from the research work and recommendations for future work.

1.5 Summary of the chapter

This chapter presented a background of the research highlighting that thermal energy storage is necessary for intermittent renewable energy resources such as solar energy. Three major types TES systems were discussed, namely; latent heat thermal energy storage (LHTES), sensible heat thermal energy storage (SHTES) and thermochemical thermal energy storage (TTES). Different types of configurations of the systems were also highlighted including their advantages and disadvantages.

The problem statement, the aim and the objectives of the study were also presented. Finally, the outline of the dissertation was also presented.

1.6 References

1. Shahid, S., 2012. Vulnerability of the power sector of Bangladesh to climate change and extreme weather events. *Regional Environmental Change 12*, 595-606.
2. World Bank report on economic growth and development, 2019.The Bangladesh Development Update. Available at https://www.thedailystar.net/world/news/ bangladesh-top-5-growing-economy-wb-1724815, accessed 4 April 2019
3. Kaygusuz, K., 2012. Energy for sustainable development: A case of developing countries. *Renewable and Sustainable Energy Reviews 16*, 1116-1126.
4. Mahadevan, R. and Asafu-Adjaye, J., 2007. Energy consumption, economic growth and prices: A reassessment using panel VECM for developed and developing countries. *Energy Policy 35*, 2481-2490.
5. Yergin, D., 2006. Ensuring energy security. *Foreign Affairs 85,* 69-82.
6. Omer, A.M., 2008. Energy, environment and sustainable development. *Renewable and Sustainable Energy Reviews 12*, 2265-2300.
7. Zhang, J., Mauzerall, D.L., Zhu, T., Liang, S., Ezzati, M. and Remais, J.V., 2010. Environmental health in China: progress towards clean air and safe water. *The Lance 375*, 1110-1119.
8. Wallack, J.S. and Ramanthan, V., 2009. The Other Climate Changers-Why Black Carbon and Ozone Also Matter. *Foreign Affairs 88*, 105-113.

9. Lewis, N.S. and Crabtree, G., 2005. Basic research needs for solar energy utilization: report of the basic energy sciences workshop on solar energy utilization April 18-21, 2005. *US Department of Energy, Office of Basic Energy Science* Washington, DC.
10. Fluri, T.P., 2009. The potential of concentrating solar power in South Africa. *Energy Policy 37*, 5075-5080.
11. Department of Energy: Report on the state of renewable and clean energy in South Africa 2015. Available at: http://www.energy.gov.za, accessed 22 July 2017.
12. De Jongh, D., Ghoorah, D. and Makina, A., 2014. South African renewable energy investment barriers: An investor perspective. *Journal of Energy in Southern Africa 25*, 15-27.
13. Pielichowska, K. and Pielichowski, K., 2014. Phase change materials for thermal energy storage. *Progress in Materials Science 65*, 67-123.
14. Cárdenas, B. and León, N., 2013. High temperature latent heat thermal energy storage: Phase change materials, design considerations and performance enhancement techniques. *Renewable and Sustainable Energy Reviews 27*, 724-737.
15. Sharma, A., Tyagi, V.V., Chen, C.R. and Buddhi, D., 2009. Review on thermal energy storage with phase change materials and applications. *Renewable and Sustainable Energy Reviews 13,* 318-345.
16. Isa, M.H.M., Zhao, X. and Yoshino, H., 2010. Preliminary study of passive cooling strategy using a combination of PCM and copper foam to increase thermal heat storage in building facade. *Sustainability 2*, 2365-2381.
17. Frigione, M., Lettieri, M. and Sarcinella, A., 2019. Phase Change Materials for Energy Efficiency in Buildings and Their Use in Mortars. *Materials 12*, 1260.
18. Watanabe, T., Kikuchi, H. and Kanzawa, A., 1993. Enhancement of charging and discharging rates in a latent heat storage system by use of PCM with different melting temperatures. *Heat Recovery Systems and CHP 13*, 57-66.
19. Sciacovelli, A., Gagliardi, F. and Verda, V., 2015. Maximization of performance of a PCM latent heat storage system with innovative fins. *Applied Energy 137*, 707-715.
20. Rathod, M.K. and Banerjee, J., 2015. Thermal performance enhancement of shell and tube Latent Heat Storage Unit using longitudinal fins. *Applied Thermal Engineering 75*, 1084-1092.

21. Xue, H.S., 2016. Experimental investigation of a domestic solar water heater with solar collector coupled phase-change energy storage. *Renewable Energy 86*, 257-261.
22. Wang, J., Ouyang, Y. and Chen, G., 2001. Experimental study on charging processes of a cylindrical heat storage capsule employing multiple-phase-change materials. *International Journal of Energy Research 25*, 439-447.
23. Xu, Y., He, Y.L., Li, Y.Q. and Song, H.J., 2016. Exergy analysis and optimization of charging–discharging processes of latent heat thermal energy storage system with three phase change materials. *Solar Energy 123*, 206-216.
24. Kumar, A. and Shukla, S.K., 2015. A review on thermal energy storage unit for solar thermal power plant application. *Energy Procedia 74*, 462-469.
25. Lugolole, R., Mawire, A., Okello, D., Lentswe, K.A., Nyeinga, K. and Shobo, A.B., 2019. Experimental analyses of sensible heat thermal energy storage systems during discharging. *Sustainable Energy Technologies and Assessments 35*, 117-130.
26. Diago, M., Iniesta, A.C., Soum-Glaude, A. and Calvet, N., 2018. Characterization of desert sand to be used as a high-temperature thermal energy storage medium in particle solar receiver technology. *Applied Energy 216*, 402-413.
27. Tian, Y. and Zhao, C.Y., 2013. A review of solar collectors and thermal energy storage in solar thermal applications. *Applied Energy 104*, 538-553.
28. Nallusamy, N., Sampath, S. and Velraj, R., 2007. Experimental investigation on a combined sensible and latent heat storage system integrated with constant/varying (solar) heat sources. *Renewable Energy 32*, 1206-1227.
29. Zanganeh, G., Khanna, R., Walser, C., Pedretti, A., Haselbacher, A. and Steinfeld, A., 2015. Experimental and numerical investigation of combined sensible–latent heat for thermal energy storage at 575 ^{o}C and above. *Solar Energy 114*, 77-90.
30. Geissbühler, L., Zavattoni, S., Barbato, M., Zanganeh, G., Haselbacher, A. and Steinfeld, A., 2015. Experimental and Numerical Investigation of Combined Sensible/Latent Thermal Energy Storage for High-Temperature Applications. *CHIMIA International Journal for Chemistry 69*, 799-803.
31. Zavattoni, S.A., Geissbühler, L., Barbato, M.C., Zanganeh, G., Haselbacher, A. and Steinfeld, A., 2017. High-temperature thermocline TES combining sensible and latent heat-CFD modeling and experimental validation. In *AIP Conference Proceedings.* Abu Dhabi, United Arab Emirates, 11–14 October, 2016.

32. Tiskatine, R., Oaddi, R., El Cadi, R.A., Bazgaou, A., Bouirden, L., Aharoune, A. and Ihlal, A., 2017. Suitability and characteristics of rocks for sensible heat storage in CSP plants. *Solar Energy Materials and Solar Cells 169*, 245-257.
33. Carrasco Portaspana, J., 2010. High temperature thermal energy storage systems based on latent and thermochemical heat storage. Master Thesis, Technischen Universität, Wien, Germerny.
34. Close, D.J. and Dunkle, R.V., 1977. Use of adsorbent beds for energy storage in drying of heating systems. *Solar Energy 19*, 233-238.
35. Kalaiselvam, S. and Parameshwaran, R., 2014. Thermal energy storage technologies for sustainability: systems design, assessment and applications. *Academic Press,* London UK.
36. Abedin, A. and Rosen, M., 2011. A critical review of thermochemical energy storage systems. *The Open Renewable Energy Journal 4,* 42-46
37. Gartler, G., Jähnig, D., Purkarthofer, G. and Wagner, W., 2004. Development of a high energy density sorption storage system. In Proceedings of the EuroSun Conference. Freiburg, Germany, 20-23 June, 2004.
38. Dicaire, D. and Tezel, F.H., 2013. Use of adsorbents for thermal energy storage of solar or excess heat: improvement of energy density. *International Journal of Energy Research 37*, 1059-1068.
39. Gong, Z.X. and Mujumdar, A.S., 1997. Thermodynamic optimization of the thermal process in energy storage using multiple phase change materials. *Applied Thermal Engineering 17,* 1067-1083.
40. Shabgard, H., Robak, C.W., Bergman, T.L. and Faghri, A., 2012. Heat transfer and exergy analysis of cascaded latent heat storage with gravity-assisted heat pipes for concentrating solar power applications. *Solar Energy 8,* 816-830.
41. Farid, M.M., Kim, Y. and Kansawa, A., 1990. Thermal performance of a heat storage module using PCM's with different melting temperature: experimental. *Journal of Solar Energy Engineering 112*, 125-131.
42. Ezra, M., Kozak, Y., Dubovsky, V. and Ziskind, G., 2016. Analysis and optimization of melting temperature span for a multiple-PCM latent heat thermal energy storage unit. *Applied Thermal Engineering 93*, 315-329.

43. Fang, M. and Chen, G., 2007. Effects of different multiple PCMs on the performance of a latent thermal energy storage system. *Applied Thermal Engineering 27*, 994-1000.
44. Mawire, A., 2016. Performance of Sunflower Oil as a sensible heat storage medium for domestic applications. *Journal of Energy Storage 5,* 1-9.
45. Mawire, A., Phori, A. and Taole, S., 2014. Performance comparison of thermal energy storage oils for solar cookers during charging. *Applied Thermal Engineering 73*, 1323-1331.
46. Nik, W.W., Ani, F.N., Masjuki, H.H. and Giap, S.E., 2005. Rheology of bio-edible oils according to several rheological models and its potential as hydraulic fluid. *Industrial Crops and Products 22*, 249-255.
47. Mawire, A., 2018. Experimental energy and exergy analyses of a discharging heat exchanger for a small hot-oil domestic storage tank. *International Journal of Green Energy 15*, 305-313.
48. Mawire, A., Lefenya, T.M., Ekwomadu, C.S., Lentswe, K.A. and Shobo, A.B., 2020. Performance comparison of medium temperature domestic packed bed latent heat storage systems. *Renewable Energy 146*, 1897-1906.

2 LITERATURE REVIEW

This chapter reviews related work done on latent heat thermal energy storage systems since this research aimed at evaluating the thermal performances of different packed bed latent heat thermal energy storage systems under different conditions.

2.1 Latent heat storage system using PCMs

In recent years, the potential of latent heat storage systems using phase change materials (PCMs) has drawn the attention of many researchers, since latent heat storage is more thermodynamically efficient in energy storage as compared to sensible heat storage [1-12]. This is due to its high storage density and its nearly isothermal storage and release of energy. Many applications of latent heat storage exist which include; electronics cooling [13-14], air-conditioning [15-16], building cooling [17-18], and solar thermal energy storage for off-sunshine hours cooking [19-28]. Farid et al., [29] and Da Cunha et al., [30] carried out comprehensive reviews on different PCMs and their applications.

Several factors should be considered in the selection of PCMs for every application. However, an ideal PCM is expected to have; a high heat of fusion, high thermal conductivity, high specific heat, high density, high rate of nucleation and crystal growth and good thermal stability. An ideal PCM is also expected to be non-toxic, be compatible with other materials (non-corrosive) and be available at low cost. Low melting temperature is not an imperfection, rather it is a property of a PCM that justifies its temperature range of application. No ideal PCM practically exists, and this is why thermal enhancement is a necessity in a PCM latent heat energy storage system. Low thermal conductivity is the main drawback associated with most PCMs, and this contributes to their low heat transfer [31-32]. Most imperfections associated with PCMs are due to their chemical structure [33]. Enhancement techniques which are of different types, include; use of high conductive materials (heat pipes) [19,34-35], addition of fins with different geometries [36-45], encapsulation/ dispersion of PCMs in shape stable structures [12, 25-28, 45-71], use of multiple PCMs [45, 61-72], addition of nanoparticles to PCMs [24,44,73-80], and the use of multiple tubes [81-83]. Employment of multiple PCMs with different melting points is one recent enhancement method with limited literature, while the majority of past work focussed on enhancement techniques using the

addition of fins. Before the introduction of the multiple PCM LHTES system, the single PCM system with different configurations was the most common, and one of the most popular is shell-and-tube configuration [35-36,39,43,58,71,72,82-86].

Due to the high efficiency of phase change materials (PCMs) in thermal energy storage, a lot of research work has been done to enhance their efficiency using different configurations and different enhancement techniques. The next sections present latent heat storage applications using single PCMs and different configurations for different temperature ranges. Low temperature applications are in temperature range of 0 to 100 ^{o}C, while medium temperature applications are in the temperature range of 100 to 300 ^{o}C. High temperature applications are considered for temperatures above 300 ^{o}C.

2.1.1 Low temperature latent heat storage (LHS) applications

The thermal energy storage characteristics of a paraffin PCM were investigated experimentally in [84] with a horizontal shell-in-tube configuration using distilled water as the HTF. This experiment was carried-out with three different inlet temperatures of 75 ^{o}C, 80 ^{o}C and 85 ^{o}C, respectively, at a constant mass flow rate of 280 kg/h. The aim of this experiment was to investigate the effect of inlet temperature on the charging and discharging characteristics. The results obtained showed that charging at higher inlet temperatures, and discharging at low temperatures enhanced the phase change process of the PCM. Rathod and Banerjee [36] investigated the enhancement of a tube and shell latent heat storage system using longitudinal fins. This experiment was done with and without longitudinal fins. The flow rate and inlet temperature were varied to compare the effect of the longitudinal fins at different flow rates and inlet temperatures. An organic PCM (stearic acid) with a melting point of 57.5 ^{o}C was used as the PCM, while water was used as the HTF. Results obtained showed that the percentage decrease in the charging time due to the presence of the longitudinal fin was 12.5 % when charged with an inlet temperature of 80 ^{o}C, and 24.5 % when charged with an inlet temperature of 85 ^{o}C. The percentage reduction in the discharging time was about 43.6 % when the fins were inserted. Liu et al., [37] investigated the melting characteristics of stearic acid in an annulus, and its thermal conductivity enhancement with fins. The charging temperature profile, the effect of the inlet water temperature, the effect of the heating flux, the influence of the fins on the temperature profile, the effect of the fin width on the melting

process and the effect of the pitch of spiral fins were investigated experimentally. The results showed that the increase in the heat flux temperature reduced the pre-melting time and shortened the charging time. The enhancement effect of the fin on the system's thermal conductivity increased as the melting process progressed. Liu et al., [38] also carried out a study on the discharging characteristics of stearic acid in an annulus, and its thermal conductivity enhancement. The experiments were done with a similar apparatus and storage medium materials as in [37] to investigate the solidification cycles of the system. Investigations were done on the discharging temperature profiles, the effect of the water inlet temperature, the effect of the Reynold's number and the influence of the fins. From the results obtained, it was confirmed that the heat transfer rate and the discharging time depended on the temperature of the cooling water. Stearic acid was recommended as a viable PCM for energy storage for domestic applications such as solar water heaters due to its phase change temperature range (67-70 ^{o}C), relatively high latent heat and insignificant supercooling. Joybari et al., [81] compared the effect of multiple tubes to a single tube experimentally and numerically in the enhancement of heat transfer in a LHTES system. A higher rate of heat transfer was observed in the multiple tube system as a result of the larger surface area which encouraged more convective heat transfer thereby shortening both the charging and discharging time. The effect of the flow rate on both charging and discharging of the two systems was also observed to be insignificant due to the nature of the flow (turbulent) inside the tubes.

Torlak and Delalić [39] investigated the influence of fins in the shell and tube TES configuration using plane and finned tubes as shown in Figure 2.1. Their results revealed that the heat transfer rate was much faster in the finned system as compared to the plane system which assisted in shortening the charging time of the finned system despite obstructing the vertical upward flow of the air during melting of the PCM.

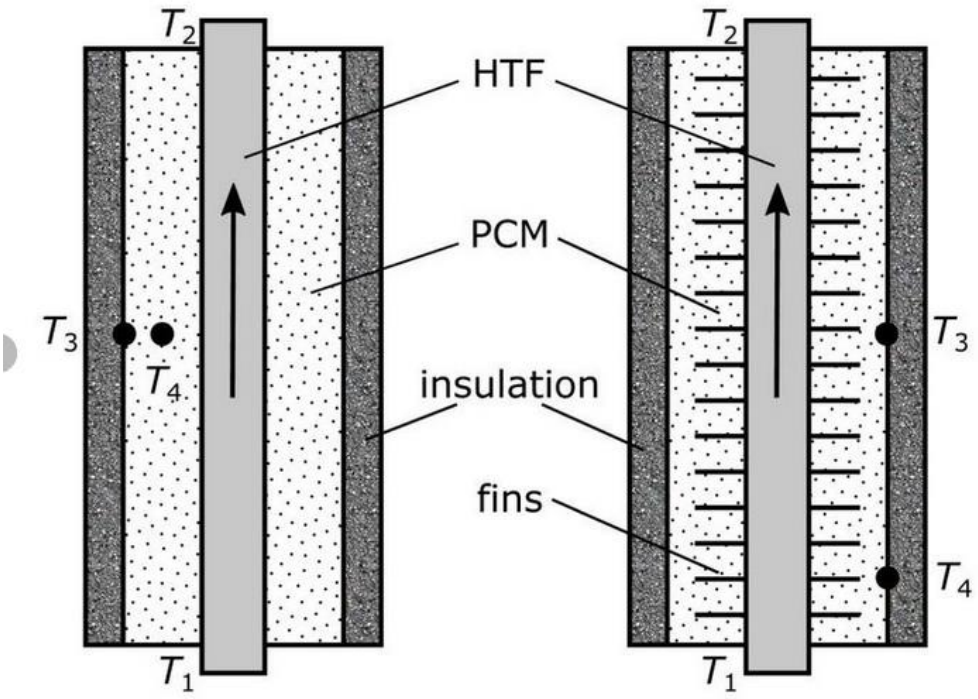

Figure 2.1: *Plane and finned shell and tube configurations investigated in [39].*

John et al., [73] investigated a LHTES system experimentally using a PCM and nano-enhanced PCMs (NEPCMs) during charging and discharging cycles. The experiments were carried out using paraffin wax as the PCM, Copper(II)Oxide (CuO) as the enhancement agent, and water as the HTF at different HTF flow rates, to investigate the effect of the flow rate on the charging and discharging cycles. The results obtained showed that the stored energy, the charging and discharging rates were improved in the NEPCM system. The performances of both systems increased with an increase in the HTF flow rate. Jesumathy et al., [74] also carried out a similar experiment in an annular storage tank and their results agreed with those obtained in [73]. Dhaidan et al., [75] investigated the enhancement effect of nanoparticles in a PCM based system using the shell and tube configuration. From their results, it was observed that the charging and discharging rate increased with an increase in the percentage of nanoparticles. Xue [76] investigated a domestic solar water heater with a solar collector coupled to a phase-change energy storage system experimentally using barium hydroxide octahydrate ($Ba(OH)_2.8H_2O$) as the PCM, barium carbonate ($BaCO_3$) as nucleant, and water as the HTF. The system was designed in such a way that the PCM was embedded in the solar collector. The evaluation of the system's thermal performance was in terms of useful energy obtained and system efficiency. The results obtained showed that the system was more efficient when the

solar collector was covered during discharging as compared to when it was exposed to environmental temperatures. Mettawee and Assassa [77] investigated the use of an aluminium powder for the enhancement of the thermal conductivity of a paraffin wax during charging and discharging cycles. The percentage of the aluminium powder was varied from 10 % to 50 % of the internal volume of the wax container. The HTF flow rate was also varied. The results showed that the charging time decreased by 60 %, and the increase in the aluminium powder increased the energy obtained.

An investigation was carried out experimentally in [19] on an indirect solar cooker integrated with an indoor PCM TES system and cooking unit as shown in Figure 2.2. The out-door flat-plate solar collector was connected to an indoor TES system using wickless heat pipes as the cooking unit, and magnesium nitrate (melting point = 89 ^{o}C) as the PCM. This experiment was investigated under Giza climatic conditions of Egypt with different types of food. The aim of this experiment was to investigate the possibility of using the PCM TES system domestically when solar radiation was not available. The results showed that the cooker could be used for both on (lunch) and off (breakfast and dinner) sunlight cooking, especially for those meals that required low temperatures for cooking. The authors also suggested eliminating heat losses by coating the absorber plate of the cooker, and increasing the thermal conductivity and heat transfer rate of the cooker by increasing the volume ratio of the steel wool inside the PCM to enhance cooker efficiency.

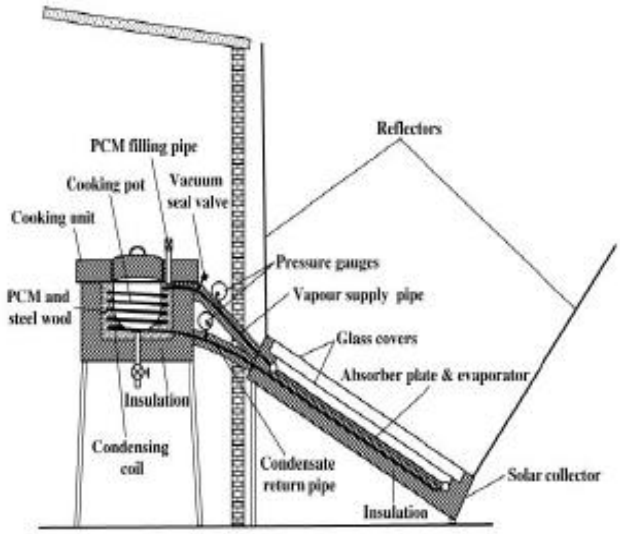

Figure 2.2: *A solar cooker integrated with a TES system for off-sunshine cooking [19].*

Kundan et al., Domanski et al., [20] investigated the possibility of using a PCM latent heat storage system for cooking during off-sunshine hours. This experiment was carried out using magnesium nitrate hexahydrate (MNHH) as the PCM, and water as the heat transfer fluid. The performance of this system was evaluated in terms of the charging/discharging time, highest temperature attained by the HTF and the time taken by the HTF to reach its highest temperature. The storage efficiency and utilization efficiency of the cooker were also evaluated. From their results, they observed that the charging time and the storage efficiency depended largely on the solar intensity and the melting temperature of the PCM. Their results also showed that the maximum temperature of the HTF during solidification (discharging) of MNHH was higher than the cooking temperatures of most food, which justified the possibility of using the PCM stored latent heat energy for cooking during off-sunshine hours. The performance of a solar water heating system integrated with a shell and tube LHTES unit was investigated experimentally in [85]. Paraffin wax and water were used as the PCM and HTF, respectively. The energy and exergy were analysed at different flow rates. The results showed that an increase in the HTF flow rate increased the energy efficiency and decreased the exergy efficiency. In addition to this, more heat losses were enhanced with higher flow rates.

Enhancement of a latent heat storage system was investigated experimentally using a heat pipe and a copper pipe [34]. A flat plate collector was used as the solar collector, while industrial grade granulated paraffin, and water were used as the PCM and HTF, respectively in the two systems. The experiments were carried out using a copper pipe on one of the setup and a heat pipe on the other. The results showed that the heat pipe enhanced thermal conductivity more than the copper pipe. The results also showed that an increase in the flow rate increased the heat storage capacity ensuring better performance. Rahimi et al., [40] investigated the effect of fins on the charging and discharging characteristics of a paraffin (R35 Paraffin). A finless system was used as the experimental control, and the inlet temperature and HTF flow rate were varied during both charging and discharging cycles to investigate their effect on both systems. At the end of the experiments, the charging and discharging rates of both systems were enhanced, but the effect of increasing the flow rate was more pronounced for the finless system, while the average heat transfer rate was higher in the finned system.

Darzi [41] studied the melting of PCMs inside concentric and eccentric horizontal annuli numerically using FLUENT software. Their results showed that the heat conduction to the PCM was dominant during the initial stages of the charging process for all locations of the storage tanks. A comparable charging rate was also observed in the two (concentric and eccentric) systems before 15 minutes of the commencement of the charging process but after that, the charging rate in the concentric array decreased as a result of conduction caused by temperature difference between the hot tube and the cold PCM. Yazici et al., [86] investigated the effect of concentric and eccentric positioning of the inner tube with regards to the centre of the outer shell on paraffin wax using a shell and tube configuration. Different values of e, the distance of the tube from the centre of the shell were investigated. The concentric case was also investigated (at e=0). The results showed that the melting time was reduced by 67 % with e=30, compared to the concentric position.

2.1.2 Medium temperature latent heat storage (LHS) applications

Saini et al., [21] carried out a review on the possibility of using a solar cooker for off-sunshine cooking. They investigated the environmental effect of using the solar cooker and the effect of the geometrical shape of the storage tank on the storage efficiency. They also commented that the use of a PCM based latent heat storage system was viable for temperatures above 100 ^{o}C. Their suggestions were that more research should carried out to increase the efficiency at an affordable cost resulting in more compact LHTES systems with high storage efficiency. Kumar et al., [82] investigated the heat transfer characteristics of a LHTES system for medium temperature solar applications using a multi-tube shell and tube configuration. The experiment was carried out with a commercial grade PCM (A164) having a melting temperature of 168.7 ^{o}C, and Hytherm 600 as the HTF. The effect of the temperature was investigated using three different HTF inlet temperatures at a constant flow rate. The effect of the flow rate was investigated using three different flow rates at a constant HTF inlet temperature. The results showed that an increase in the HTF inlet temperature decreased the thermal efficiency of the system, while the heat transfer rate increased with an increase in the flow rate. Agyenim et al., [83] carried out a study on a latent heat storage system for powering a LiBr/H_2O absorption cooling system using single and multiple tube shell and tube configurations. The heat spread radially and angularly within the storage tank in both the

single and multiple tube systems during charging but natural convection dominated the multiple tube system as a result of the higher volume flow as compared to the single tube (control) system.

Agyenim et al., [42] carried out an experimental comparison of the heat-transfer enhancement efficiency of longitudinal fins and circular fins on a LHTES system using erythritol and silicon oil as the PCM and HTF, respectively. The results obtained showed that the system with longitudinal fins had complete phase change, while the control system with circular fins system had incomplete phase change suggesting better heat transfer in the longitudinal finned system. Also the longitudinal fined system showed better solidification characteristics of erythritol with insignificant supercooling. Agyenim et al., [43] studied the enhancement effect of a longitudinal fin on a LHTES system using a shell and tube configuration designed for the operation of a $HiBr/H_2O$ absorption cooling system during charging and solidification cycles. The PCM used was erythritol with a melting temperature of 119.7 ^oC, and the HTF was silicon oil. The results obtained showed that the energy output from the storage system as a result of the enhancement, reached the maximum level for the $HiBr/H_2O$ absorption cooling system. The thermal properties of D-mannitol were studied in [87] for latent heat thermal energy storage using a differential scanning calorimeter (DSC) and thermo-gravimetry (TG). The investigations were focused on the melting temperature and the enthalpy of fusion. Different temperatures were used in the tests. The results revealed that the melting temperature was in the range of 162.15 to 167.8 ^oC, and the enthalpy of fusion was 326.8 J/g. Decomposition was also observed from the results starting from around 300.15 ^oC. From the conclusions drawn, D-mannitol was found to be a promising PCM for medium temperature applications since it showed a large temperature difference between the melting temperature and the decomposition temperature. Stability tests were carried out on three sugar alcohol PCMs (D-mannitol, myo-insositol and galactitol) by Sole et al., [88] using DSC and fourier-transform infrared spectroscopy (FTIR) techniques. The results showed that myo-insositol was a stable PCM although a change in the chemical structure was observed from the FTIR measurement which had no effect on its thermophysical properties. Galactitol showed a very poor cycling stability, which was evident on the wide change in the solidification temperature after 18 cycles. D-mannitol showed a tendency of reacting with atmospheric oxygen, and it produced a non-stable mixture with a low energy storage density.

The use PCMs for off-sunlight cooking using medium temperatures has been reported recently [22-23]. El-Sebaii et al., [22] investigated the charging and discharging characteristics of commercial-grade magnesium chloride hexahydrate ($MgCl_2.6H_2O$) in a sealed storage tank under the extra water principle. This extra water principle helps to avert the common problem of incongruent melting of salt hydrate PCMs as a result of phase segregation, and it has been used in [89-90]. The results obtained confirmed that $MgCl_2.6H_2O$ was a good PCM for off-sunlight cooking provided the extra water principle was applied, although, small degrees of supercooling were observed. A box type solar cooker with four reflectors and a single reflector type were investigated in [23]. Both cookers were integrated with thermal energy storage (TES) systems. Oxalic acid dehydrate ($C_2H_6O_6$) was used as the phase change material (PCM) in the TES systems. Loads (food) of two different masses (400g and 800g) were tested. From the results obtained, it was observed that the efficiency of the solar cooker increased with an increase in the load, and the higher the number of reflectors the faster was the cooking speed. Oxalic acid dehydrate was confirmed as a promising PCM for off sunshine cooking due to its efficiency of discharging heat energy.

2.1.3 High temperature latent heat storage (LHS) applications

Shabgard et al., [35] developed a model to compare different arrangements of a heat pipe in a shell and tube configuration for a high temperature LHTES system for solar thermal electricity generation during both charging and discharging cycles. The difference in the two systems was the location of the PCM and the HTF. In system 1, the HTF flowed in the tube, while the shell contained the PCM. System 2 was the reverse configuration where the PCM was in tube and the HTF flowed in the shell. From the results obtained, system 2 showed a better performance as compared to system 1. Kenisarin [78] carried out a review on investigations and practices for finding more unknown PCMs, enhancement of existing high temperature PCMs, and for the creation of more efficient PCMs through combinations of two or more salts using suitable ratios and other PCM types. Their thermophysical properties and applications were also investigated and discussed. Zhao et al., [79] investigated the performance of a mixture of calcium nitrate ($Ca(NO_3)_2$) and sodium nitrate ($NaNO_3$) mixed in different proportions for high temperature PCM applications. The results showed a ratio of

3:7 as the best mixture ratio with a melting temperature of 217 ^{o}C which was cheaper than the two pure solar salts.

Mosleh and Ahmadi [91] carried out a dynamic analysis on the performance of a parabolic trough concentrated solar power plant in Shiraz, Iran using TRNSYS software to investigate the PCM that was capable of improving its performance. In this investigation, many high temperature PCMs were tested, and $NaNO_3$ was selected as the best PCM with a solar fraction of 34.4 %. The selected PCM enhanced the solar fraction of the power plant by 90.5 % when compared to other solar plants without LHTES, and the cost of power generation was reduced. Myers et al., [80] investigated the enhancement of nitrate salts (KNO_3 and $NaNO_3$) by doping them with nanoparticles (CuO) to improve their thermal conductivity and thermal diffusivity. The results obtained revealed that the thermal conductivity and the thermal diffusivity of the two eutectic salts were significantly increased as a result of the doping. However, the effect of nanoparticles on the individual eutectic salts was limited to a particular temperature. The eutectic mixture was confirmed to be stable after several cycles. Foong et al., [24] studied a small-scale double reflector solar concentrating system with high temperature heat storage for an off-sunlight cooking application. A direct heating method was used (no HTF) and a 40 %:60 % mixture of $NaNO_3$ and KNO_3 was used as the PCM in the storage medium. The performance of this system was analysed using a finite element model that was validated with experimental results. The results showed effective melting within 2 to 2.5 hrs of charging, and a temperature of about 260 ^{o}C was attained which was suitable for cooking any kind of food at night. Foong et al., [44] also carried out another numerical investigation on a similar storage system as reported in [24], for a higher temperature range that was integrated with aluminium fins to investigate the effect of aluminium fins during charging cycles. The results showed an appreciable reduction in the melting time for the system with aluminium fins.

2.2 Packed bed latent heat thermal energy storage (LHTES) systems

This section will review low, medium and high temperature packed bed LHTES systems. A packed bed LHTES system is a configuration of encapsulated phase change materials with similar of different geometries packed in a storage tank. Spherically encapsulated PCMs in a packed bed storage configuration are shown in Figure 2.3. It is one of the oldest and common configuration of latent heat storage system. A recent study has shown that the packed bed

storage system is more efficient and economically more viable as compared to the tube-and-shell configuration and this justifies carrying out a study on this configuration regardless of the larger pressure drop [58].

Figure 2.3: *A schematic view of a packed bed LHTES unit [51].*

2.2.1 Low temperature packed bed LHTES systems

Senthil et al., [46] investigated a paraffin wax packed bed LHTES system experimentally for a concentrated solar collector. The flow rate was varied to investigate its effect on the charging and discharging cycles. The results showed that an increase in flow rate increased the charging and discharging rates and reduced the thermal efficiency. Abu-Hamdeh and Alnefaie [25] investigated experimentally the use of stored latent heat energy in a solar stove for off-sunshine cooking of rice. This experiment was carried out on a sunny day with encapsulated acetamide as the PCM and air as the HTF. A parabolic reflector was used as the solar collector for the charging process, and a fan was used as the HTF circulator. The performance of the system was evaluated using four different values of the air flow rate. The results showed that increasing the air flow rate increased the energy transfer effectiveness of the system. They also recommended acetamide as a promising PCM for solar cooking applications. Nallusamy et al., [47] investigated the performance of a solar water heating system using a packed bed LHTES unit. The effects of porosity and the HTF flow rate on the performance of the storage unit were investigated. Paraffin wax and water were used as the PCM and HTF, respectively. The charging cycles were done with varying inlet fluid temperatures. Continuous and batch-wise processes were used to recover the stored energy during discharging cycles. The

parameters used for evaluation of the performance of the system were the instantaneous heat stored, the cumulative heat stored, the charging rate and the system efficiency. The results showed that the rate at which heat was extracted from the solar collector and the charging rate depended largely on the mass flow rate.

Karthikeyan et al., [48] carried out a parametric study on a spherically encapsulated PCM in a packed bed storage configuration. The effects of the capsule size, inlet temperature, flow rate and the effective thermal conductivity of the PCMs were investigated. Numerical results were validated with experimental results. The results showed that an increase in all parameters investigated enhanced the performance of the charging cycle, but the effect of the inlet temperature was more pronounced when compared to other parameters. Regin et al., [49] carried out a numerical investigation on charging and discharging thermal characteristics of a packed bed LHTES system using paraffin wax as the PCM. The results showed that the discharging time was longer as compared to the charging time due to low heat transfer during discharging. The results obtained also showed that the charging time could be reduced by increasing the inlet temperature and the capsule radius.

Wu and Fang [50] carried out an investigation on the dynamic performance a packed bed LHTES system during discharging cycles. The influence of the initial inlet temperature of the HTF and the mass flow rate were investigated. Their results showed that an increase in flow rate increased the rate of heat transfer and decreased the discharging time, while an increase in the initial inlet temperature increased the discharging efficiency and reduced the rate of heat transfer. Pakrouh et al., [51] investigated numerically the solidification characteristics of a packed bed of a paraffin wax using water as the HTF. The parameters investigated were the capsule diameter and the inlet temperature. The results obtained showed that both decreasing the capsule diameter and HTF inlet temperature increased the entropy generation rate which had no influence on the system's storage efficiency. Also, reducing the inlet temperature decreased the system's efficiency. They also observed that decreasing the capsule diameter increased the rate of heat transfer by creating more surface area for heat interaction which in turn enhanced the system's efficiency. This reduction was limited only to a decrease of up to 20 mm, and further reduction of the diameter showed no significant effects.

Oró et al., [12] carried out a comparative analysis numerically and experimentally on the stratification of a packed bed LHTES system. This investigation was done with a sensible heat storage system (water) and a PCM packed bed storage tank comprising of ethyl acetate (pk6). The results showed that the thermal stratification of the PCM packed bed system decreases with an increase in the bed volume during charging cycles. They also observed that the thermal stratification was more pronounced in the sensible heat storage system in both charging and discharging cycles, while the degree of thermal stratification in the PCM packed bed system more was pronounced during the discharging cycles as compared to its charging cycles. The results also suggested that enhancement of thermal stratification for the PCM system could be achieved by using thinner layer of the PCM packed bed instead of a high volume of PCM in the packed bed. Ismail and Henrıquez [52] investigated the use of a spherical capsule for a packed bed system experimentally and numerically. Investigations were carried out on the effect of the external diameter of the PCM capsule, the wall thickness of the capsule and the charging /discharging temperature profiles. The experimental results were in good agreement with the simulated results and a copper capsule exhibited the best heat transfer characteristics. The heat transfer rate decreased with an increase in the temperature, and it increased with the increase of the flow rate causing the charging time to reduce. Oró et al., [53] carried out a comparative study on two different numerical models of a packed bed LHTES system. The two models were the Brinkman's equation model and the energy equation model. Both models were validated with experimental results, and the results showed that forced convection was more critical when compared to free convection except in few cases with low flow rates or static fluids.

2.2.2 Medium temperature packed bed LHTES systems

Mawire et al., [54] compared the thermal performances of a packed bed latent heat storage of adipic acid, erythritol and eutectic solder using sunflower oil as the HTF with three different flow rates. The temperature profiles, total energy and total exergy, useful energy and useful exergy during both charging and discharging cycles were compared. The charging results showed that the eutectic solder packed bed LHTES stored the greatest useful energy but its overall performance was lower than the other systems due to lower degree of thermal stratification and longer charging time. Erythritol showed the highest energy and exergy

efficiencies in all the experiments despite possessing more supercooling. Shobo and Mawire [55] also observed the supercooling effect in erythritol while comparing the performances of three PCM capsules for packed bed systems (acetanilide, erythritol and an In-Sn alloy). From their results, a high degree of supercooling was observed in acetanilide and erythritol, which reduced the quality of the useful energy expected from them. The issue of supercooling in erythritol was tackled using different techniques as reported in [91-92]. Wang et al [92] minimized the supercooling effects of erythritol and boost its heat releasing ability through encapsulation and doping. This enhancement practice was carried out using polysiloxane capsules which contained erythritol and carboxy-methyl-cellulose as the nucleating agent and nano-alumina as the thickener. The results obtained showed that the degree of supercooling was decreased by 83.6 %, the heat releasing ability was increased by 59 % and the thermal conductivity was increased by 29.2 %. The results also revealed that the melting and the freezing point of erythritol were retained. Zeng et al., [93] carried out a cyclic DSC experiment on nine nucleants to investigate the most suitable nucleant that could supress the supercooling defect in erythritol without altering its crystallisation point after several cycles. The nucleants investigated were; calcium pimelate (CaPi), bicyclic [1, 2, 2] heptane di-carboxylate (HPN-68), aryl amide (TMB-5), calcium salt of hexahydrophthalic acid (HPN-20E), 1,3:2,4-di-p-methylbenzylidene sorbitol (MDBS), calcium salt of benzene-1, 3, 5-tricarboxylic acid (Ca_3BTC_2), sodium salt of benzene-1, 3, 5-tricarboxylic acid (Na_3BTC), potassium salt of benzene-1, 3, 5-tricarboxylic acid (K_3BTC) and magnesium salt of benzene-1, 3, 5-tricarboxylic acid and (Mg_3BTC_2). The results showed that CaPi (calcium pimelate) and TMB-5 (aryl amide) were the best since they could melt and crystalize erythritol at a nearly constant temperature with a high phase change enthalpy.

The use of a PCM latent heat storage unit for off-sunshine solar cooking was investigated in [26]. Experiments were carried out during the winter season with two different set-ups; one with one reflector, and the other with three reflectors to investigate the effect of the reflectors using different loads (food). The storage units comprised of a cylindrical tank filled with commercial grade acetanilide with a melting temperature of 118.9 ^{o}C as the PCM. The results showed that the set-up with three reflectors was more efficient, and the possibility of cooking with the stored PCM latent energy during the evening was guaranteed. Kumaresan et al., [27] carried out an experimental investigation on the performance of a double walled cooking unit integrated with a TES system. This experiment was done with a packed bed of D-

mannitol as the PCM and therminol 55 as the HTF. The heat distribution analysis was evaluated, and it was found that the heat loss was high. They suggested that minimizing the heat loss would enhance the efficiency of the system. Klein et al., [56] investigated the efficiency of sodium sulphate as a PCM in a packed bed storage configuration for a solar gas turbine. This investigation was carried out numerically during both charging and discharging cycles using a Dispersion-Concentric (D-C) model that was reported in [94]. The results obtained were compared with a SHTES packed bed system of alumina particles, and it was observed that the discharging time improved by 10 %, the storage mass was reduced by 31 %, and it was more cost effective. Shobo and Mawire [28] investigated numerically a packed bed LHTES system of aluminium-encapsulated erythritol for solar cooking using sunflower oil as the HTF. The model was based on dual phase heat transfer equations and it was validated with experimental results. The results showed that the charging time decreased with an increase of the HTF flow rate, and the increase in the inlet temperature only improved the energy stored.

2.2.3 High temperature packed bed LHTES systems

A laboratory scale packed bed LHTES was investigated experimentally by Alam et al., [57]. This investigation was carried out for both charging and discharging cycles using sodium nitrate ($NaNO_3$) encapsulated in spherical capsules as the PCM and air as the HTF. The HTF flow rate was varied during both charging and discharging cycles to investigate its effect on the charging and discharging cycles. The results obtained showed that an increase in the flow rate increased the heat transfer rate and shortened the charging and discharging times. Li et al., [58] investigated the performance of a macro-encapsulated molten salt packed bed TES system experimentally and numerically. The temperature profiles for the charging and discharging processes at different inlet temperatures and flow rates were presented. The numerical results were validated with experimental results and reasonably good agreement was obtained. The overall performance of the system was compared with the performance of a shell and tube configuration. The results showed that both an increase in the inlet temperature and the flow rate improved the charging/discharging rates and the charging efficiency, but the effect of the temperature increase was more pronounced compared to the effect of the flow rate. The results also showed that the packed bed LHTES system had a better

overall efficiency as compared to the shell and tube system. Ma and Zhang [59] developed a three dimensional numerical model to evaluate the performances of a packed bed LHTES system and a SHTES system. The charging and discharging cycles of a LHTES system composed Al-Si capsules and a SHTES system composed of rocks were evaluated. Numerical results were validated with the experimental results, and reasonably good agreement was obtained between the two results. From the results obtained, the packed bed LHTES system showed a larger energy storage density and a more stabilized outlet temperature as compared to the SHTES system. A more uniform temperature distribution was exhibited by the LHTES system which was due to radiation heat transfer. This radiation heat transfer increased the temperature difference between the storage medium temperature and the HTF temperature making the charging/discharging time shorter. Peng et al., [60] used a concentric-dispersion model to investigate the behaviour of a packed bed LHTES system. The effect of the PCM capsule diameter, flow rate and the effect of the storage tank height were analysed using a finite difference approach after validating the model experimentally. The results obtained showed that the charging efficiency was increased by decreasing the flow rate, decreasing the PCM capsule size and by increasing the height of the storage tank.

2.3 Cascaded latent heat thermal energy storage (CLHTES) system

The cascaded latent heat thermal energy storage (CLHTES) system of PCMs with different melting points is a very promising enhancement technique proposed in the recent years. This storage method has drawn the attention of researchers in recent years due to its advantages over the single stage PCM LHTES system. Some of the advantages of the CLTES include; uniformity of the outlet temperature, a higher heat transfer rate, higher energy and exergy rates, fast charging and discharging rates and higher energy and exergy efficiencies. The performance of this system depends largely on the selection of PCM for the storage medium [62,68,85,96]. Recent literature evaluating the efficiency of CLHTES systems is rather limited [45,61-72]. The cascaded arrangement of PCMs is shown in Figure 2.4.

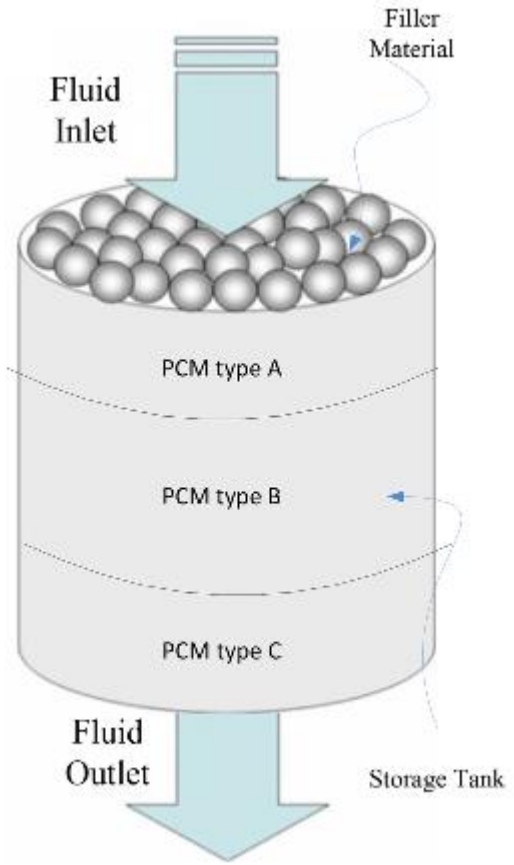

***Figure 2.4**: A schematic view of a cascaded LHTES unit [69].*

Aldoss and Raman [61] investigated the charging and discharging performances of different number of stages of multiple PCMs compared to a single PCM packed bed system. The results obtained showed that multiple PCM systems had a better performance in both charging and discharging cycles compared to the single PCM system. The performance tended to increase with an increase in number of stages, and the optimal number of stages was found to be three. Ezra et al., [62] analysed numerically the optimal range of the charging temperature of a multiple PCM LHTES system using a mathematical model. Many parameters were investigated such as the effect of the inlet temperature, flow rate, number of rows, number of materials and the PCM's melting temperature range. An optimal way was found of attaining the shortest melting (charging) time for an entire multiple-PCM unit under given conditions. Xu et al., [63] developed a mathematical model for analysing and optimization of the overall exergy efficiency of combined charging/discharging processes of a three PCM cascaded LHTES system. Different parameters such as the effect of the inlet temperature, the optimum melting temperature of the PCMs and the number of heat transfer units (NTU) were

considered based on a lumped model. Their results revealed that the increase in the overall exergy efficiency as a result of the inlet temperature increase depended on the NTUs. Shabgard et al., [64] developed a model to investigate the thermal performances of different configurations of high temperature (280-390 ^{o}C) cascaded and non-cascaded LHTES systems. The parameters investigated included, the heat transfer rate and the energy and exergy analyses in both cycles. The results obtained showed that the highest exergy efficiency was obtained in the non-cascaded LHTES system with the lowest melting temperature, while maximum exergy recovery for 24 hours of charging and discharging was seen with the cascaded system.

Wu et al., [65] carried out a comparative investigation on the cyclic behaviour of cascaded and non-cascaded LHTES systems. Their results showed that the cascaded system had a faster charging and discharging rate compared to the non-cascaded system, which contributed to its higher accumulated efficiency. Cheng et al., [66] analysed the performance of a cascaded cold storage system of PCMs experimentally and numerically during discharging cycles. Its performance was compared to that of a single PCM system, and better discharging performances were obtained for the cascaded system. Tian and Zhou [67] investigated the enhancement effect of a metal-foam on a cascaded LHTES system experimentally and numerically. The numerical results were validated with the experimental results, and good agreement was obtained between these two results. In this investigation, the heat transfer rate and exergy efficiency of a single-stage TES system, a cascaded TES and a metal-foam enhanced cascaded thermal energy storage (MF-CTES) were compared. The results showed the shortest charging time was seen with the MF-CTES. Peiro et al., [68] compared the thermal performance of a cascaded LHTES system with a single-stage LHTES system at pilot plant scales. The results obtained showed a higher heat transfer rate and an overall efficiency that was enhanced by 19.36 % for the cascaded system when compared to the single PCM packed bed system.

Shamsi et al., [69] carried out an evaluation and optimization investigations of the thermal performances of a cascaded multi-PCM latent heat thermal energy storage system. In this study, different PCMs were used in different proportions with different HTFs for optimization reasons. Also, many parameters such as the storage volume, charging time and the mass flow rate were varied with different cascaded stages to investigate their effects. The numerical

results obtained were validated with the experimental results and there was a good agreement. A 2-stage cascaded system was compared with the single PCM system, and the energy stored was 5.12 % more than the stored energy in the single PCM system. The simulation results also showed that the bottom PCM had a vital role of gathering more energy during charging which enhanced the heat transfer rate of the system. Wang et al., [70] carried out a study on a cascaded LHTES system encapsulated with cylindrical capsules. A 3-stage multiple PCM LHTES system was compared experimentally with a single stage PCM LHTES system during charging cycles with two different charging temperatures. The results showed a faster charging rate for the cascaded system compared to the single PCM system. Fang and Chen [71] investigated the performance of a multiple PCM LHTES system numerically using a shell and tube configuration during charging and discharging cycles. The parameters investigated were the effect of different PCMs on the melting fraction, the energy stored and the outlet temperature of the storage tank. Results obtained showed that the performance of the cascaded system depended largely on the PCM selection.

Michel and Ritz-Paal [72] investigated experimentally and numerically the use of a cascaded LHTES system of alkaline nitrate salts in a vertical shell and tube configuration for a parabolic trough power plant. Results showed that the performance of the cascaded LHTES system depended largely on the value of the thermal conductivity and the heat of fusion of the medium PCMs. Seeniraj and Narasimhan [42] investigated the enhancement effect of fins in a cascaded LHTES system numerically during charging cycles. The modelled energy equation that governs the behaviour of the LHTES system was developed and used on both the single PCM system and the finned cascaded system. The charging thermal characteristics were compared, and the finned cascaded system showed higher stored energy and a nearly uniform outlet temperature when compared with the single PCM unit.

2.4 Summary of the chapter

This chapter presented a literature review of PCM latent heat thermal energy storage systems. The systems were classified for applications using three temperature categories (low, medium and high). The review of the systems was based on the method of design, applications and results obtained. The literature confirmed that a lot of investigations have been done on LHTES systems in terms of enhancement techniques, energy and exergy

evaluation and charging/discharging characteristics of storage systems. The literature also revealed that limited work has been done on cascaded latent heat energy storage systems using the packed bed storage configuration for medium temperature applications. Furthermore, no literature has been reported on metallic PCM based cascaded systems using sunflower oil as the heat transfer fluid which justifies the scope of the current study.

2.5 References

1. Verma, P. and Singal, S.K., 2008. Review of mathematical modeling on latent heat thermal energy storage systems using phase-change material. *Renewable and Sustainable Energy Reviews 12*, 999-1031.
2. Watanabe, T. and Kanzawa, A., 1995. Second law optimization of a latent heat storage system with PCMs having different melting points. *Heat Recovery Systems and CHP 15*, 641-653.
3. Beemkumar, N., Karthikeyan, A., Manoj, A., Keerthan, J.S., Stallan, J.P. and Amithkishore, P., 2017. Investigation of Sensible and Latent Heat Storage System using various HTF. In *IOP Conference Series: Materials Science and Engineering* 7–9 July, 2016. Sathyabama University, Chennai, India.
4. Sharma, S.D. and Sagara, K., 2005. Latent heat storage materials and systems: a review. *International Journal of Green Energy 2*, 1-56.
5. Sarbu, I. and Sebarchievici, C., 2018. A comprehensive review of thermal energy storage. *Sustainability 10*, 191.
6. Jegadheeswaran, S., Pohekar, S.D. and Kousksou, T., 2010. Exergy based performance evaluation of latent heat thermal storage system: a review. *Renewable and Sustainable Energy Reviews 14*, 2580-2595.
7. Rathod, M.K. and Banerjee, J., 2013. Thermal stability of phase change materials used in latent heat energy storage systems: A review. *Renewable and Sustainable Energy Reviews 18*, 246-258.
8. Pielichowska, K. and Pielichowski, K., 2014. Phase change materials for thermal energy storage. *Progress in Materials Science 65*, 67-123.
9. Liu, M., Tay, N.S., Bell, S., Belusko, M., Jacob, R., Will, G., Saman, W. and Bruno, F., 2016. Review on concentrating solar power plants and new developments in high temperature

thermal energy storage technologies. *Renewable and Sustainable Energy Reviews 53*, 1411-1432.

10. Ma, F. and Zhang, P., 2017. Investigation on the performance of a high-temperature packed bed latent heat thermal energy storage system using Al-Si alloy. *Energy Conversion and Management 150*, 500-514.
11. Alva, G., Lin, Y. and Fang, G., 2018. An overview of thermal energy storage systems. *Energy 144*, 341-378.
12. Oró, E., Castell, A., Chiu, J., Martin, V. and Cabeza, L.F., 2013. Stratification analysis in packed bed thermal energy storage systems. *Applied Energy 109*, 476-487.
13. Khudhair, A.M. and Farid, M.M., 2008. Use of phase change materials for thermal comfort and electrical energy peak load shifting: experimental investigations. In *Proceedings of the ISES Solar World Congress 2007,* Abu Dhabi, UAE, 30 October-2 November 2017, *283-288.*
14. Tan, F.L. and Tso, C.P., 2004. Cooling of mobile electronic devices using phase change materials. *Applied Thermal Engineering 24*, 159-169.
15. Parameshwaran, R. and Kalaiselvam, S., 2014. Energy conservative air conditioning system using silver nano-based PCM thermal storage for modern buildings. *Energy and Buildings 69*, 202-212.
16. Nagano, K., Takeda, S., Mochida, T., Shimakura, K. and Nakamura, T., 2006. Study of a floor supply air conditioning system using granular phase change material to augment building mass thermal storage—heat response in small scale experiments. *Energy and Buildings 38*, 436-446.
17. Kośny, J., 2015. PCM-enhanced building components: an application of phase change materials in building envelopes and internal structures. *Springer* Boston, USA, 1-54.
18. Gracia, A. and Cabeza, L.F., 2015. Phase change materials and thermal energy storage for buildings. *Energy and Buildings 103*, 414-419.
19. Hussein, H.M.S., El-Ghetany, H.H. and Nada, S.A., 2008. Experimental investigation of novel indirect solar cooker with indoor PCM thermal storage and cooking unit. *Energy Conversion and Management 49*, 2237-2246.
20. Domanski, R., El-Sebaii, A.A. and Jaworski, M., 1995. Cooking during off-sunshine hours using PCMs as storage media. *Energy 20*, 607-616.
21. Saini, P., Sharma, V., Singh, C. and Singh, S., 2015. Solar cooker for off-sunshine cooking. *Journal of Academia and Industrial Research 3*, 438-444.

22. El-Sebaii, A.A., Al-Heniti, S., Al-Agel, F., Al-Ghamdi, A.A. and Al-Marzouki, F., 2011. One thousand thermal cycles of magnesium chloride hexahydrate as a promising PCM for indoor solar cooking. *Energy Conversion and Management 52*, 1771-1777.
23. Vigneswaran, V.S., Kumaresan, G., Sudhakar, P. and Santosh, R., 2017. Performance evaluation of solar box cooker assisted with latent heat energy storage system for cooking application. IOP conference series: In Proceedings of the 7th International Conference on Environment and Industrial Innovation, 24–26 April 2017, Kuala Lumpur, Malaysia.
24. Foong, C.W., Nydal, O.J. and Løvseth, J., 2011. Investigation of a small-scale double-reflector solar concentrating system with high temperature heat storage. *Applied Thermal Engineering 31*, 1807-1815.
25. Abu-Hamdeh, N.H. and Alnefaie, K.A., 2019. Assessment of thermal performance of PCM in latent heat storage system for different applications. *Solar Energy 177*, 317-323.
26. Buddhi, D., Sharma, S.D. and Sharma, A., 2003. Thermal performance evaluation of a latent heat storage unit for late evening cooking in a solar cooker having three reflectors. *Energy Conversion and Management 44*, 809-817.
27. Kumaresan, G., Vigneswaran, V.S., Esakkimuthu, S. and Velraj, R., 2016. Performance assessment of a solar domestic cooking unit integrated with thermal energy storage system. *Journal of Energy Storage 6,* 70-79.
28. Shobo, A.B. and Mawire, A., 2016. Investigation of aluminum encapsulation of a PCM for domestic cooking. In Proceedings of the 24th Domestic Use of Energy (DUE). Cape Town, South Africa 30-31 March, 2016, 1-6.
29. Farid, M.M., Khudhair, A.M., Razack, S.A.K. and Al-Hallaj, S., 2004. A review on phase change-energy storage: materials and applications. *Energy Conversion and Management 45*, 1597-1615.
30. Da Cunha, J.P. and Eames, P., 2016. Thermal energy storage for low and medium temperature applications using phase change materials–a review. *Applied Energy 177*, 227-238.
31. Zhou, D. and Zhao, C.Y., 2011. Experimental investigations on heat transfer in phase change materials (PCMs) embedded in porous materials. *Applied Thermal Engineering 31*, 970-977.

32. Pincemin, S., Olives, R., Py, X. and Christ, M., 2008. Highly conductive composites made of phase change materials and graphite for thermal storage. *Solar Energy Materials and Solar Cells 92*, 603-613.
33. Frigione, M., Lettieri, M. and Sarcinella, A., 2019. Phase change materials for energy efficiency in buildings and their use in mortars. *Materials 12*, 1260.
34. Patil, R.M. and Ladekar, C., 2014. Experimental investigation for enhancement of latent heat storage using heat pipes in comparison with copper pipes. *International Refereed Journal of Engineering and Science 3*, 44-52
35. Shabgard, H., Bergman, T.L., Sharifi, N. and Faghri, A., 2010. High temperature latent heat thermal energy storage using heat pipes. *International Journal of Heat and Mass Transfer 53*, 2979-2988.
36. Rathod, M.K. and Banerjee, J., 2015. Thermal performance enhancement of shell and tube latent heat storage unit using longitudinal fins. *Applied Thermal Engineering 75*, 1084-1092.
37. Liu, Z., Sun, X. and Ma, C., 2005. Experimental investigations on the characteristics of melting processes of stearic acid in an annulus and its thermal conductivity enhancement by fins. *Energy Conversion and Management 46*, 959-969.
38. Liu, Z., Sun, X. and Ma, C., 2005. Experimental study of the characteristics of solidification of stearic acid in an annulus and its thermal conductivity enhancement. *Energy Conversion and Management 46*, 971-984.
39. Torlak, M. and Delalić, N., 2017, June. Latent-heat thermal-energy storage in heat exchanger with plain and finned tube. In *Proceedings of the 3rd World Congress on Mechanical, Chemical, and Material Engineering (MCM'17), Rome, Italy* 8-10 June, 2017.
40. Rahimi, M., Ranjbar, A.A., Ganji, D.D., Sedighi, K. and Hosseini, M.J., 2014. Experimental investigation of phase change inside a finned-tube heat exchanger. *Journal of Engineering 2014*, 641954.
41. Darzi, A.R., Farhadi, M. and Sedighi, K., 2012. Numerical study of melting inside concentric and eccentric horizontal annulus. *Applied Mathematical Modelling 36*, 4080-4086.
42. Agyenim, F., Eames, P. and Smyth, M., 2009. A comparison of heat transfer enhancement in a medium temperature thermal energy storage heat exchanger using fins. *Solar Energy 83*, 1509-1520.

43. Agyenim, F., Eames, P. and Smyth, M., 2011. Experimental study on the melting and solidification behaviour of a medium temperature phase-change storage material (Erythritol) system augmented with fins to power a LiBr/H2O absorption cooling system. *Renewable Energy 36*, 108-117.
44. Foong, C.W., Hustad, J.E., Løvseth, J. and Nydal, O.J., 2010. Numerical Study of a High Temperature Latent Heat Storage (200-300 0 C) Using Eutectic Nitrate Salt of Sodium Nitrate and Potassium Nitrate. In *Proceedings of the COMSOL Conference*, Newton, USA, 7-9 October 2010.
45. Seeniraj, R.V. and Narasimhan, N.L., 2008. Performance enhancement of a solar dynamic LHTS module having both fins and multiple PCMs. *Solar Energy 82*, 535-542.
46. Senthil, R., Sundaram, P. and Kumar, M., 2018. Experimental investigation on packed bed thermal energy storage using paraffin wax for concentrated solar collector. *Materials Today: Proceedings 5,* 8916-8922.
47. Nallusamy, N., Sampath, S. and Velraj, R., 2006. Study on performance of a packed bed latent heat thermal energy storage unit integrated with solar water heating system. *Journal of Zhejiang University-SCIENCE A7*, 1422-1430.
48. Karthikeyan, S., Solomon, G.R., Kumaresan, V. and Velraj, R., 2014. Parametric studies on packed bed storage unit filled with PCM encapsulated spherical containers for low temperature solar air heating applications. *Energy Conversion and Management 78*, 74-80.
49. Regin, A.F., Solanki, S.C. and Saini, J.S., 2009. An analysis of a packed bed latent heat thermal energy storage system using PCM capsules: Numerical investigation. *Renewable Energy 34*, 1765-1773.
50. Wu, S. and Fang, G., 2011. Dynamic performances of solar heat storage system with packed bed using myristic acid as phase change material. *Energy and Buildings 43*, 1091-1096.
51. Pakrouh, R., Hosseini, M.J., Ranjbar, A.A. and Bahrampoury, R., 2017. Thermodynamic analysis of a packed bed latent heat thermal storage system simulated by an effective packed bed model. *Energy 140*, 861-878.
52. Ismail, K.A.R. and Henrıquez, J.R., 2002. Numerical and experimental study of spherical capsules packed bed latent heat storage system. *Applied Thermal Engineering 22*, 1705-1716.

53. Oró, E., Chiu, J., Martin, V. and Cabeza, L.F., 2013. Comparative study of different numerical models of packed bed thermal energy storage systems. *Applied Thermal Engineering 50*, 384-392.
54. Mawire, A., Lefenya, T.M., Ekwomadu, C.S., Lentswe, K.A. and Shobo, A.B., 2020. Performance comparison of medium temperature domestic packed bed latent heat storage systems. *Renewable Energy 146*, 1897-1906.
55. Shobo, A.B. and Mawire, A., 2017. Experimental comparison of the thermal performances of acetanilide, meso-erythritol and an In-Sn alloy in similar spherical capsules. *Applied Thermal Engineering 124*, 871-882.
56. Klein, P., Roos, T. and Sheer, J., 2014. High temperature thermal storage for solar gas turbines using encapsulated phase change materials. In Proceedings of the 2nd Southern African Solar Energy Conference ,Nelson Mandela Bay (Port Elizabeth), South Africa. 27-29 January, 2014.
57. Alam, T.E., Dhau, J., Goswami, D.Y., Rahman, M.M. and Stefankos, E., 2015. Experimental investigation of a packed bed latent heat thermal storage system with encapsulated phase change material. In the ASME 2014 International Mechanical Engineering Congress and Exposition. American Society of Mechanical Engineers Digital Collection, Montreal, Quebec, Canada. 14-20 November, 2014.
58. Li, M.J., Jin, B., Ma, Z. and Yuan, F., 2018. Experimental and numerical study on the performance of a new high-temperature packed bed thermal energy storage system with macro-encapsulation of molten salt phase-change material. *Applied Energy*, *221*, 1-15.
59. Ma, F. and Zhang, P., 2017. Investigation on the performance of a high-temperature packed bed latent heat thermal energy storage system using Al-Si alloy. *Energy Conversion and Management 150*, 500-514.
60. Peng, H., Dong, H. and Ling, X., 2014. Thermal investigation of PCM-based high temperature thermal energy storage in packed bed. *Energy Conversion and Management 81*, 420-427.
61. Aldoss, T.K. and Rahman, M.M., 2014. Comparison between the single-PCM and multi-PCM thermal energy storage design. *Energy Conversion and Management 83*, 79-87.
62. Ezra, M., Kozak, Y., Dubovsky, V. and Ziskind, G., 2016. Analysis and optimization of melting temperature span for a multiple-PCM latent heat thermal energy storage unit. *Applied Thermal Engineering 93*, 315-329.

63. Xu, Y., He, Y.L., Li, Y.Q. and Song, H.J., 2016. Exergy analysis and optimization of charging–discharging processes of latent heat thermal energy storage system with three phase change materials. *Solar Energy 123*, 206-216.
64. Shabgard, H., Robak, C.W., Bergman, T.L. and Faghri, A., 2012. Heat transfer and exergy analysis of cascaded latent heat storage with gravity-assisted heat pipes for concentrating solar power applications. *Solar Energy 86*, 816-830.
65. Wu, M., Xu, C. and He, Y., 2016. Cyclic behaviors of the molten-salt packed bed thermal storage system filled with cascaded phase-change material capsules. *Applied Thermal Engineering 93*, 1061-1073.
66. Cheng, X. and Zhai, X., 2018. Thermal performance analysis and optimization of a cascaded packed bed cool thermal energy storage unit using multiple phase change materials. *Applied Energy 215*, 566-576.
67. Tian, Y. and Zhao, C.Y., 2013. Thermal and exergetic analysis of metal foam-enhanced cascaded thermal energy storage (MF-CTES). *International Journal of Heat and Mass Transfer 58*, 86-96.
68. Peiró, G., Gasia, J., Miró, L. and Cabeza, L.F., 2015. Experimental evaluation at pilot plant scale of multiple PCMs (cascaded) vs. single PCM configuration for thermal energy storage. *Renewable Energy 83*, 729-736.
69. Shamsi, H., Boroushaki, M. and Geraei, H., 2017. Performance evaluation and optimization of encapsulated cascade PCM thermal storage. *Journal of Energy Storage*, *11*, 64-75.
70. Wang, J., Ouyang, Y. and Chen, G., 2001. Experimental study on charging processes of a cylindrical heat storage capsule employing multiple-phase-change materials. *International Journal of Energy Research 25*, 439-447.
71. Fang, M. and Chen, G., 2007. Effects of different multiple PCMs on the performance of a latent thermal energy storage system. *Applied Thermal Engineering 27*, 994-1000.
72. Michels, H. and Pitz-Paal, R., 2007. Cascaded latent heat storage for parabolic trough solar power plants. *Solar Energy 81*, 829-837.
73. John, M.W., Mamidi, T., Subendran, S. and Subramanian, L.G., 2018. Experimental investigation of low-temperature latent heat thermal energy storage system using PCM and NEPCM. In *IOP Conference Series: Materials Science and Engineering* 402, 012197.

74. Jesumathy, S., Udayakumar, M. and Suresh, S., 2012. Experimental study of enhanced heat transfer by addition of CuO nanoparticle. *Heat and Mass Transfer 48*, 965-978.
75. Dhaidan, N.S., Khodadadi, J.M., Al-Hattab, T.A. and Al-Mashat, S.M., 2013. Experimental and numerical investigation of melting of NePCM inside an annular container under a constant heat flux including the effect of eccentricity. *International Journal of Heat and Mass Transfer 67*, 455-468.
76. Xue, H.S., 2016. Experimental investigation of a domestic solar water heater with solar collector coupled phase-change energy storage. *Renewable Energy 86*, 257-261.
77. Mettawee, E.B.S. and Assassa, G.M., 2007. Thermal conductivity enhancement in a latent heat storage system. *Solar Energy 81*, 839-845.
78. Kenisarin, M.M., 2010. High-temperature phase change materials for thermal energy storage. *Renewable and Sustainable Energy Reviews 14*, 955-970.
79. Zhao, C.Y., Ji, Y. and Xu, Z., 2015. Investigation of the Ca (NO3) 2–NaNO3 mixture for latent heat storage. *Solar Energy Materials and Solar Cells 140*, 281-288.
80. Myers Jr, P.D., Alam, T.E., Kamal, R., Goswami, D.Y. and Stefanakos, E., 2016. Nitrate salts doped with CuO nanoparticles for thermal energy storage with improved heat transfer. *Applied Energy 165*, 225-233.
81. Joybari, M.M., Seddegh, S., Wang, X. and Haghighat, F., 2019. Experimental investigation of multiple tube heat transfer enhancement in a vertical cylindrical latent heat thermal energy storage system. *Renewable Energy 140*, 234-244.
82. Kumar, A., Shahi, P. and Saha, S.K., 2018. Experimental Study of Latent Heat Thermal Energy Storage System for Medium Temperature Solar Applications. *In Proceedings of the 4thWorld Congress on Mechanical, Chemical, and Material Engineering (MCM'18*), Madrid, Spain 16 –18 August 2018.
83. Agyenim, F., Eames, P. and Smyth, M., 2010. Heat transfer enhancement in medium temperature thermal energy storage system using a multitube heat transfer array. *Renewable Energy 35*, 198-207.
84. Avci, M. and Yazici, M.Y., 2013. Experimental study of thermal energy storage characteristics of a paraffin in a horizontal tube-in-shell storage unit. *Energy Conversion and Management 73*, 271-277.
85. Mahfuz, M.H., Anisur, M.R., Kibria, M.A., Saidur, R. and Metselaar, I.H.S.C., 2014. Performance investigation of thermal energy storage system with Phase Change Material

(PCM) for solar water heating application. *International Communications in Heat and Mass Transfer 57*, 132-139.

86. Yazıcı, M.Y., Avcı, M., Aydın, O. and Akgun, M., 2014. Effect of eccentricity on melting behavior of paraffin in a horizontal tube-in-shell storage unit: An experimental study. *Solar Energy 101*, 291-298.
87. Kumaresan, G., Velraj, R. and Iniyan, S., 2011. Thermal analysis of d-mannitol for use as phase change material for latent heat storage. *Journal Applied Science 11*, 3044-3048.
88. Solé, A., Neumann, H., Niedermaier, S., Martorell, I., Schossig, P. and Cabeza, L.F., 2014. Stability of sugar alcohols as PCM for thermal energy storage. *Solar Energy Materials and Solar Cells 126*, 125-134.
89. Furbo, S., 1981. Heat storage with an incongruently melting salt hydrate as storage medium based on the extra water principle. In *Thermal Storage of Solar Energy* 135-145 Springer, Dordrecht.
90. Furbo, S., 1980. Investigation of heat storages with salt hydrate as storage medium based on the extra water principle. *NASA Sti/recon Technical Report.*
91. Mosleh, H.J. and Ahmadi, R., 2019. Linear parabolic trough solar power plant assisted with latent thermal energy storage system: A dynamic simulation. *Applied Thermal Engineering 161*, 114204.
92. Wang, Y., Li, S., Zhang, T., Zhang, D. and Ji, H., 2017. Supercooling suppression and thermal behavior improvement of erythritol as phase change material for thermal energy storage. *Solar Energy Materials and Solar Cells 171*, 60-71.
93. Zeng, J.L., Zhou, L., Zhang, Y.F., Sun, S.L., Chen, Y.H., Shu, L., Yu, L.P., Zhu, L., Song, L.B. and Cao, Z., 2017. Effects of some nucleating agents on the supercooling of erythritol to be applied as phase change material. *Journal of Thermal Analysis and Calorimetry 129*, 1291-1299.
94. Amiri, A., Vafai, K. and Kuzay, T.M., 1995. Effects of boundary conditions on non-Darcian heat transfer through porous media and experimental comparisons. *Numerical Heat Transfer, Part A: Applications 27*, 651-664.
95. Mahfuz, M.H., Anisur, M.R., Kibria, M.A., Saidur, R. and Metselaar, I.H.S.C., 2014. Performance investigation of thermal energy storage system with Phase Change Material (PCM) for solar water heating application. *International Communications in Heat and Mass Transfer 57*, 132-139.

96. Chidambaram, L.A., Ramana, A.S., Kamaraj, G. and Velraj, R., 2011. Review of solar cooling methods and thermal storage options. *Renewable and Sustainable Energy Reviews 15*, 3220-3228.

3. EXPERIMENTAL METHOD AND ANALYSES

The experimental method and thermal analyses used in the evaluation of the thermal performances of four latent heat thermal energy storage systems are presented in this chapter for the charging and discharging processes. The first system (a) is a single latent heat storage system comprised of a packed bed of 40 spherical aluminium capsules encapsulated with eutectic solder (Sn63Pb37). The second system (b) is a 2-PCM cascaded latent heat storage system of eutectic solder and erythritol consisting of eutectic solder at the top (20 capsules) and erythritol (20 capsules) at the bottom making a 50 %: 50 % storage ratio. The third system (c) is also a 2-PCM cascaded latent heat thermal energy storage system with 20 eutectic solder capsules at the top, and 20 adipic acid capsules at the bottom in a storage ratio of 50 %: 50 %. The fourth storage system (d), is a 3 PCM cascaded system with 14 eutectic solder capsules at the top, 14 adipic acid capsules at the middle and 14 erythritol capsules at the bottom making a storage ratio of 33 %: 33 %: 33 %.

3.1 Experimental setup and method

The schematic diagram of the experimental set-up is shown in Figure 3.1. The experimental set-up consisted of (a) a vertical cylindrical insulated stainless steel tank with diameter of 0.123 m and a height of 0.54 m. K-type thermocouples were inserted at four axial levels (A, B, C and D) of the storage tank. Each of the four levels had three radial K-type thermocouples (accuracy ± 2.2 ^{o}C) situated at radial distances of 0.013 m, 0.038 m and 0.064 m, respectively [1]. The axial temperature at each axial level (TA, TB, TC, and TD) was obtained as a numerical average of the temperatures of the three radial thermocouples at each level. Another two thermocouples were placed at the inlet and the outlet ports of the storage tank to measure the inlet and outlet temperatures (Tin and Tout) of the TES tank.

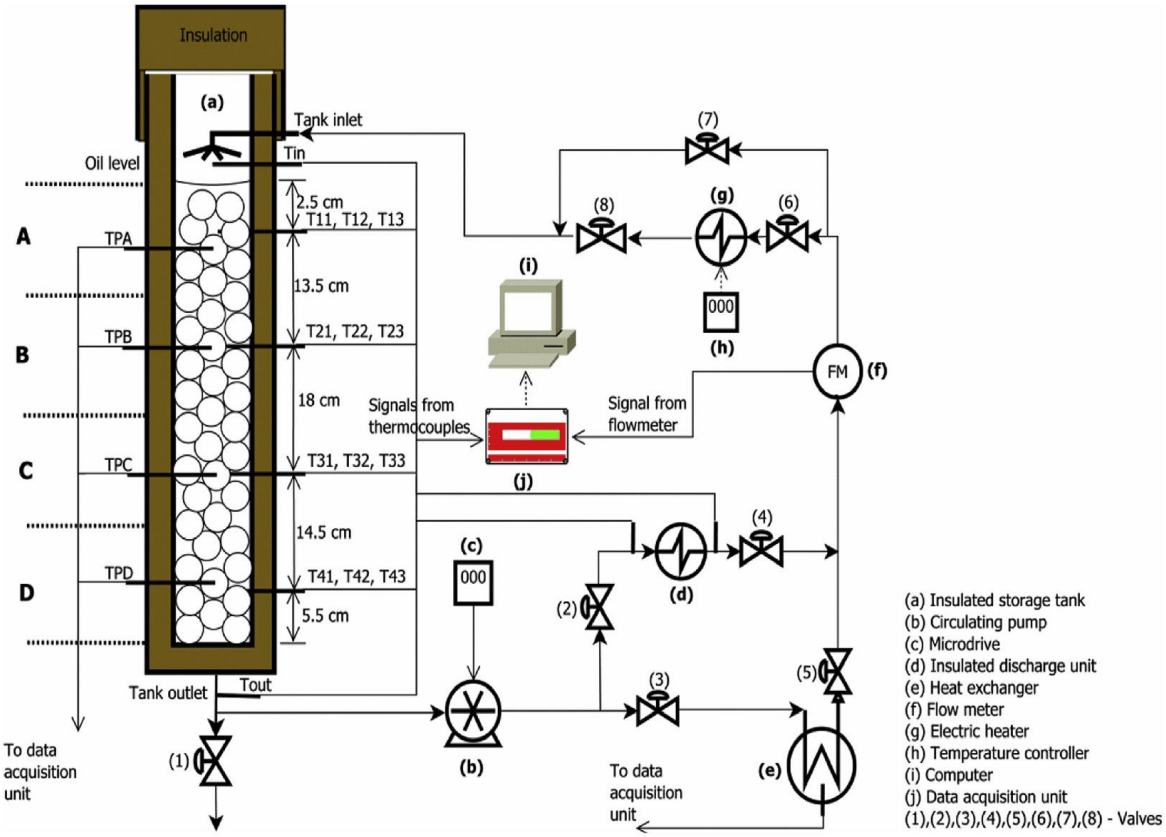

Figure 3.1: *Schematic diagram of the experimental setup [5].*

During the charging cycle, thermal energy was supplied by two electrical heating elements (g) each with a power rating of 900 W. The two electrical heating elements were connected to the TZN4S temperature controller (h) with an accuracy of ± 0.3 %. An oil circulating copper coil was embedded in between the two heating elements, which heated up the oil as it passed through it during charging cycles. From the design of the experimental system, the charging and discharging cycles proceeded from the top to the bottom of the storage tank to limit the cost of the system since only one expensive circulating pump was utilized. The experimental system consisted of several control valves for controlling the fluid flow during charging and discharging cycles. During the charging cycles, valves (1), (2), (4) and (7) were closed, while valves (3) (5) (6) and (8) were opened to circulate the fluid through the electrical heating elements. During discharging cycles, valves (1), (3), (5), (6) and (8) were closed, while valves (2), (4) and (7) were opened.

Before the commencement of the charging process, it was ensured that the inlet temperature, the outlet temperature and all the axial level temperatures were close to the

ambient temperature of around 20 ^{o}C. However, in some cases the temperatures were lower than 20 ^{o}C thus slight pre-heating to make the temperatures close to 20 ^{o}C was required. It is also important to note that exact initial temperatures of 20 ^{o}C were not possible, and a range of ± 2 ^{o}C was deemed to be acceptable. On the other-hand, when the storage temperatures were higher than the ambient temperature as a result of accumulated heat in the storage tank after charging, the oil was circulated through the discharging loop to discharge the accumulated energy to attain temperatures close to the ambient experimental conditions. The experimental charging experiments were carried out firstly with three different charging flow rates of 4 ml/s, 6 ml/s and 8 ml/s, respectively, using a set heater charging temperature of 280 ^{o}C. Experiments with three different set charging temperatures of 260 ^{o}C, 280 ^{o}C and 300 ^{o}C were also carried out using the same charging flow rate of 6 ml/s. The maximum set heater charging temperature for every experiment and the required flow rate were set at the beginning of each of the charging experiment using the TZN4S temperature controller(h) and the VLT micro drive (c), respectively. The charging termination time in each experiment was determined by the bottom average axial temperature (TD) obtained from the average of the temperature of the three radial thermocouples (TD1, TD2 and TD3) at the bottom (D- level) of the TES system. The bottom limiting charging temperature was 180 ^{o}C for the three cascaded PCM TES systems as this ensured that the all the bottom level PCM capsules had melted. Erythritol has a melting temperature of around 120 ^{o}C, while adipic acid has a melting temperature of around 150 ^{o}C, and this bottom charging temperature ensured that these two PCMs were going to melt. However, in the case of the eutectic solder packed bed system, the termination time was determined when TD was around 190 ^{o}C due to its higher melting temperature of around 183 ^{o}C. This bottom limiting temperature ensured that eutectic solder capsules at the bottom of the storage tank melted.

A positive displacement oil circulating pump (GPA series, Green-pumps, Padova, Italy) (b) with a frequency controlled by a VLT micro-drive (c) (maximum error of 0.8 % of the full scale reading) was used to circulate sunflower oil through the desired flow lines during the charging and discharging processes. A Macnaught series MISSP pulsed type of positive displacement flow-meter (f) (accuracy ± 1 %) [2] was used to measure the flow rate of the heat transfer fluid as it circulated in the charging and discharging loops. All the measured temperatures and flow rate were collected in 10 s intervals using an Agilent 34970 A data acquisition unit (j)

(accuracy ± 0.1 ^{o}C) [3] which was connected to a personal computer which recorded the data and saved it as comma separated values (CSV) excel files. The personal computer was also used to visualize the charging and discharging processes. Figure 3.2 shows the photograph of the main components of the experimental set-up which include the TES tank, discharging tank, oil circulating pump, data-logger, electrical heater, flow-meter and the computer [4].

Figure 3.2: *Photograph of the experimental setup [4].*

The discharging process was carried out immediately after the charging process. Before discharging commenced, the two electrical heating elements were switched off and sunflower oil was circulated through the discharging unit at a set flow rate with the help of the discharging valves (2), (4) and (7) as shown in Figure 3.1. The discharging unit was comprised of a copper coil heat exchanger immersed inside a 5 litre water bath. K-type of thermocouples were used to monitor the discharging inlet temperature ($T_{dischin}$), the

discharging outlet temperature ($T_{dischout}$) and the water bath temperature (T_w). As the hot oil passed through the discharging unit, the thermal energy from the circulating oil was transferred to the water bath through the walls of the heat exchanger water making the water temperature to rise. The discharging cycles were terminated when the $T_{dischin}$, $T_{dischout}$ and T_w were approximately equal. At the point of termination, the temperature differences between the TES temperatures and the discharging unit temperatures (T_W, $T_{dischin}$ and $T_{dischout}$) were small. The hot oil was discharged from the top to the bottom as in the charging case since one pump was used to limit the cost of the experimental system. The high temperature pump costs around R 40,000 (USD 2,500), and it was deemed not economical to operate two pumps due to budget constraints. The discharging processes were carried with three discharging flow rates of 4 ml/s, 6 ml/s and 8 ml/s respectively, immediately after charging with different set heater temperatures (260 ^oC, 280 ^oC and 300 ^oC) and different charging flow rates.

3.1.1 Encapsulation of PCM spherical capsules and thermophysical properties

Hollow spherical aluminum capsules with diameters of 0.05 m and wall thicknesses of 0.001 m were filled with adipic acid, erythritol and eutectic solder. About 80 % of the total internal volume of each capsule was filled with PCM leaving an allowance of 20 % for thermal expansion. Most of the capsules were closed and sealed with screw caps, and a few with thermocouple screw caps (to measure the PCM temperature) after pouring the PCMs as shown in Figure 3.3. The volume to be poured into the capsule was estimated by the mass of PCM inside each capsule for the three PCMs. It was ensured that the mass for a particular PCM type was almost constant in each individual capsule.

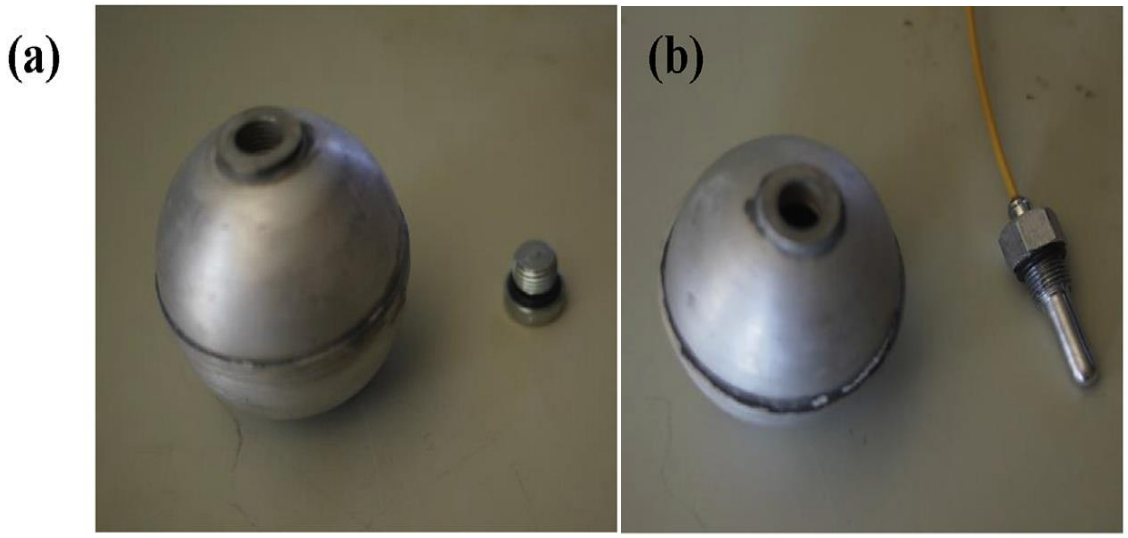

Figure 3.3: *(a) Aluminium PCM capsule with a screw cap, (b) aluminium PCM capsule with a thermocouple screw cap [5].*

The crystal sizes for adipic acid and erythritol were ~~t~~oo small to enable easy pouring of the PCMs even in their solid form. 20 aluminum capsules of each adipic acid and erythritol were filled to 80 % on their internal volume and their masses were carefully measured with an electronic balance. However, the process involved in the encapsulating of eutectic solder was different and more difficult as compared to adipic acid and erythritol due to its physical nature. 2 mm thick solder wire was inserted into 40 capsules from the top opening until an internal volume 80% was covered. The volume of the PCM wire in the capsules was also about 80 % of the total internal volume of the capsule to allow for thermal expansion. A screw driver was used to press down on the solder wire to ensure that the solder occupied the maximum volume. Care was also taken to ensure that all 40 capsules had approximately the same mass of solder inside them. All the 60 PCM capsules were heated up to their melting point in an oil bath to ensure that there were no PCM leakages before they were put into the storage tank. The photographs of the PCMs used for this study are shown in Figure 3.4.

(a) (b) (c)

Figure 3.4: *Photographs showing (a) adipic acid, (b)erythritol and (c) eutectic solder used as PCMs in the spherical aluminium capsules [6].*

Table 3.1 shows the thermophysical properties of erythritol, adipic acid and the eutectic solder. The values shown in Table 3.1 were not obtained experimentally but from open recent literature because of the high cost of the laboratory equipment used for the experimental measurements of the thermal properties. With regards to the scope of this experimental work, it was deemed unnecessary to perform practical thermal properties measurements since the bulk performance of the TES systems was the main aim of the research. Although the same volume was maintained for all the three PCMs, the masses of the encapsulated PCMs were different due to their different densities. Eutectic solder with the highest density shows the highest mass, while erythritol and adipic have comparable masses. Eutectic solder also shows the highest thermal conductivity while adipic acid and erythritol show comparable thermal conductivities. Adipic acid shows the highest phase change enthalpy while the eutectic solder shows the least. Although quite a number of experimental studies have been reported on cascaded LHTES systems, no study has been done using the mentioned PCMs in a cascaded packed bed system.

Table 3.1: *The thermophysical properties of the three PCMs.*

Properties	Adipic acid	Erythritol	Eutectic solder (Sn63Pb37)
Melting temperature (^oC)	150-152 [7]	118-122 [5]	183 [12]
Specific heat capacity (kJ/kg)	1.59(20^oC), 2.26(150^oC) [8]	1.38(20^oC), 2.76(140 ^oC) [5]	0.21 (30 ^oC) [12]
Phase change Enthalpy (kJ/kg)	213-260 [7]	139.7 [5]	52.1 [13-14]
Density (kg/m^3)	1360(20^oC), 1093(163 ^oC) [8]	1210 [5]	8400 [11]
Thermal conductivity (W/mK)	0.142-0.162 [8]	0.130(120^oC) [5]	50 [11]
Average mass of the PCM in the capsules (g)	40	44	164

3.1.2 Single PCM packed bed latent heat storage system

The single PCM TES system (TES system (a)) was made-up of forty capsules of encapsulated eutectic solder packed randomly into the storage tank up to the top level of the storage tank (TA) as shown in Figure 3.5. Four PCM capsules with thermocouple capsules shown in red in Figure 3.5 were placed at four axial levels (TA, TB, TC, TD) to measure the PCM temperature. Sunflower oil was poured up to Level A to fill in the void fraction of the storage tank. The void fraction of the storage tank was estimated to be around 0.49 as reported in [5].

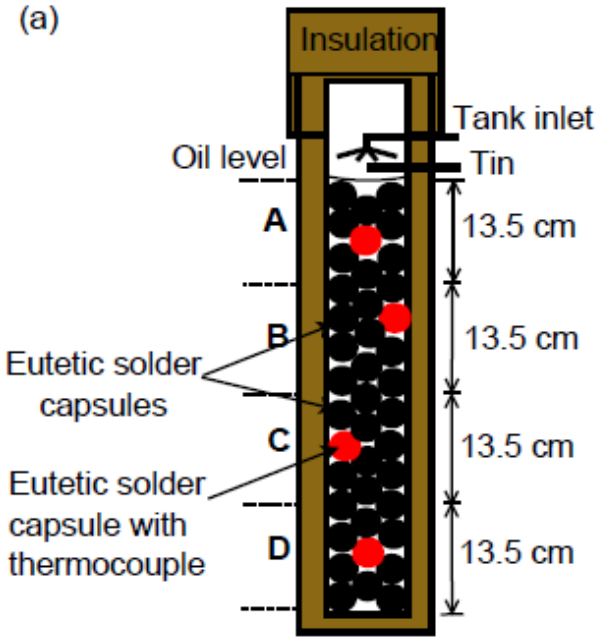

Figure 3.5: *The schematic diagram of storage system (a) which was the single PCM TES system. It shows forty PCM capsules in the storage tank with four capsules having thermocouples (red).*

3.1.3 Cascaded latent heat storage system 1

Figure 3.6 presents a 2-stage cascaded LHTES (TES system (b)) system of twenty capsules of eutectic solder (black) at the top and twenty capsules of erythritol (brown) at the bottom. The PCM temperatures are monitored with four PCM capsules shown in red and green colours placed at the four axial levels of the TES tank. Two red capsules with thermocouples are used to monitor the PCM temperature at the two top axial levels (level A and level B), while the two green capsules with thermocouples are used to monitor the PCM temperature at levels C and D. Sunflower oil was also used to fill up the void fraction of the storage tank as with single PCM case.

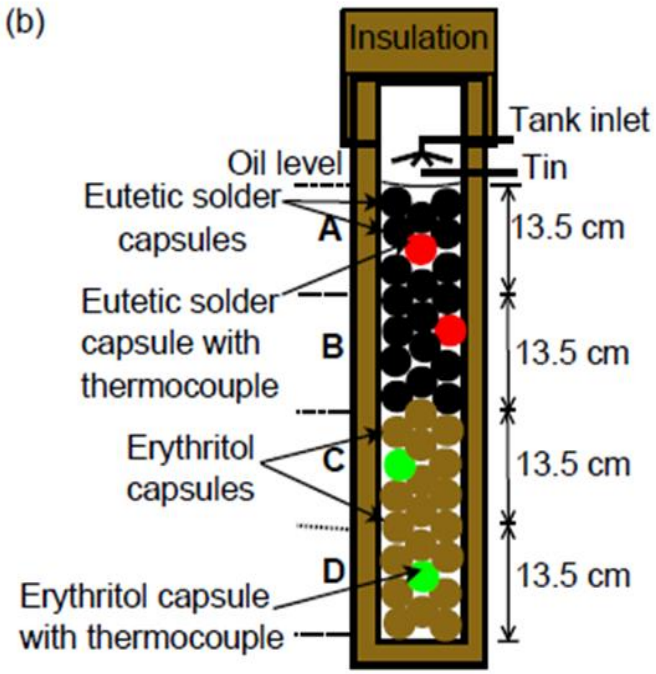

Figure 3.6: *The schematic diagram of storage system (b) which was a 2-PCM cascaded TES system. It shows twenty eutectic solder PCM capsules at the top and twenty erythritol PCM capsules at the bottom of the storage tank with four capsules having thermocouples (red and green).*

3.1.4 Cascaded latent heat storage system 2

Figure 3.7 shows cascaded system 2 (TES system (c)) which is also a 2-stage cascaded LHTES system consisting of twenty eutectic solder capsules at the top (black) and twenty adipic acid capsules at the bottom (white). The PCM temperatures at the four axial levels (A, B, C, D) of the storage tank are also monitored using the two red capsules with thermocouples (eutectic solder). and two blue capsules (erythritol) with thermocouples. The tank was also filled with up sunflower oil in a similar manner to TES system (a) and system (b).

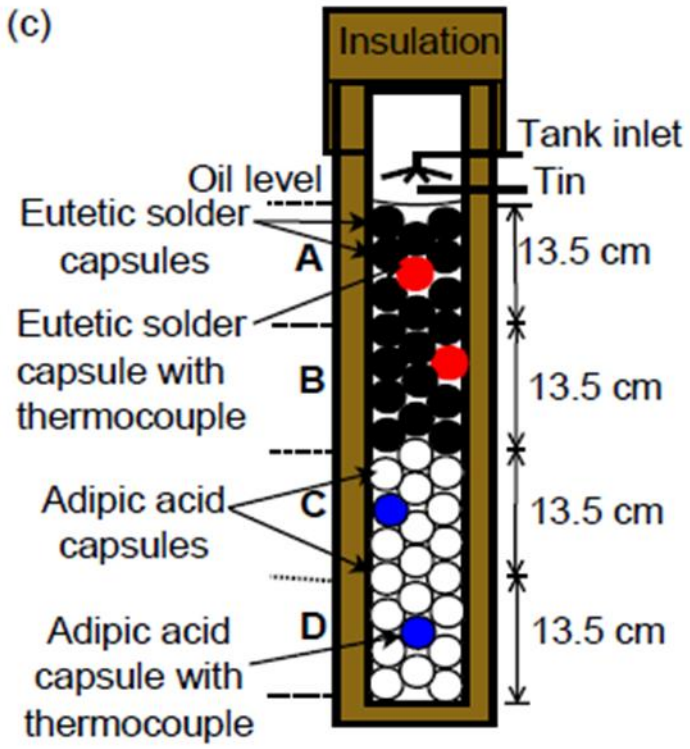

***Figure 3.7**: The schematic diagram of storage system (c) which was a 2- PCM cascaded TES system. It shows twenty eutectic solder PCM capsules at the top and twenty adipic acid PCM capsules at the bottom of the storage tank with four capsules having thermocouples (red and blue).*

3.1.5 Cascaded latent heat storage system 3

A 3 PCM cascaded system (TES system (d)) of eutectic solder, adipic acid and erythritol capsules is shown in Figure 3.7. This system consists of fourteen capsules of eutectic solder at the top (black), fourteen capsules of adipic acid in the middle (white) and fourteen capsules of erythritol-at the bottom (brown). Two PCM capsules of each type with thermocouples monitor the PCM temperatures in the storage tank (red, blue and green). The void fraction is also similar to three other systems and sunflower oil fills up the void fraction in the storage tank.

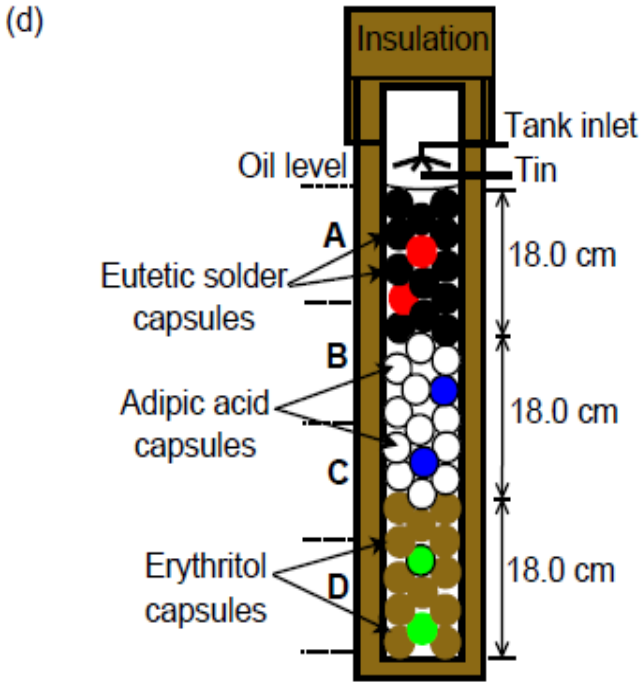

***Figure 3.8**: The schematic diagram of storage system (d) which was a 3-PCM cascaded TES system. It shows fourteen eutectic solder PCM capsules at the top, fourteen adipic acid PCM capsules at the middle and fourteen erythritol PCM capsules at the bottom of the storage tank with six capsules having thermocouples (red, blue and green).*

3.2 Experimental thermal analysis

The temperature difference between the charging inlet and the charging outlet temperatures $(T_{chin} - T_{disout})$ of the storage tank determines the charging energy rate value, and it is expressed as;

$$\dot{E_{ch}} = \rho_{av} C_{av} \dot{V}_{ch} (T_{chin} - T_{chout}) \quad (3.1)$$

,where ρ_{av} is the temperature dependent average density of the oil, C_{av} is the temperature dependent average specific heat capacity of the oil, $\dot{V}_{ch}$ is the volumetric charging flow rate, T_{chin} is the inlet charging temperature at the top of the storage tank and T_{chout} is the outlet charging temperature at the bottom of the storage tank. The total thermal energy stored (E_{ST}) in the storage tank during charging cycles was estimated by integrating from the start of charging (t_{ini}) to the end of the charging (t_f) for each small temperature measurement interval, and this can be expressed as [14-15];

$$E_{ST} = \int_{t_{ini}}^{t_f} \rho_{av} C_{av} \dot{V}_{ch} (T_{chin} - T_{chout}) dt. \quad (3.2)$$

The charging exergy rate can be expressed as [15];

$$E_{xch} = \rho_{av} C_{av} \dot{V_{ch}} \left[(T_{chin} - T_{hout}) - T_{amb} ln \left(\frac{T_{chin}}{T_{chout}} \right) \right] \quad (3.3)$$

, where T_{amb} is the ambient temperature. The total charging exergy is also evaluated by integrating and it is expressed as;

$$E_{XCH} = \int_{t_{ini}}^{t_f} \rho_{av} C_{av} \dot{V_{ch}} \left[(T_{chin} - T_{chout}) - T_{amb} ln \left(\frac{T_{chin}}{T_{chout}} \right) \right] dt. \quad (3.4)$$

The discharging energy rate can be expressed as;

$$E_{dis} = \rho_{av} C_{av} \dot{V}_{dis} (T_{disin} - T_{disout}) \quad (3.5)$$

,where $\dot{V}_{dis}$ is the discharging volumetric flow rate, T_{disin} is the discharging inlet temperature from the storage tank to the discharging coil and T_{disout} is the discharging outlet temperature from discharging coil to the storage tank. The total energy discharged from the stored tank can be estimated by integrating Eq. (3.5) from the start of discharging to the end of discharging for each small temperature measurement interval and this can be expressed as;

$$E_{DIST} = \int_{t_{ini}}^{t_f} \rho_{av} C_{av} \dot{V_{dis}} (T_{disin} - T_{disout}) dt. \quad (3.6)$$

The discharging exergy rate is expressed as;

$$\dot{E}_{xdis} = \rho_{av} C_{av} \dot{V_{dis}} \left[(T_{disin} - T_{disout}) - T_{amb} ln \left(\frac{T_{disin}}{T_{disout}} \right) \right] \quad (3.7)$$

, and it can be integrated to give the total exergy discharged as;

$$E_{XDIST} = \int_{t_{ini}}^{t_f} \rho_{av} C_{av} \dot{V_{dis}} \left[(T_{disin} - T_{disout}) - T_{amb} ln \left(\frac{T_{disin}}{T_{disout}} \right) \right] dt. \quad (3.8)$$

The overall energy efficiency can be expressed by the ratio of the total energy discharged to the total energy stored and this is expressed as [16-17];

$$\eta_e = \frac{E_{DIST}}{E_{ST}}. \quad (3.9)$$

The overall exergy efficiency can also be expressed as the ratio of the total exergy discharged to the total charging exergy and this is given as;[18-19]

$$\eta_{ex} = \frac{E_{XDIST}}{E_{XCHT}}. \quad (3.10)$$

The variation of the density and the specific heat capacity of sunflower oil with temperature is given [4, 16,17] as;

$$\rho_S = 930.62 - 0.65T \tag{3.11}$$

, and

$$C_S = 2115.0 + 3.13T. \tag{3.12}$$

3.3 Experimental uncertainty

The uncertainty in the temperature measurements was estimated to be ±2 °C from the accuracy of the thermocouples. For the flow meter, the uncertainty in the flow rate was estimated to be ±1 % of the measured value as determined from the accuracy of the flow meter [2]. The values of the uncertainties in the average density and the average specific heat capacity were $\partial\rho_{av}$ = ± 0.069 g/cm^3 and ∂C_{av} = ± 0.021 J/gK as obtained from previous related work [18, 19].

Experimental uncertainties in the calculated quantities (energy/exergy charging/discharging rates as well as energy/exergy storage efficiencies) were determined as reported in [18, 19]. As an example, for the energy charging rate the uncertainty is given as;

$$\partial \dot{E}_{ch} = \sqrt{\left(\frac{\partial \dot{E}_{ch}}{\partial \rho_{av}}\right)^2 + \left(\frac{\partial \dot{E}_{ch}}{\partial C_{av}}\right)^2 (\partial C_{av})^2 + \left(\frac{\partial \dot{E}_{ch}}{\partial \dot{V}_{av}}\right)^2 (\partial \dot{V}_{av})^2 + \left(\frac{\partial \dot{E}_{ch}}{\partial T_{out}}\right)^2 (\partial T_{out})^2 + \left(\frac{\partial \dot{E}_{ch}}{\partial T_{in}}\right)^2 (\partial T_{in})^2}. \tag{3.13}$$

The same procedure was repeated for the other calculated values. The range of the percentage uncertainties varied between 1–5 % of the calculated values and this was deemed to be acceptable in the experiments.

3.4 Summary of the chapter

In this chapter, the experimental method and setup were presented. The thermophysical properties of the PCMs used were also presented including the encapsulation method of the PCMs. The different TES configurations were also presented and thermal analyses to evaluate the performance of these TES configurations.

3.5 References

1. Stephenson, D.A., 1993. Tool-work thermocouple temperature measurements—theory and implementation issues. *Journal of Engineering for Industry 115*, 432-437.
2. Website 3: Macnaught Flow-meter Datasheet. Available at http://www.macnaught .com.au/, accessed August 2011.
3. Website 2: HP 34970A Datasheet. Available at http://cp.literature.agilent.com/litweb /pdf/34970-90002.pdf, accessed August 2011.
4. Lugolole, R., Mawire, A., Lentswe, K.A., Okello, D. and Nyeinga, K., 2018. Thermal performance comparison of three sensible heat thermal energy storage systems during charging cycles. *Sustainable Energy Technologies and Assessments 30*, 37-51.
5. Mawire, A., Ekwomadu, C.S., Lefenya, T.M. and Shobo, A., 2020. Performance comparison of two metallic eutectic solder based medium-temperature domestic thermal energy storage systems. *Energy*, 116828.
6. Ekwomadu C.S., Mawire A., Lefenya T.M., Shobo A.B., 2019. Comparison of the Thermal Behaviour of two Eutectic Solder Cascaded Latent Heat Thermal Energy Storage during charging. In *Proceedings of the* 6th Southern African Solar Energy Conference, (SASEC 2019), East London, South Africa, 25-27 November, 2019.
7. Seki, Y., Inca, Ş., Ezan, M.A., Turgut, A. and Erek, A., 2015. Graphite nanoplates loading into eutectic mixture of adipic acid and sebacic acid as phase change material. *Solar Energy Materials and Solar Cells 140*, 457-463.
8. Chemistry Dashboard. Available at https://comptox.epa.gov/dashboard/dsstoxdb/ results ?search =Adipic+acid2%2C2%2C5%2C5-d4, accessed March 2018.
9. Wu YK, Lin KL, Salam B., 2009. Specific heat capacities of Sn-Zn-Based solders measured using differential scanning calorimetry. *Journal of Electronic Materials* 38, 227-230.
10. Höhlein, S., König-Haagen, A. and Brüggemann, D., 2017. Thermophysical characterization of $MgCl_2 \cdot 6H_2O$, xylitol and erythritol as phase change materials (PCM) for latent heat thermal energy storage (LHTES). *Materials 10*, 444.
11. Hart, M.B. and Young, R.C., Topline Corp, 2015. Disposable apparatus for aligning and dispensing solder columns in an array. U.S. Patent 9,108,262.

12. Morando, C., Fornaro, O., Garbellini, O. and Palacio, H., 2014. Thermal properties of Sn-based solder alloys. *Journal of Materials Science: Materials in Electronics 25*, 3440-3447.

13. Technical Data Sheet 2018 of Sn63Pb37 RA Solder Wire4880–4888. Available at https://images-na.ssl-images-amazon.com/images/I/81h+ZhgF19L.pdf, accessed June 2018.

14. Alam, T.E., 2015. Experimental investigation of encapsulated phase change materials for thermal energy storage. PhD thesis*,* University of South Florida, Florida.

15. Jegadheeswaran, S., Pohekar, S.D. and Kousksou, T., 2010. Exergy based performance evaluation of latent heat thermal storage system: a review. *Renewable and Sustainable Energy Reviews 14*, 2580-2595.

16. Mawire, A., Phori, A. and Taole, S., 2014. Performance comparison of thermal energy storage oils for solar cookers during charging. *Applied Thermal Engineering 73*, 1323-1331.

17. Mawire, A., 2016. Performance of Sunflower Oil as a sensible heat storage medium for domestic applications. *Journal of Energy Storage 5*, 1-9.

18. Mawire, A., 2018. Experimental energy and exergy analyses of a discharging heat exchanger for a small hot-oil domestic storage tank. *International Journal of Green Energy 15*, 305-313.

19. Mawire, A. and Taole, S.H., 2014. Experimental energy and exergy performance of a solar receiver for a domestic parabolic dish concentrator for teaching purposes. *Energy for Sustainable Development 19*, 162-169.

4 RESULTS AND DISCUSSION

This chapter presents results obtained from the experimental tests of the four latent heat thermal energy storage systems carried out under South African weather conditions in the North-West province. The evaluation of the performances of the four TES systems is done in this chapter.

4.1 Charging results

This section presents the profiles of the charging temperature, energy rates and exergy rates of the four LHTES systems charged with different set heater temperatures and diffrernt flow rates. The first set of the experiments investigated the effect of the flow rate. Three different flow rates (4ml/s, 6 ml/s and 8 ml/s) were used at a constant set heater charging temperature of 280 ^{o}C . The second set of experiments investigated the effect of the charging temperature on thermal performance and three different set charging heater temperatures (260 ^{o}C, 280 ^{o}C, and 300 ^{o}C) were used with the same constant flow rate of 6 ml/s. To ensure repeatability, the first the first four tests were done twice.

4.1.1 Effect of the flow rate

The effect of the flow rate on the profiles of the charging temperature, energy rate and exergy rate of the four storage systems are presented in this section. The flow rates used in the experiments were 4 ml/s, 6 ml/s and 8 ml/s, respectively , using the same set heater charging temperature of 280 ^{o}C.

4.1.1.1 Profiles of charging temperatures

Figure 4.1 shows average charging fluid temperature profiles for four storage systems with a low charging flow rate of 4 ml/s.

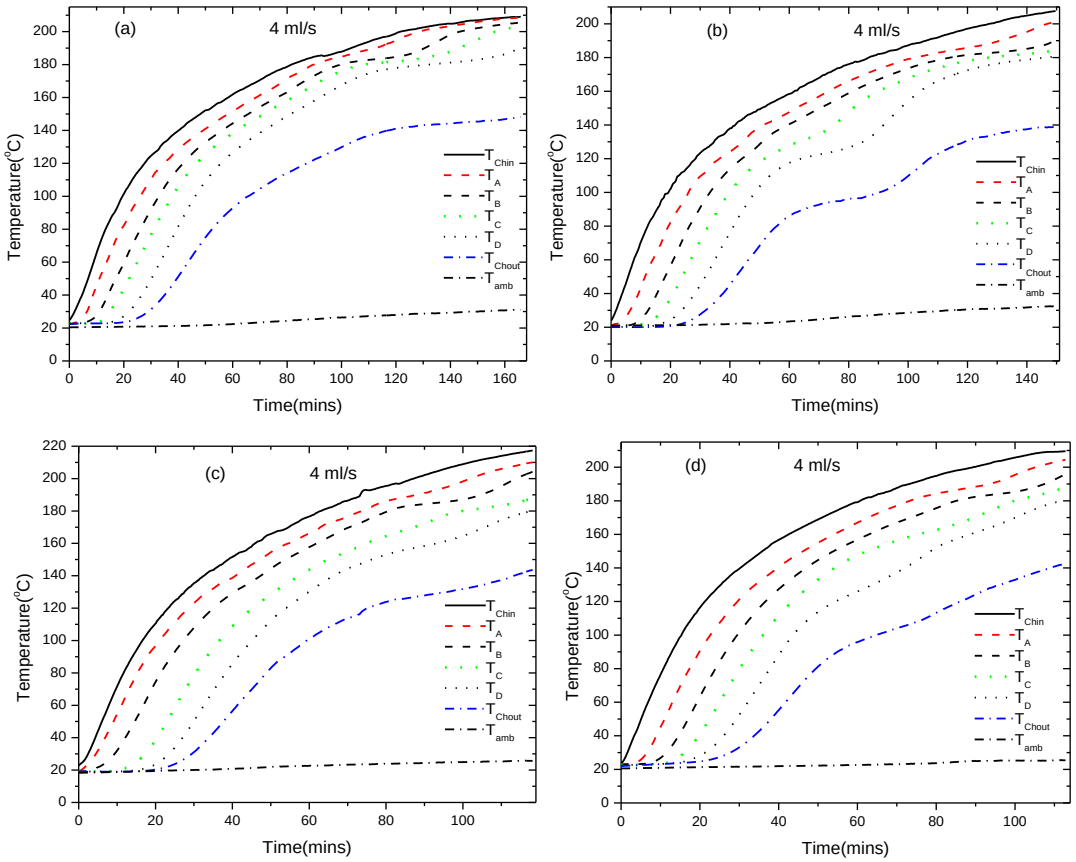

Figure 4.1: *Average charging temperature profiles at a heater set temperature of 280 °C using a low flow rate of 4 ml/s for (a) the single PCM system, (b) cascaded system 1, (c) cascaded system 2 and (d) cascaded system 3.*

The figure shows plots of the single PCM system composed of 40 eutectic solder (Sn63/Pb37) capsules, cascaded system 1, cascaded system 2 and cascaded system 3. Cascaded system 1 comprises of 20 eutectic solder PCM capsules at the top and 20 erythritol PCM capsules at the bottom. Cascaded system 2 consists of 20 eutectic solder PCM capsules at the top and 20 adipic acid PCM capsules at the bottom. Cascaded system 3 consists three PCM capsule layers of eutectic solder at the top (14 capsules), adipic acid in the middle (14 capsules) and erythritol at the bottom (14 capsules). In Figure 4.1, T_{Chin} is the charging inlet temperature at the top of the storage tank, T_A to T_D are the average temperatures at the four different levels of the storage tank (taken from the top to the bottom), T_{Chout} is the outlet charging temperature at the bottom of the storage tank and T_{amb} is the ambient surrounding temperature. For the cascaded storage systems, the charging experiments are terminated when T_D, the bottom storage temperature is around 180 °C as a precaution to ensure that the flash point of adipic acid which is 196 °C [1], is not exceeded. For the single PCM system, the

charging experiments are terminated when T_D is 190 ^oC to ensure that the bottom layer PCM (T_D) melts since the melting temperature of the eutectic solder is around 183 ^oC [2].

The single PCM system shows the longest charging time of around 170 mins possibly due to the larger thermal mass of metallic PCMs in the storage tank, and the slightly higher charging termination temperature. The temperature rise at the top of the storage for the single PCM is also slower as compared to the cascaded systems possibly due to larger thermal mass. Cascaded system 1 with erythritol capsules at the bottom shows a charging time slower than the other cascaded systems, possibly due to the lower melting temperature of erythritol which is 120 ^oC. The phase change process at the bottom thus occurs earlier and for a longer duration as compared to the other cascaded systems making the bottom limiting temperature to be approached later. The phase change process at the bottom for cascaded system 1 occurs for a longer time as compared to the other cascaded systems. Another possible reason for the longer charging time for cascaded system 1 is the lower thermal conductivity of erythritol in the liquid phase as compared to adipic acid which slows down heat transfer in the liquid phase such that the two cascaded systems with adipic acid have faster temperature rises after the phase change processes [3-4].

The charging time for cascaded system 1 is comparable to that of single PCM system, whereas the charging times of cascaded system 2 and cascaded system 3 with adipic acid are considerably shorter and comparable. Cascaded system 3, the three PCM system charges up in the shortest duration of around 112 mins possibly due to the shorter PCM transitions at three different temperatures making the combined thermal mass of the storage tank after all three PCMs have melted lower as compared to the other systems. Heat transfer thus occurs slightly faster for cascaded system 3. This charging time is, however, slightly lower than the charging time of cascaded system 2 which is around 118 mins. It seems the slightly higher thermal conductivity of adipic acid in the liquid phase for cascaded system 2 and cascaded system 3 has an effect on the charging time since the densities of adipic acid and erythritol are very similar [3-4].

In terms of the charging phase change transitions, the single PCM shows phase change transitions which commence from the top to the bottom since charging occurs from the top to the bottom. In contrast to this behaviour, the cascaded systems with lower meting temperature PCMs at the bottom, show phase change transitions that commence from the

bottom lower temperature PCMs to the upper high melting temperature PCMs at the top. The most pronounced phase change transitions at the bottom are seen with cascaded system 1 consisting of eutectic solder and erythritol. This is possibly due to the larger phase change enthalpy of erythritol [3] when compared to the other PCMs. The lowest degree of thermal stratification along the height of the storage tank during the charging process is seen with single PCM system due to the higher axial thermal conductivity of the metallic PCM. The greatest degree of the thermal stratification along the height of the storage tank is seen with cascaded system 3 (3 PCM) possibly due to the three phase change transitions at different temperatures implying that it has the greatest potential of storing thermal energy.

Figure 4.2 shows temperature profiles of the storage tank for the four storage systems using a medium charging flow rate of 6 ml/s. The charging times for all storage systems are longer as compared to the 4 ml/s case. This has also been observed in previous work done on the same storage system [4-5]. The reason of the longer charging time with the higher flow rate is due to the lower inlet temperature attained with the higher flow rate of 6 ml/s. The lower inlet temperature to the storage tank with 6 ml/s is probably a direct result of more pronounced cooling of the electrical heater with this flow rate. This is because the same heating power was used for the two flow rates as measure of ensuring controlled experiments. With an increase of flow rate, the heater was slightly cooled more at the same heating power output resulting in a lower inlet temperature to the storage tank from the outlet of the charging heater. Another possible reason for the longer charging time with an increase in the flow rate is that at a faster flow rate, the interaction time of the oil (HTF) with heating chamber will be shorter compared to the lower flow rate making the inlet temperature to be lower. However, when the flow is slow, the HTF will acquire more heat as compared to the faster flowing HTF thereby making the charging inlet temperature to be higher. The lower inlet charging temperatures for charging with 6 ml/s resulted in the bottom limiting experimental temperatures (190 ^{o}C) to be approached at later times when compared to charging with 4 ml/s. Due to the higher charging flow rate, the degree of thermal stratification along the height of the storage system is lower as compared to the 4 ml/s case for all four storage systems. As with the 4 ml/s case, cascaded system 3 shows a greater degree of thermal stratification along the height of the storage tank possibly due to the number of phase change transitions as compared to the other systems.

Cascaded system 3 also shows the shortest charging time of close to 120 mins due to the combined effect of the low duration phase change transitions, lower combined thermal mass after phase change and the slightly higher thermal conductivity of adipic acid as compared to erythritol. The charging time for cascaded system 2 of around 121 mins is also nearly identical to that of cascaded system 3. The metallic single PCM system with the largest thermal mass shows the longest charging time of around 180 mins. This is comparable to that of cascaded system 1 which is around 176 mins.

In terms of phase change transitions, cascaded system 2 shows the longest phase change duration at the bottom of the storage tank as with the 4 ml/s case. The single PCM system with the higher melting temperature PCMs shows phase change transitions which occur much later as compared to the other systems as with the 4 ml/s case. Its degree of thermal stratification is also lower along the height of the storage tank when compared to the other systems due its higher thermal conductivity. The outlet temperatures for all the storage systems show higher values at the end of charging with 6 ml/s as compared to 4 ml/s due to the higher degree of heat transfer.

The temperature profiles during charging with the highest flow rate of 8 ml/s are shown in Figure 4.3. The highest flow rate induces the highest heat transfer rates such that corresponding temperatures rises in the storage tank are also higher thus increasing heat losses such that the bottom limiting temperatures are approached later as compared to the other two lower flow rates. The metallic solder shows the longest charging time of around 230 mins followed by cascaded system 2 (205 mins) due to the reasons mentioned earlier. The shortest charging duration as with the other cases is seen with cascaded system 3 (125 mins), and this is almost identical to the charging time for cascaded system 2 of around 127 mins

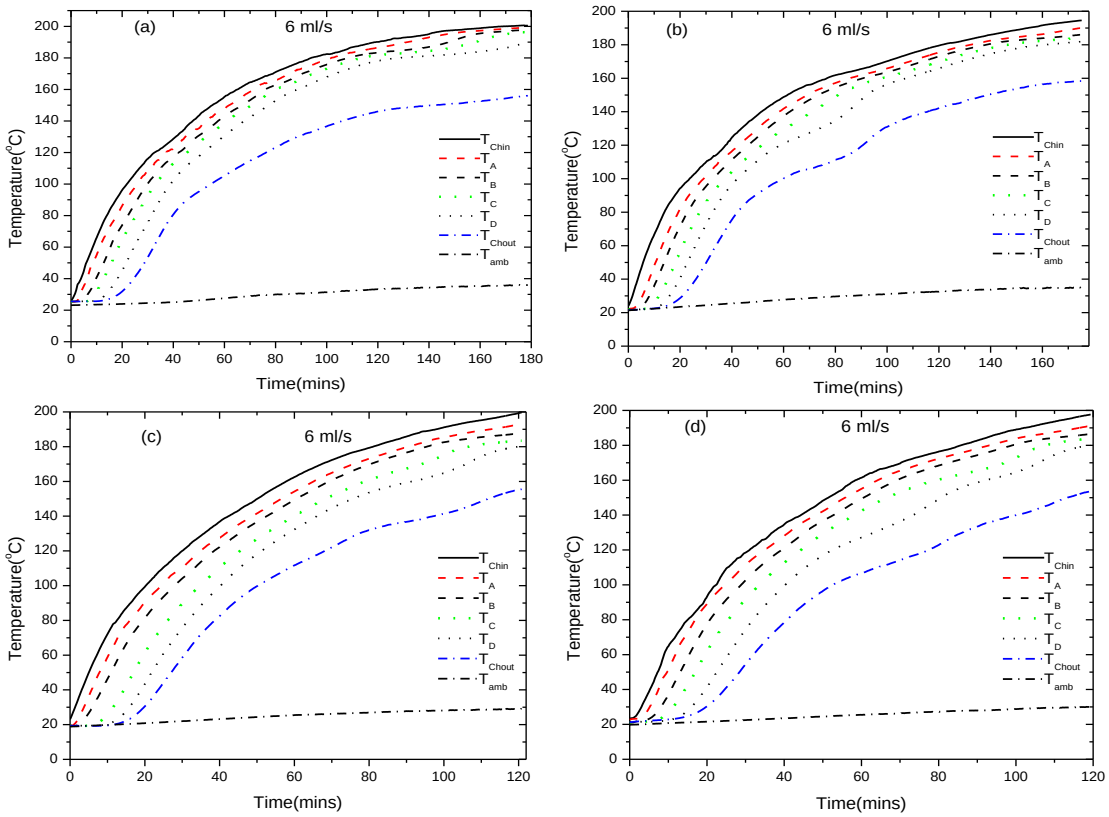

Figure 4.2: *Average charging temperature profiles at a heater set temperature of 280 °C using a medium flow rate of 6 ml/s for (a) the single PCM system, (b) cascaded system 1, (c) cascaded system 2 and (d) cascaded system 3.*

The degree of thermal stratification along the height of the storage tank with this flow rate is lower for all the four storage tanks as compared to the other flow rates. This is due to the higher heat transfer rates which lower the thermal axial thermal gradients for all the systems. The single PCM system shows the lowest thermal gradient at the end of the charging process and higher TES temperatures. Cascaded system 3 as with the other flow rates, shows the greatest degree of thermal stratification and its outlet temperature is slightly lower at the end of charging as compared to the other storage systems. The charging outlet temperatures show higher values at the end of charging for this flow rate as compared to the other lower flow rate possibly due to the higher heat transfer rates. The phase change transition duration periods are comparable for the three cascaded systems using this high charging flow rate.

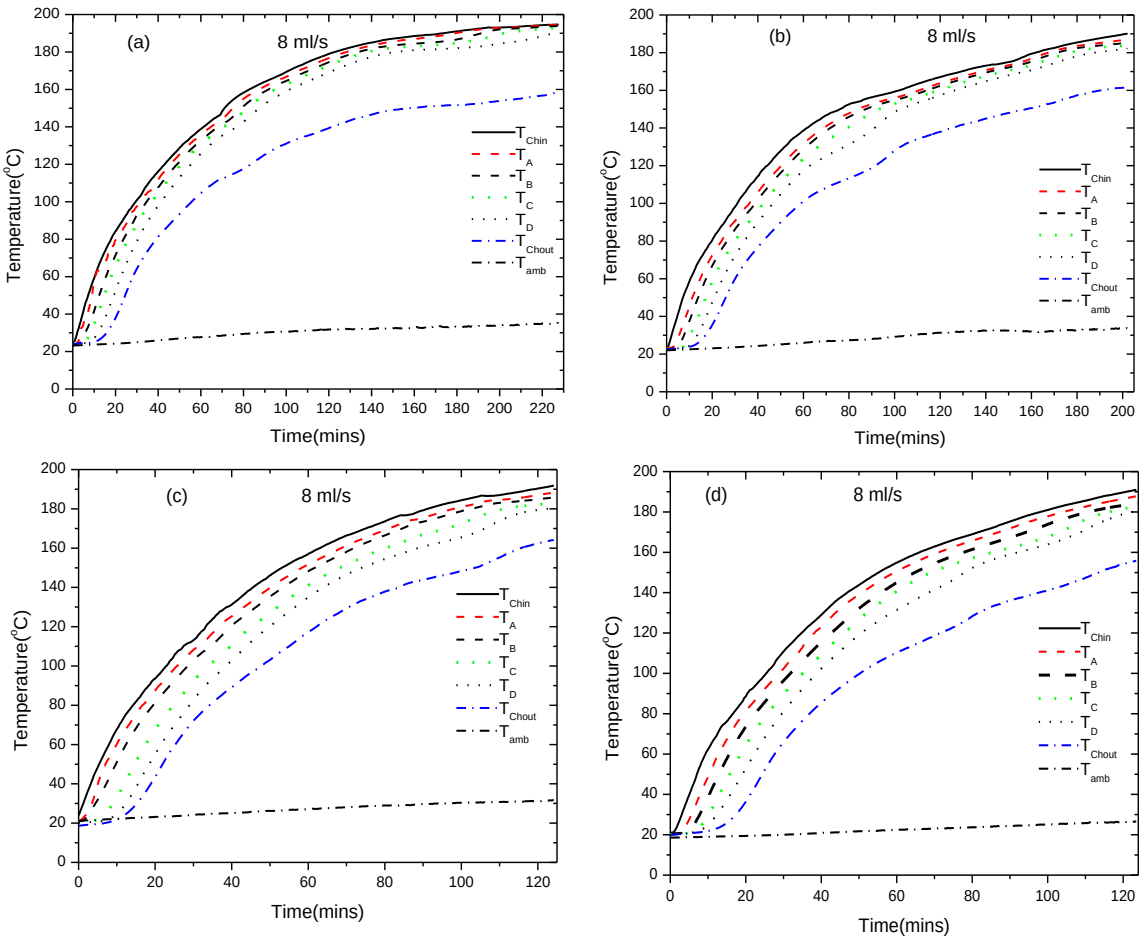

Figure 4.3: *Average charging temperature profiles at a heater set temperature of 280 °C using a high flow rate of 8 ml/s for (a) the single PCM system, (b) cascaded system 1, (c) cascaded system 2 and (d) cascaded system 3.*

4.1.1.2 Charging energy and exergy rates

To quantify the amount of energy storage during the charging processes with different flow rates, energy charging rates are presented in Figure 4.4.

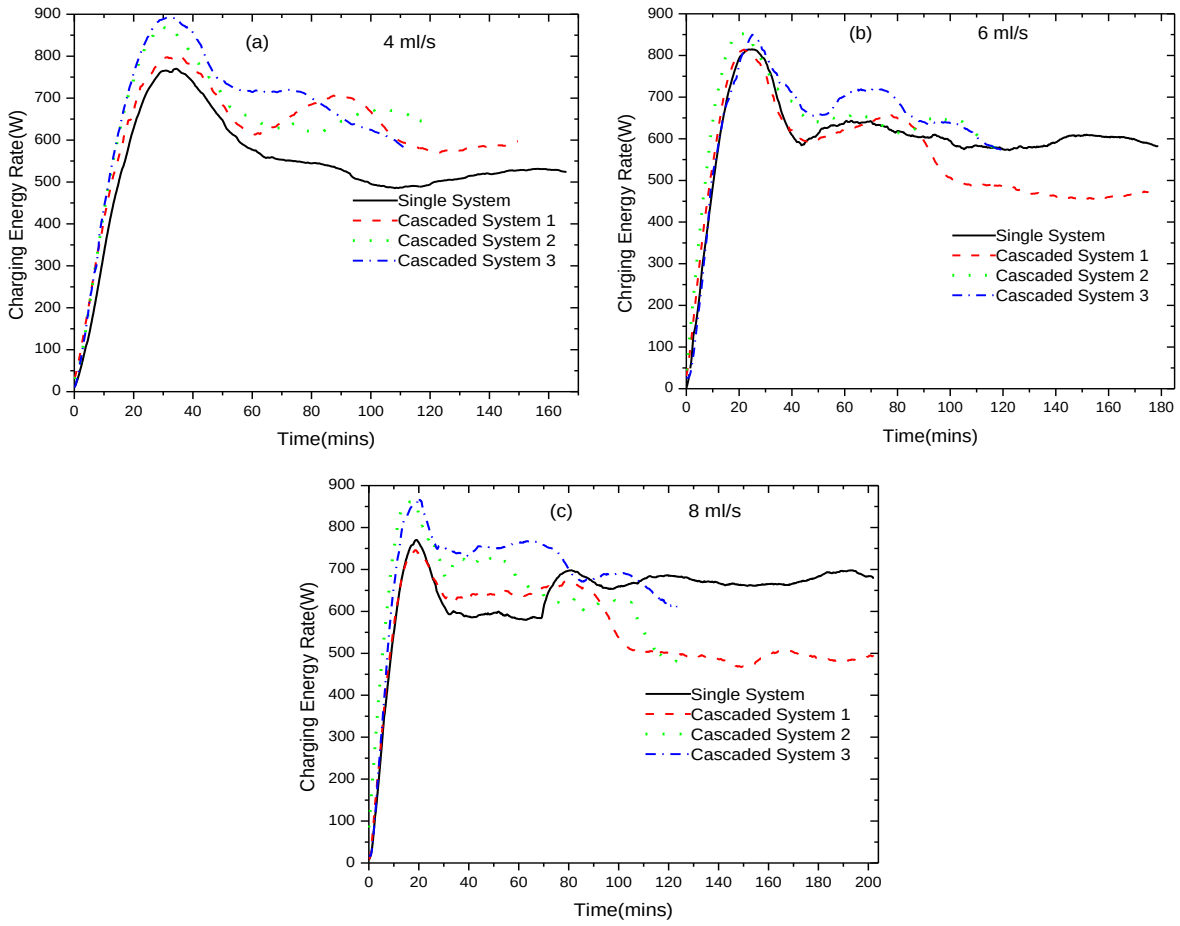

Figure 4.4: *Charging energy rate profiles at (a) low, (b) medium and (c) high flow rates for the four storage systems.*

For the lowest charging flow rate, in Figure 4.4 (plot (a), the energy rate profiles for all storage systems are seen to initially rise to peak values within the first 30 mins of charging as the inlet temperatures rise rapidly when the outlet temperatures are not significantly increasing as depicted in Figure 4.1. Cascaded system 3 with the highest degree of stratification shows the highest peak energy rate value close to 900 W, which is comparable to the peak value of cascaded system 2 which is around 870 W. The single PCM with the largest thermal mass and the least degree of axial thermal stratification shows the least peak value of around 750 W, which is comparable to about 800 W for cascaded system 1. After these initial rises, energy rates drop from the peak values as the outlet charging temperatures start to rise appreciably. Cascaded system 3 maintains higher energy rate values from the commencement of charging to around 80 mins possibly due to the greater degree of axial thermal stratification. After 80

mins, the energy rate profile for cascaded system 3 drops from around 700 W to 600 W at the end of the charging process. In contrast to the behaviour cascaded system 3, secondary peak values are seen for cascaded system 1 and 2 at around 90 mins and 110 mins, respectively. These secondary peaks can be explained by the phase change processes at the bottom of the storage tanks between 60 and 90 mins for cascaded system 1, and between 80 and 110 mins for cascaded system 2. These phase change processes induce lower outlet temperature gradient rises which consequently increases the temperature difference between the top and the bottom of the storage tank thus increasing the energy charging rates to secondary peak values. The secondary peaks can be qualitatively used to identify the time when the phase change process is occurring at the bottom of cascaded system 1 and cascaded system 2. For the single PCM system, the slight rise in the energy rate from 110 mins to the end of charging also corresponds to time when the phase process is occurring at the bottom of the storage tank. For cascaded system 3, the phase change process occurs for a shorter duration, however, the flattened almost constant energy rate profile from around 50 mins to 80 mins corresponds to the time when the phase change process is occurring at the bottom with erythritol melting inducing a slower outlet temperature rise as shown in Figure 4.1 (d). Generally, the highest energy rate values are seen with cascaded system 3, followed by cascaded system 2, cascaded system 1 and lastly by the single PCM system. It is also important to note that cascaded system 2 and cascaded system 3 also show slightly faster rises to the peak energy rates.

Figure 4.4 (b) shows energy rate profiles with a higher charging flow rate of 6 ml/s. Due to the increased heat transfer rates, the rise to the peak values is faster as compared to charging with 4 ml/s. The peak energy rate values for cascaded system 2 and cascaded system 3 are comparable but lower than the 4 ml/s case possibly due to a loss of thermal stratification with the higher flow rate which also increases the outlet charging temperatures. For the single PCM system and cascaded system 1, the peak energy rate values are marginally higher and comparable to the 4 ml/s case. This suggests that the increase in the flow rate slightly improves the charging performance of the single PCM. A secondary peak with higher energy rate values as compared to the other storage systems is seen with cascaded system 3. Cascaded system 3 as with the 4 ml/s case, shows greater energy rate values for most of the duration of charging. In contrast to the 4 ml/s case, cascaded system 1 shows lower energy

rates values when compared to the single PCM after around 90 mins. This due to the lower density of erythritol in the liquid state which causes the rate of temperature rise at the bottom to be faster thus reducing the thermal gradient between the top and the bottom of the storage tank. This reduction in the thermal gradient causes the drop in the charging energy rate for cascaded system 1 after 90 mins. In terms of the thermal performance with this flow rate, cascaded system 3 shows the highest energy rates followed by cascaded system 2, the single PCM system and lastly by cascaded system 1.

Figure 4.4 (c) shows the energy rates of the four systems with the highest charging flow rate of 8 ml/s. The fastest rise to the peak values is shown with this flow rate since it has the greatest heat transfer rates. As with the other flow rates, cascaded system 3 shows generally higher energy rate values, and its peak value is comparable to that of cascaded system 2. The flattened almost constant energy rate value is seen with cascaded system 3 for a longer duration (20 mins to 70 mins) as compared to the other flow rates suggesting efficient charging despite of the fact that the degree thermal stratification is lower with this flow rate. The peak values for cascaded system 1 and the single PCM system are comparable and lower than those of cascaded system 2 and 3, as is the case with the lower flow rates. The single PCM system also shows greater energy rates after melting of the bottom PCM in cascaded system 1. A sharp rise in the energy rate profile of the single PCM system is seen between 70 and 80 mins. This is possibly due to an external disturbance like a wind breeze which causes the thermal gradient of the outlet temperature to drop as depicted in Figure 4.3 (a). The drop in thermal gradient of the outlet temperature from 70 mins to 80 mins is most probably due to an external factor since eutectic solder will not have melted during this period. As with the 6 ml/s case, the highest energy rate values are seen with the 3 PCM cascaded system 3, followed by cascaded system 2, the single PCM system and lastly by cascaded system 1. As an overall observation, cascaded system 3 shows the highest energy rate values and the metallic single PCM shows the lowest. The performance of the single PCM system is, however, better than that of cascaded system 1 for 6 ml/s and 8 ml/s, after the bottom PCM has melted. This result suggests that a lower melting point PCM tends to lower the performance of cascaded systems if charging is continued to significantly higher temperatures above its melting point. On a closer observation, the highest flow rate also seems to lower the performance of cascaded system 2 with the higher meting point PCM at the bottom as it energy rate values

become lower than those of the single PCM between 70 mins to the end of charging. The highest flow rate increases the heat transfer rate, and also increases the temperature rise in the cascaded systems such that appreciably higher temperatures above the melting temperatures of the bottom PCMs are obtained. These significantly higher temperatures at the bottom seem to lower the thermal performance of the cascaded systems.

Energy rate profiles are only adequate in evaluating the quantity of the stored energy. To evaluate the quality of the stored energy, exergy rate profiles are presented in Figure 4.5.

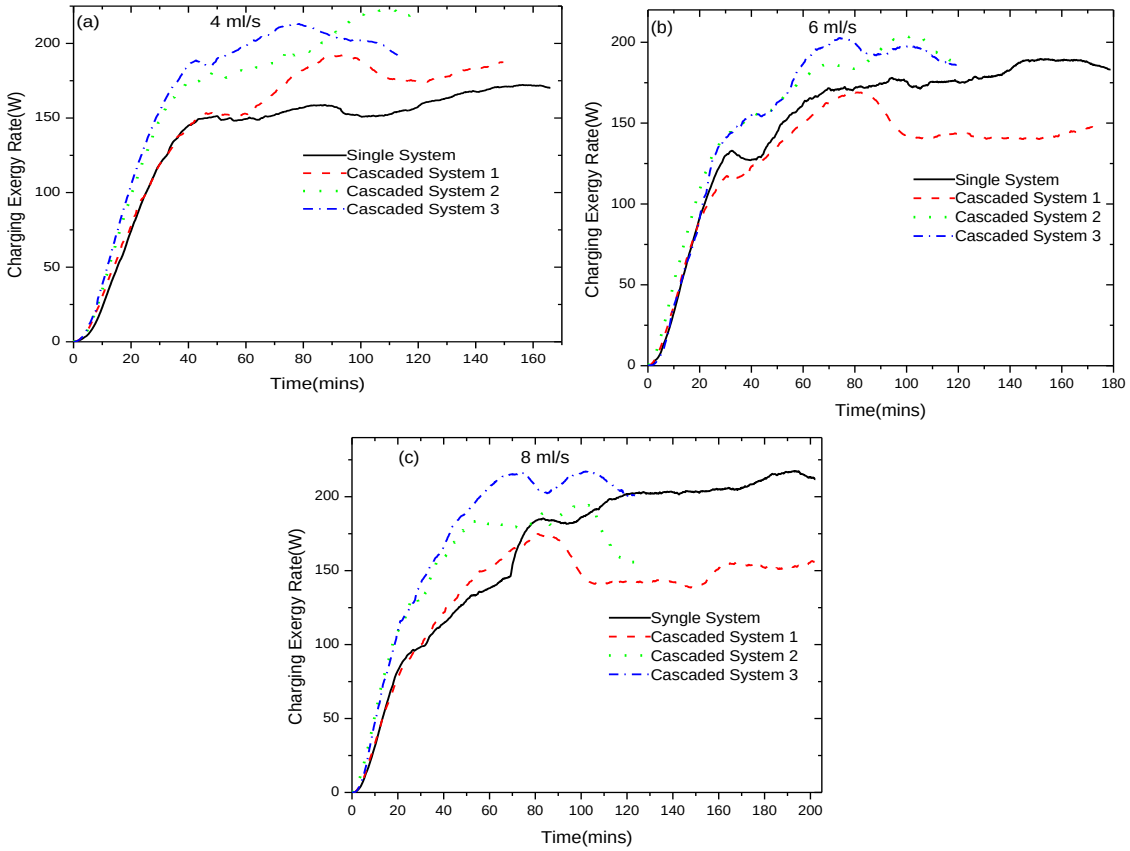

Figure 4.5**:** *Charging exergy rate profiles at (a) low, (b) medium and (c) high flow rates for the four storage systems.*

Charging exergy rates are considerably lower than the corresponding charging energy rates since heat losses are accounted for. For the lowest charging flow rate, cascaded system 3 shows higher exergy rate values from around 30 mins to 90 mins as compared to the other storage systems. This is due to the larger degree of thermal stratification during this period induced by the release of latent heat from erythritol followed by adipic acid during this period

for this 3 PCM system. Cascaded system 2 shows the second best thermal performance in terms of the exergy rate values for the lowest flow rate, and its exergy rate values become greater than those of cascaded system 3 after 90 mins of charging. This is possibly due its earlier release of latent heat of the eutectic solder at the top of the storage tank when compared to cascaded system 3 as depicted in Figure 4.1. Cascaded system 1 shows the third best thermal performance as it is charged for a longer period as compared with cascaded system 2 which has adipic acid at the bottom with a higher thermal conductivity. The least thermally stratified single PCM system due its higher thermal conductivity shows the lowest exergy rate values during the charging cycle.

The secondary peaks depicted by the energy profiles in Figure 4.4 are not as clearly defined for the exergy rate profiles, however, the period of phase change is shown by exergy rate profiles with lower gradients as compared to the initial exergy rate gradients at the start of the charging process. For example, for cascaded system 1, the phase change process at bottom of the storage tank occurs between 50 to 90 mins (Figure 4.1), and this is clearly shown by the exergy rate profile rising from around 150 W to around 185 W with a gradient that is lower than the initial gradient. For the same system, the exergy rate shows a slight rise from 110 mins up to the end of charging which corresponds to the time when the top eutectic solder PCM starts to melt. Exergy rate values range from 0 W to around 225 W. The highest exergy values at the end of charging processes are seen with cascaded system 2, followed by cascaded system 3, cascaded system 1 and lastly by the single PCM system.

Plot (b) of Figure 4.5 shows the exergy rate profiles when charging with a flow rate of 6 ml/s. Cascaded system 3 shows the highest initial exergy rate values as compared to the other storage systems as with 4 ml/s case. The exergy rate rises are faster as compared to the 4 ml/s case due to the higher degree of heat transfer. The change in the exergy rate gradients can also be used to qualitatively represent the phase change processes as with the 4 ml/s case. The cascaded systems show slightly lower values as compared to the 4 ml/s case due to the loss in thermal stratification. In contrast to this behaviour, the single PCM system actually improves its performance with the higher flow rate, and it shows a higher exergy rates values when compared to cascaded system 1 possibly due the greater heat transfer rate with the higher flow rate induced by its high thermal conductivity. The time when the bottom PCM has finished melting is shown by the drop of the exergy rate profile for cascaded system 1 at

around 90 mins as in the case of the energy rate profile. This is due to a substantially lower thermal mass at the bottom which lowers the axial thermal gradient as there is a faster temperature rise at the bottom of the storage tank. Cascaded system 1 thus shows the worst thermal performance in terms of the exergy rates when charging with a flow rate of 6 ml/s.

Increasing the flow rate from 6 ml/s to 8 ml/s is seen to further improve the performance of the single PCM system such that it shows the greatest exergy rate values with the highest charging flow rate. In fact, the exergy rate values for the single PCM systems are greater than those of cascaded system 1 and 2 after 100 mins of charging further supporting the idea that the greater charging flow rate enhances more pronounced heat transfer in the single PCM as compared to the cascaded systems. Generally, as with the other flow rates, cascaded system 3 shows greater exergy rate values as compared to the other storage systems. The performance of cascaded system 2 is second best followed by the single PCM system. Cascaded system 1 shows lower exergy rate values for most of the charging duration, except for a brief period between 30 and 70 mins where it shows slightly greater exergy rate values when compared to the single PCM system. The exergy rate profiles values are comparable for three cascaded systems when using the three different flow rates, whereas the single PCM system shows appreciably higher exergy rate values with an increase in the charging flow rate.

4.1.2 Effect of the temperature

4.1.2.1 Profiles of charging temperatures

Charging temperature profiles at three different set heater temperatures of 260 ^{o}C, 280 ^{o}C and 300 ^{o}C at a set flow rate of 6 ml/s are presented in this section. This is carried out to investigate the thermal behaviour of the systems at different set charging temperatures. Figure 4.6 shows the thermal behaviours of the four latent heat thermal energy storage (LHTES) systems during charging with a set flow rate of 6 ml/s at a low set heater temperature of 260 ^{o}C.

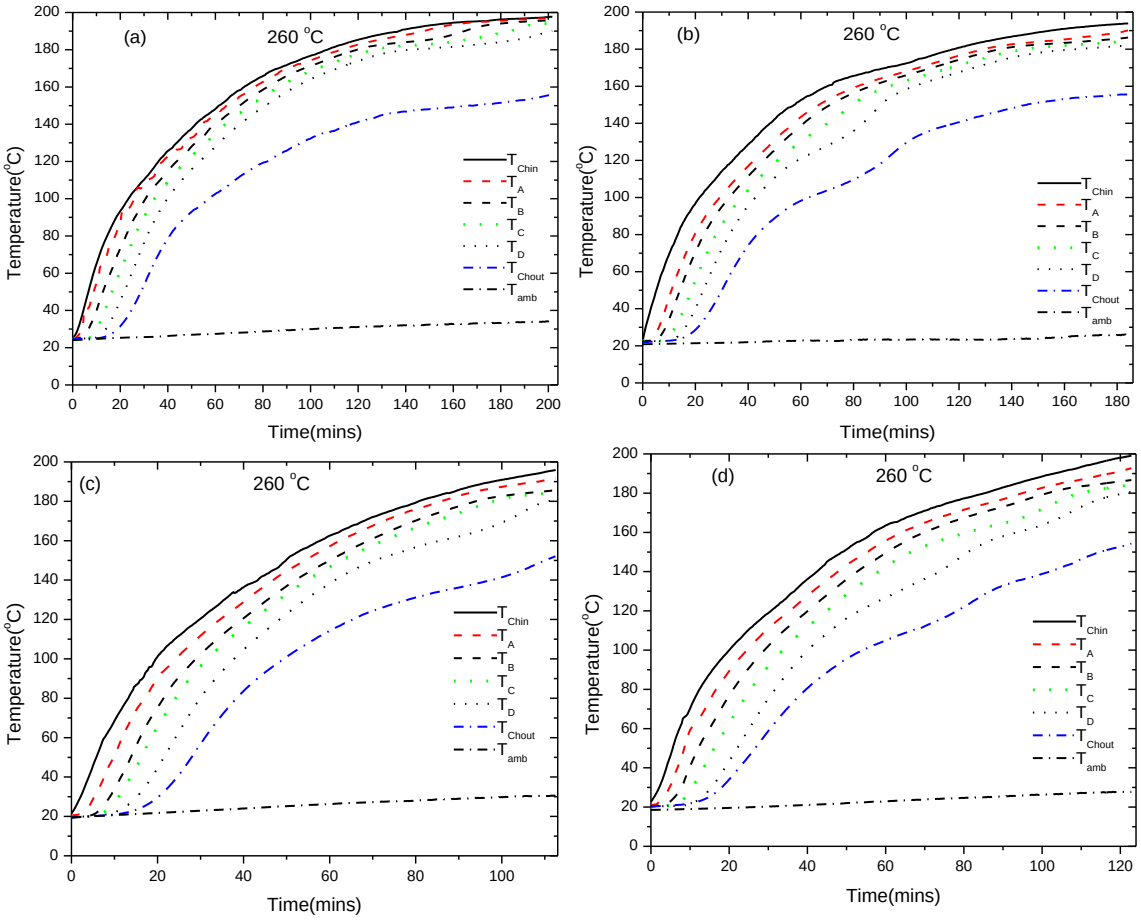

Figure 4.6: *Average charging temperature profiles at a low set heater temperature of 260 °C with a flow rate of 6 ml/s for (a) the single PCM system, (b) cascaded system 1, (c) a cascaded system 2 and (d) cascaded system 3.*

The single PCM system shows the longest charging duration of about 210 mins, followed by cascaded system 1 with a charging duration of about 185 mins. This trend is due to reasons mentioned earlier of the larger thermal mass of metallic PCMs in the storage tank, and the slightly higher charging termination temperature for the single PCM system. In the case of cascaded system 1, the longer charging time is a result of the lower melting temperature of erythritol (120 °C). The phase change process at the bottom occurs earlier for a longer duration as compared to the other cascaded systems making the bottom limiting temperature to be approached later. Cascaded system 2 shows a slight shorter charging time compared to cascaded system 3. This is likely due to a slightly lower initial ambient temperature when the charging experiment for cascaded system 3 commenced which resulted in the lower rise of the initial storage temperatures as compared to cascaded system 2. The lower ambient temperatures for cascaded system 3 resulted in slightly higher heat losses such that the

bottom limiting temperature was achieved at a slightly later time. The change in the ambient temperature in the cascaded system 2 is from about 20 ^{o}C to about 30 ^{o}C, while the change in the ambient temperature for cascaded system 3 is from around 19 ^{o}C to 26 ^{o}C. As in the case of the different flow rates, the lowest degree of thermal stratification is seen with the single PCM system due to the large axial thermal conductivity. Cascaded system 3 also shows the largest temperature difference during charging as explained earlier in the effect of flow rate.

Figure 4.7 presents the charging temperature profiles of the four latent heat thermal energy storage systems at a set heater temperature of 280 ^{o}C using a flow rate of 6 ml/s.

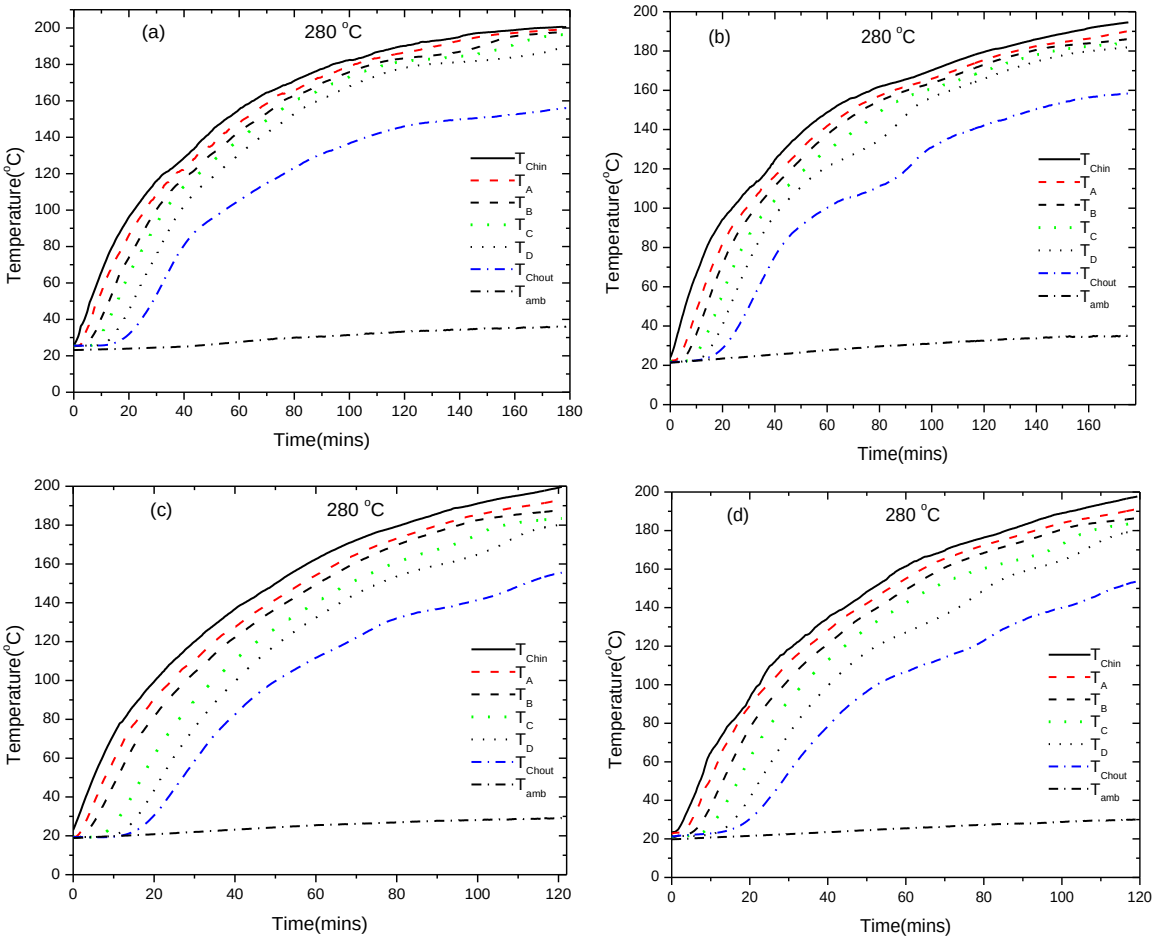

Figure 4.7: *Average charging temperature profiles at a medium set heater temperature of 280 ^{o}C with a flow rate of 6 ml/s for (a) the single PCM system, (b) cascaded system 1, (c) cascaded system 2 and (d) cascaded system 3.*

All the systems show a reduction in the charging times as compared to temperature profiles depicted in Figure 4.6. This is as a result of a higher thermal gradient between the HTF inlet temperature and the PCM temperature which encourages more convective heat transfer thereby making the bottom limit temperature to be reached earlier. There is no significant change in the degree of thermal stratification as a result of the change in temperature. Cascaded system 3 charges up in a shortest time interval of about 120 mins, while the single system shows the longest charging time interval due to the reasons mentioned earlier. Cascaded system 1 and the single PCM system show a charging time that is almost the same. Cascaded system 2 and cascaded system 3 also show comparable charging times. All the TES systems in Figure 4.7 experience earlier phase change when compared to the systems in Figure 4.6. This is because of the increase in the inlet charging temperatures which also increases the thermal gradients between the HTF temperatures and the PCM temperatures in all the levels along the storage tanks.

Temperature profiles of the four latent heat thermal energy storage systems with a set heat charging temperature of 300 ^{o}C using a flow rate of 6 ml/s are presented in Figure 4.8. The single PCM system shows a longer charging time as compared to the 280 ^{o}C case, possibly due the lower ambient temperature conditions for this test with more associated heat losses making the bottom limiting storage tank temperature to be approached later. The effect of the increase of the inlet temperature seems to be superseded by the lower ambient conditions, thus the ambient temperature also has a significant effect on the charging time. The effect of the set heater charging temperature which affects the inlet charging temperatures of the systems seems to be more pronounced for a set heater temperature rise from 260 ^{o}C to 280 ^{o}C as compared to a set temperature rise from 280 ^{o}C to 300 ^{o}C. This is shown by the very small drop in the charging times of the cascaded TES systems for an increase in the set heater temperature from 280 ^{o}C to 300 ^{o}C. The best charging temperature is thus 280 ^{o}C for these cascaded systems since an increase in the charging temperature to

300 °C seems to have an almost insignificant effect of the charging times. The set temperature of 300 °C also results in more heat losses.

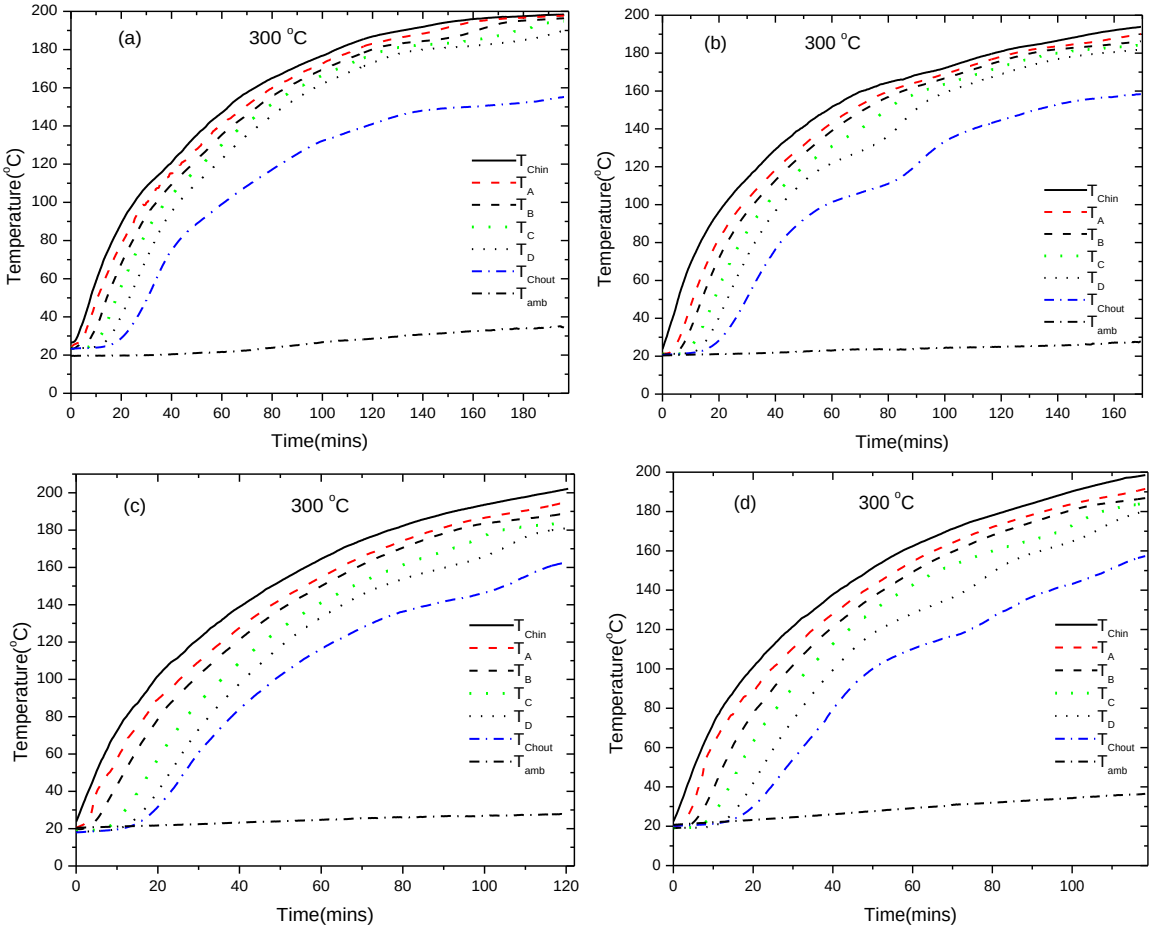

Figure 4.8: *Average charging temperature profiles at a high set heater temperature of 300 °C with a flow rate of 6 ml/s for (a) the single PCM system, (b) cascaded system 1, (c) a cascaded system 2 and (d) cascaded system 3.*

4.1.2.2 Charging energy and exergy rates

The effect of set heater charging temperature on the energy rates for four storage systems is shown in Figure 4.9. Figure 4.9(a) shows the energy rates of the four TES systems at a low set heater temperature of 260 °C.

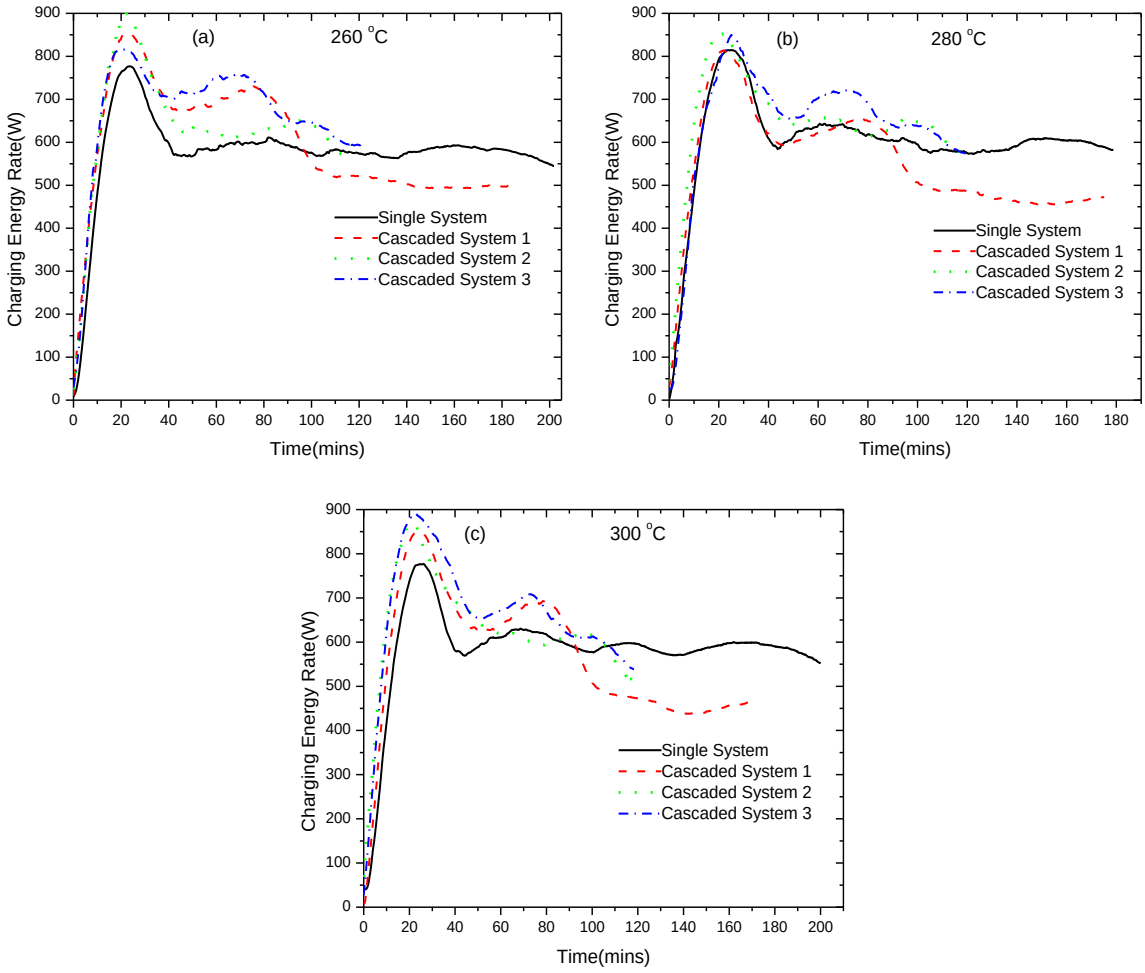

Figure 4.9: *Charging energy rate profiles at (a) low, (b) medium and (c) high set heater temperatures for the four storage systems.*

The energy rate rises to the peaks for the three cascaded systems are almost identical, showing peak values just after 20 mins. Cascaded system 2 shows the highest energy rate peak value of about 900 W due to the highest degree of initial thermal stratification obtained due to the slightly faster rise of the inlet charging temperature. The single PCM system as a result of its higher axial thermal conductivity shows the lowest degree of axial thermal stratification resulting in the lowest peak value of about 790 W. Due to the gradual increase of the outlet temperatures, all the systems experience drops from the peak values after 20 mins as in the case with the effect of the flow rate. Secondary peak values are also observed in the energy rate profiles of the cascaded systems as explained earlier, and these signify the phase change processes at the bottom of the storage tank. Cascaded system 3 shows the

greater energy rate values at the occurrence of secondary peak due to latent heat being release in multiple sequences. After the occurrence of the secondary peak value for cascaded system 1, it shows lower energy rate values after 90 mins when compared to the single PCM system as explained earlier in the effect of the flow rate (Figure 4.4 (b)). The drop to lower energy rate values for cascaded system 1 is due to the lower density of erythritol in the liquid state which causes the rate of temperature rise at the bottom of the storage tank to be faster thereby reducing the thermal gradient between the top and the bottom of the storage tank.

Figure 4.9(b) shows the charging energy rate profiles at a higher heater set temperature of 280 ^{o}C. There is no significant change observed in the time of the occurrence of peak energy rate values as a result of the increase in the heater temperature from 260 ^{o}C to 280 ^{o}C. Cascaded system 1 and cascaded 2 show a reduction in their peak values, from 860 W to 810 W and from 900 W to 850 W, respectively as a result of the slightly higher initial outlet temperature rise induced by the greater heat transfer at the higher set temperature. Thus, the initial thermal gradient is reduced. On the other hand, the peak energy rate values for cascaded system 3 and the single PCM system are slightly higher at around 850 W and 820 W respectively, for 280 ^{o}C as compared to 820 W and 790 W for 260 ^{o}C. This could be a result of the greater degree of initial thermal stratification for these two storage systems for the 280 ^{o}C case. Secondary peak values are also evident in the energy rates profiles of the cascaded systems which can be used as a qualitative inference of the phase change processes in the storage systems. Cascaded system 1 also shows lower energy rate values after erythritol has melted when compared to the single PCM system after 90 mins.

The highest set temperature (300 ^{o}C) charging energy rates of the four TES systems are shown in Figure 4.9 (c). Figure 4.9 (c) also shows no significant shift in the time of occurrence of the peak values as a result of the temperature increase. This justifies the observation that an increase in temperature has little or no effect on the time of occurance of the peak values of the systems. Cascaded system 3 shows the highest peak energy rate value of 900 W which is comparable to that of cascaded system 2 (850 W), and that of cascaded system 1 (850 W). This is due to higher degree of thermal stratification in cascaded system 3 which seems to increase with an increase in the set temperature as the peak energy rate increases from 820 W to 900 W for set temperature increases from 260 ^{o}C to 300 ^{o}C. The peak value of cascaded system 2 using 280 ^{o}C is comparable with the one obtained with 300 ^{o}C, whereas for 260 ^{o}C a

higher peak value is seen suggesting that higher temperatures tend to degrade the performance of this system. On the other hand, for cascaded system 1 and the single PCM system, the peak values show no predictable trend and cannot be used to infer the effect of the set temperature clearly. The peak energy rate values of the single PCM system is lower at a set temperature of 300 ^{o}C as compared to the 280 ^{o}C case possibly due the lower ambient temperature conditions for the former which results in more heat losses and a longer charging time. It is important to note that with similar ambient conditions for the 300 ^{o}C case, it will be expected that the charging energy rate of the single PCM system should increase. The secondary peak values as with the other set temperatures infer the phase change transitions at the bottom of the storage systems. Cascaded system 1 also shows lower values after erythritol has melted as with the other cases. In general, the increase in the set temperature slightly reduces the charging time only for the cascaded storage systems.

Figure 4.10 shows the exergy rate variations using different set heater temperatures. Cascaded system 3 which releases latent heat from three different PCMs shows greater exergy rate values with lowest set temperature of 260 ^{o}C. Cascaded system 2 shows the second best thermal performance in terms of the exergy rate values for the lowest set temperature, although it shows lower values when compared to cascaded system 1 from 40 to 70 mins. The lowest exergy rates are shown with the eutectic solder single PCM system with the lowest degree of thermal stratification, however, after erythritol has melted, the single PCM shows higher exergy rate values as compared to cascaded system 1. The small secondary peaks signifying the phase change transitions at the bottom are also evident for the exergy rate profiles as with the case of the different flow rates.

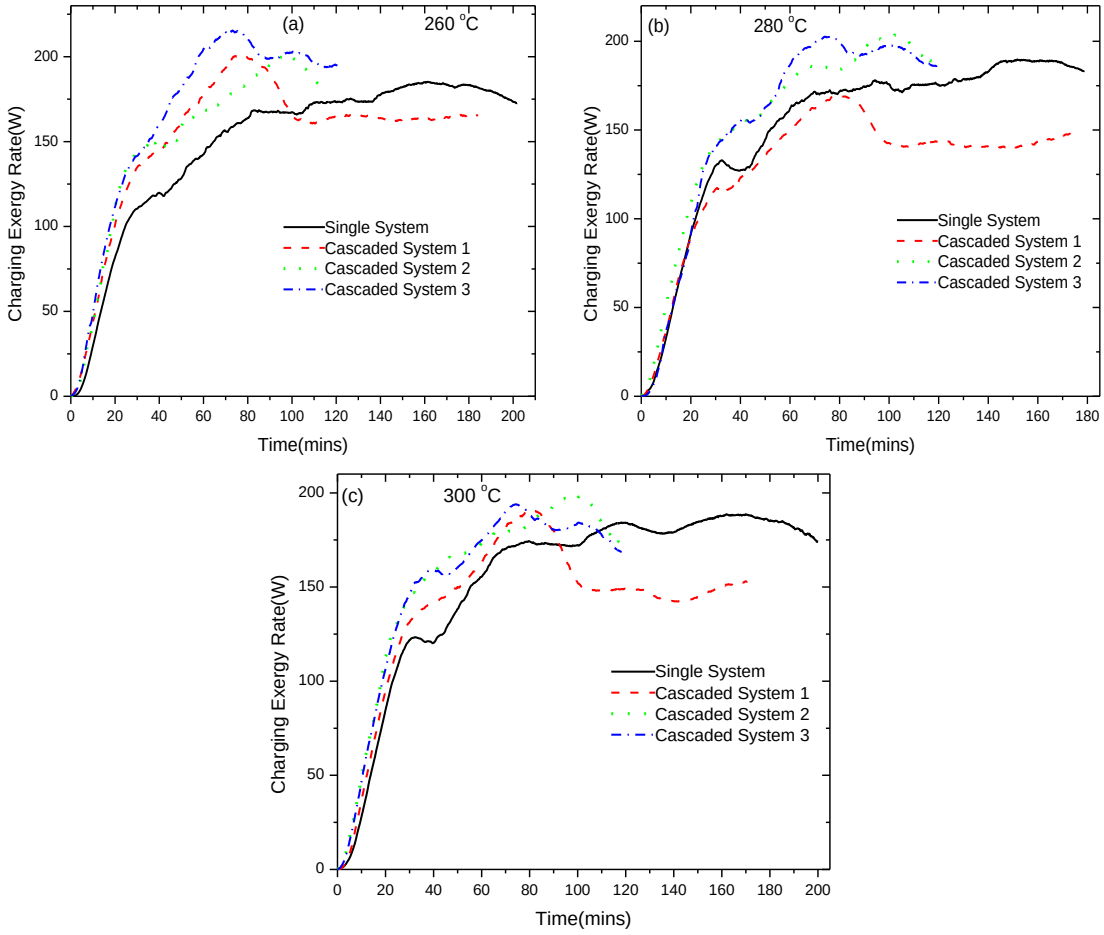

Figure 4.10: *Charging exergy rate profiles at (a) low, (b) medium and (c) high set heater temperatures for the four storage systems.*

Figure 4.10 (b) shows charging exergy rates for the four storage systems at a set heater charging temperature of 280 °C. Cascaded system 3 with the greatest degree of thermal stratification shows the highest values for most of the duration of charging. However, from after 90 mins of charging to the end, cascaded system 2 shows slightly higher values due to earlier melting of eutectic solder at the top of cascaded system 2. Cascaded system 1 shows much lower values as compared to the other storage systems due to the lower charging energy rate (Figure 4.9(b)). Except for cascaded system 2, the exergy rate values for other three storage systems show comparable values with an increase in the set charging temperature from 260 °C to 280 °C suggesting that a change in the set temperature has a marginal effect on the rate of storing exergy. It is also important as with the energy rate

values, the maximum exergy rate values occur at nearly the same time for two set temperatures.

For the highest set temperature of 300 ^{o}C (Figure 4.10 (c)), cascaded system 2 shows slightly higher exergy rate values when compared to the other storage systems, however, cascaded system 1 and cascaded system 3 shows slightly higher values for a brief duration between 60 and 80 mins. At 300 ^{o}C, the single PCM system shows lower exergy rate values except after around 110 mins, when erythritol in cascaded system 1 has melted. All four storage systems, show more comparable initial exergy rate values with this set temperature. The exergy rate values for this set temperature are also comparable to the other set temperatures firmly providing evidence that the set charging temperature has a minimal effect on the amount of exergy that can be stored in the cascaded storage systems.

4.2 Discharging results

4.2.1 Effect of flow rate

The effect of the flow rate on the discharging processes is presented in this section.

4.2.1.1 Profiles of discharging temperatures

Figure 4.11 presents the discharging thermal profiles for the four storage systems at a low flow rate of 4 ml/s. The discharging process is from the top to the bottom of the storage tank immediately after the charging process. This process is terminated when the inlet temperature of the discharging unit is approximately equal to the outlet temperature. At the end of the discharging process, all the stored thermal energy has been extracted making the load (water) temperature, and the temperatures of the discharging unit to be nearly equal. Cascaded systems show longer discharging durations as compared to the single PCM system. This is due to the multiple release of the stored latent heat in the cascaded systems. However, a slightly longer discharging time is observed in cascaded system 2 instead of cascaded system 3 consisting of three PCMs. This is possibly due to the slightly lower temperature of the water at the beginning of the discharging process. This results in a slightly larger temperature difference between the discharging inlet oil temperature and the water temperature which results in a slightly longer discharging duration.

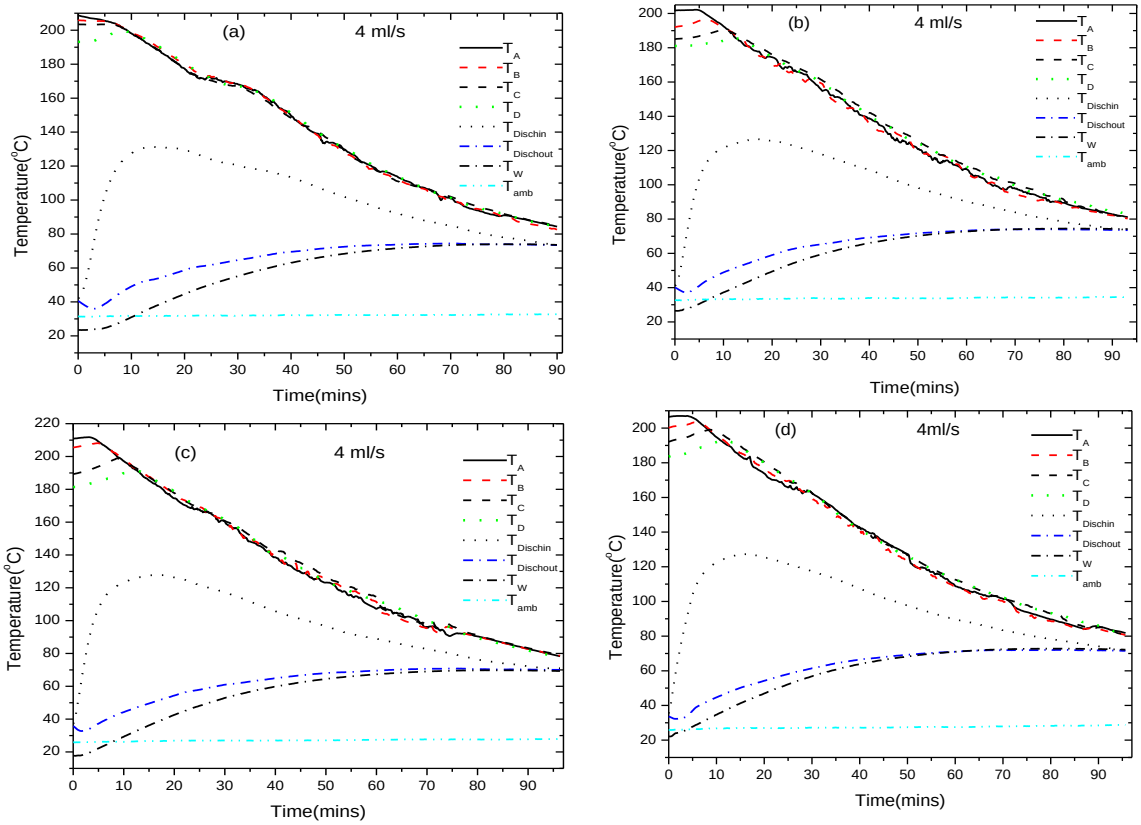

Figure 4.11: *Average discharging temperature profiles at a low flow rate of 4 ml/s for (a) the single PCM system, (b) cascaded system 1, (c) cascaded system 2 and, (d) cascaded system 3.*

The discharging unit inlet temperatures ($T_{Dischin}$) for the four storage systems rise to peak values within the first 15 mins of the discharging as the stored thermal energy is extracted from the storage tank. The single PCM shows a slightly higher peak value of the discharging inlet temperature due to the higher initial temperature of the system before discharging. The three cascaded systems with approximately equal initial temperatures show comparable peak values. All the four storage systems show steady drops after the peak values as the thermal energy is used to heat up the water. The discharging outlet temperatures ($T_{Dischout}$) of all the systems show a brief initial drop as the discharging process commences. This drop is as a result of the surrounding water at a slightly lower temperature which initially cools down the oil at the outlet port.

All systems show a rise in the water temperature (T_W) as the thermal energy is transferred from the storage tank to the water until the inlet and the outlet temperatures of discharging unit are almost equal. Cascaded system 2 shows a slightly lower water temperature at the end of the discharging process. This is due to the slightly lower initial water temperature as a

result of a slightly lower ambient temperature at the start of discharging. The faster rise in the water temperature is seen with cascaded system 3 which suggests that it has the best initial heat transfer rate. However, the water temperatures at the end of discharging are comparable for the storage systems. Unlike the cascaded systems with an immediate rise in the water temperature at the start of the discharging process, the single PCM system takes a longer time to rise. This shows that the heat transfer during the initial stages of the discharging process is less pronounced in the single PCM as compared to the cascaded systems.

Initial rises in the storage tank temperatures (T_A-T_D) are observed in all the systems within the first 10 mins of the commencement of the discharging process. This is due to the hot oil resident in the heating coil that is pumped down through the storage tank. The hot oil causes the bottom storage tank temperature to initially rise. The most pronounced rise with a longer duration is seen with T_D at the bottom of the storage tank. After the initial rise, the storage tank temperatures begin to fall as heat is extracted to heat up the water in the discharging unit. A longer solidification phase change transition of the single PCM system is observed by the flattening of the temperature profiles with very small thermal gradients from 20 to 35 mins within the temperature range of 175 ^oC to 170 ^oC. This indicates more pronounced nucleation and efficient release of the stored thermal energy. Cascaded system 2 shows the least thermal gradient in eutectic solder during discharging when compared to the other two cascaded systems suggesting that it has better nucleation during solidification. However, less pronounced and short solidification phase change transitions of eutectic solder with large thermal gradients are observed in the cascaded systems between 20 to 30 mins as compared to the single PCM system. Other PCMs (adipic acid and erythritol) in the cascaded systems show insignificant phase change transitions. Unlike the single PCM system with little or no axial thermal gradients, cascaded systems show more pronounced axial thermal gradients with temperature profile reversals (i.e. T_D becomes higher than other levels during the discharging process). The top storage tank temperature (T_A) of the cascaded system 1 shows the greatest temperature reversals during the discharging process implying that it has the poorest heat transfer characteristics. The temperature gradients and temperature reversals for the cascaded system 2 and cascaded system 3 are comparable implying similar discharging performances. The insignificant axial thermal gradient observed in the single PCM system is

as a result of the homogenous nature of the system which helps to maintain a uniform temperature across the system during the discharging process.

Thermal profiles at a medium discharging flow rate of 6 ml/s for the four storage systems are shown in Figure 4.12. Apart from the increase in the flow rate, all other conditions are observed as with the flow rate of 6 ml/s. The increase in the flow rate of the HTF from 4 ml/s to 6 ml/s increases the rate of heat transfer thereby shortening the discharging time. The occurrence of the peak values of the discharging unit inlet temperatures is observed earlier as compared to the lower flow rate (4 ml/s). This is as a result of the increase in the flow rates which facilitates the flow of the hot oil from the storage tank outlet faster along the flow-line. A slight increase is also observed in the peak values of $T_{Dischin}$ possibly due to the faster flow of the hot oil from the storage tank outlet along the flow-line. The initial brief drop of the discharging unit outlet temperature observed in Figure 4.11 is reduced. This is as a result of the faster flow of the hot oil which displaces the cooler resident oil at the outlet port in a shorter time. Both the water temperature and the outlet temperature of the discharging unit show faster rises as compared to the lower flow rate due to the faster heat transfer rate.

The rise of the storage tank temperatures during the initial stages of the discharging process is lower, and it occurs for a shorter time as compared to the lower flow rate. This can be caused by the increase of the flow rate which encourages more axial heat transfer thereby inducing a greater degree of thermal mixing in adjacent levels of the TES tank. The solidification phase change transition of the eutectic solder in the single PCM occurred earlier with a comparable thermal gradient to the 6 ml/s case around 15 to 20 mins within the temperature range of 165 ^{o}C to 170 ^{o}C. All the TES systems show earlier solidification phase change transitions of the eutectic solder during the discharging process due to the faster heat transfer rate. Cascaded system 3 shows the greatest thermal gradient of the eutectic solder during discharging indicating the worst degree of nucleation during the discharging process. The phase change transition of erythritol is not seen in cascaded system 1 and in cascaded system 3, whereas very small durations of phase change transitions of adipic acid are seen with cascaded system 3 and cascaded system 2 after 20 mins. The minimum temperature reversals are seen in the single PCM system as in the case with the lower flow rate. Cascaded system 2 shows the most pronounced axial thermal gradient as discharging progresses when compared to other systems.

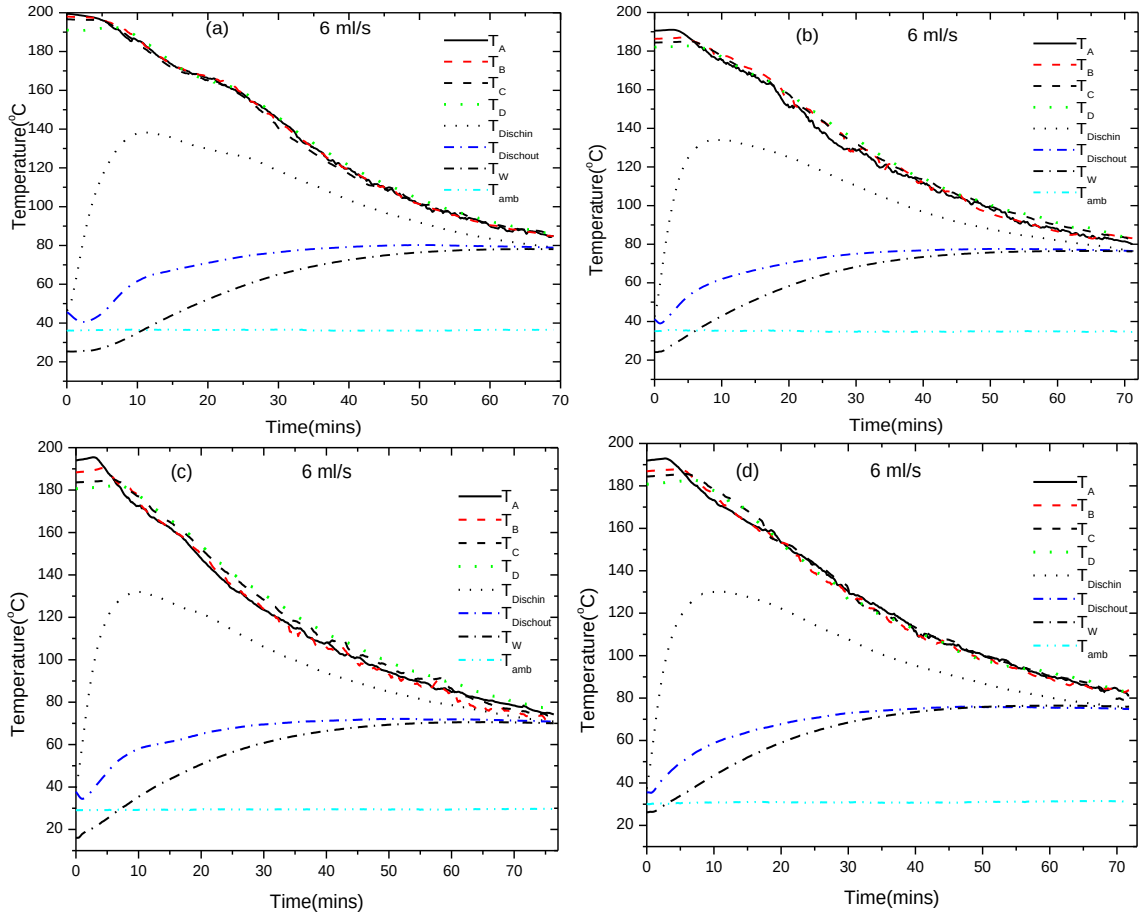

Figure 4.12: *Average discharging temperature profiles at a medium flow rate of 6 ml/s for (a) the single PCM system, (b) cascaded system 1, (c) cascaded system 2 and (d) cascaded system 3*.

Thermal profiles of the four storage systems during discharging with a high flow rate of 8 ml/s are shown in Figure 4.13. All the systems show a shorter discharging duration due to the highest heat transfer rate induced by the highest discharging flow rate. The inlet, outlet and the water temperatures of the discharging unit rise up faster and earlier as compared to the lower flow rates. The peak values of the inlet temperatures and the rises of the water and the outlet temperatures of the discharging unit increase slightly with this increase of the flow rate. The initial rise of the storage tank temperatures particularly at the bottom of the tank is reduced due to more axial thermal mixing between adjacent storage tank levels. The solidification phase change transition of the eutectic solder TES occurred earlier and in a very short time. There are temperature reversals in the eutectic solder system with the bottom temperatures becoming slightly higher than top storage temperatures for this system after 10 mins resulting in larger axial thermal gradients as compared to the lower flow rates. This

is a result of the higher flow rate inducing faster heat transfer at the top resulting in a faster temperature drop at the top after solidification as compared to the bottom.

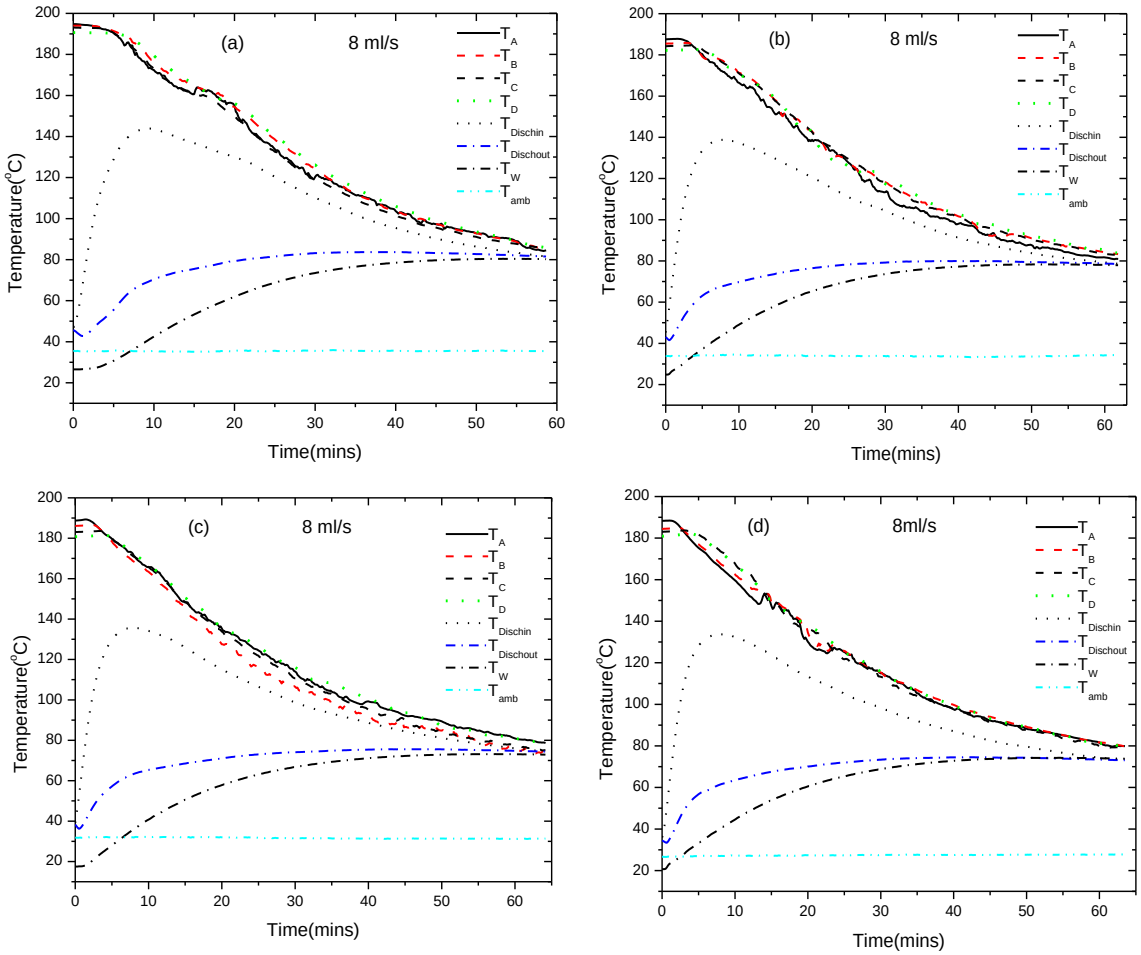

Figure 4.13: *Average discharging temperature profiles at a high flow rate of 8 ml/s for (a) the single PCM system, (b) cascaded system 1, (c) cascaded system 2 and (d) cascaded system 3.*

The widening of the thermal gradients increases with this flow rate for all the storage systems, as both axial and radial convection and conduction is enhanced with the increase in the flow rate. Cascaded system 3 shows the least widening of the thermal gradient along the storage tank with the highest flow rate (8 ml/s) after the slightly evident small phase change transitions for adipic acid and erythritol at around 15 mins and 20 mins, respectively. This implies better heat transfer for this system with the highest discharging flow rate. On the other-hand, the greatest temperature reversals between the top and bottom storage temperatures is seen with cascaded system 1 (eutectic solder/erythritol), implying that it has

the worst thermal performance. The phase change transition for erythritol is also slightly evident for cascaded system 1 between 25 to 30 mins. For cascaded system 2, the brief phase change transition of adipic acid is seen around 15 mins. Cascaded system 2 also showed wider thermal gradients as compared to the other PCMs after the phase change transition of adipic acid, implying a deterioration in its thermal performance. Generally, the highest flow rate seems to induce the phase change processes at the bottom of storage more effectively qualitatively implying more effective nucleation of the PCMs.

4.2.1.3 Discharging energy and exergy rates

To evaluate the quantity and the quality of the performances of the storage systems during discharging with the three different flow rates, energy and exergy rate profiles are presented in this section. The discharging energy rates of the thermal storage systems at three different flow rates are presented in Figure 4.14. For the lowest flow rate, cascaded system 1 shows the lowest energy rate for the whole discharging duration due to the lower rise of the inlet discharging temperature which reduced heat transfer as a result of the slight temperature reversals in the storage tank temperatures confirmed by Figure 4.11 (b). The peak value of the discharging energy rate for the cascaded system 1 is about 620 W, whereas other systems show comparable peak values of around 690 W. The peak values occur at more or less the same time when the discharging inlet temperatures depicted in Figure 4.11 show peak values. Cascaded system 2 with the largest temperature difference between the discharging unit temperatures and the lower storage tank temperature reversals for the cascaded systems, shows slightly higher values from 0 to 40 mins. The single PCM system with the least axial thermal gradients and the least temperature reversals (Figure 4.11(b)) shows slightly higher energy rate values from 35 to 50 mins. Comparable and slightly higher energy rate values for cascaded systems 2 and 3 are seen from 65 mins to the end of the discharging process.

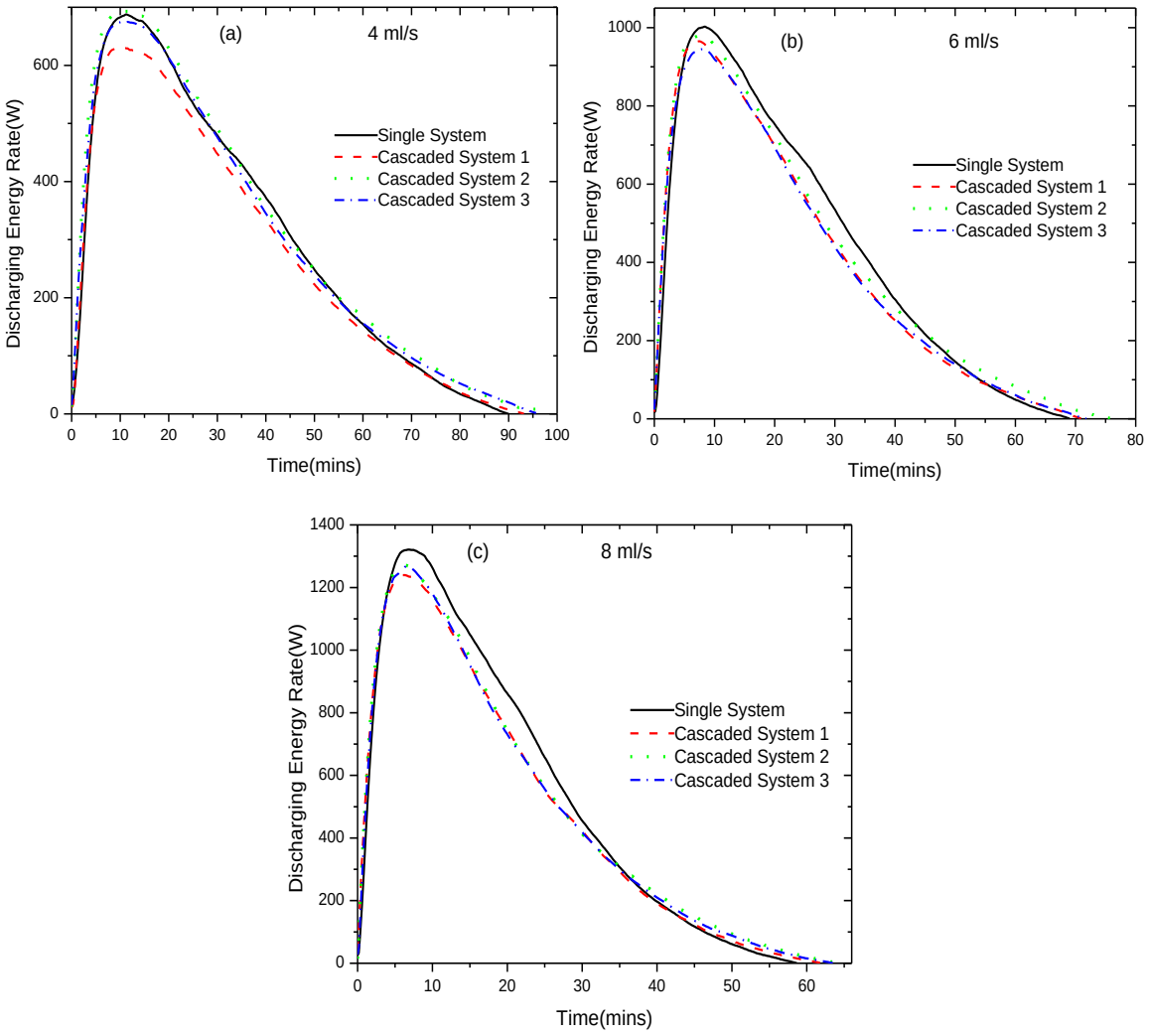

Figure 4.14: *Discharging energy rate profiles at (a) low, (b) medium and (c) high flow rates for the four storage systems.*

In Figure 4.14 (b), the peak values occurred earlier with higher energy rate values as compared to the low flow rate due to the increase in the rate of heat transfer. The single PCM system shows the highest energy rate values for the most duration of discharging (5 to 50 mins) as a result of its higher efficiency of discharging thermal energy with well-defined phase change transitions, negligible axial thermal gradients and minimum temperature reversals. The discharging energy rate peak value of the single PCM system is around 1000 W followed by cascaded system 1 and cascaded system 2 with a comparable peak energy rate values of around 970 W. Cascaded system 3 shows a marginally lower peak of the energy rate and comparable energy rate values to the other cascaded systems for the duration of charging

since the storage tank temperature profiles are comparable with the flow rate of 6 ml/s. Cascaded system 2 shows slightly greater energy rate values from 50 mins up to the end of discharging due to the slightly larger temperature difference of the discharging unit temperatures induced by the greater storage tank thermal stratification in this stipulated period.

Increasing the flow rate from 6 ml/s to 8 ml/s results in higher peak energy rate values which occur earlier as compared the lower flow rates. The discharging time is further reduced due to the increase in the heat transfer rate. The single PCM system also shows higher energy rate values from the peak to around 35 mins of the discharging process due to the larger temperature difference of the discharging unit induced by the slightly higher temperature stored energy. The energy rate for the eutectic solder system drops to slightly lower values from 35 mins to the end of discharging compared to the other storage systems. This because its discharging unit temperatures become lower when compared to the cascaded systems. This can possibly be explained by the occurrence of more pronounced temperature reversals with the highest flow rate and the slight release of latent heat by the lower temperature PCMs at the bottom of the cascaded storage systems. The three cascaded systems show comparable energy rate values for the duration of the discharging process suggesting effective heat transfer that results in noticeable phase change transitions in the cascaded systems.

Profiles of discharging exergy rates for the storage systems at different flow rates are shown in Figure 4.15 for the evaluation of the quality of the thermal energy discharged. In a similar manner to the discharging energy rate profiles, the peak values of the exergy rate profiles increase with the flow rate, and the time for the occurrence of the peak values decreases with the flow rate. Exergy rate values are much lower than the energy rate values since they account for heat losses. For the lowest flow rate (4 ml/s), cascaded system 2 generally shows higher exergy rate values due to the largest temperature difference between the discharging unit temperatures and lower storage tank temperature reversals for the cascaded systems considered. The exergy rate values for cascaded system 2 are, however, comparable to those of the eutectic solder system and cascaded system 3 from 35 mins to the end of discharging. Cascaded system 1 also shows the lowest exergy rate values for the whole discharging duration due to the lower rise on the inlet discharging temperature which reduced heat

transfer as a result of the slight temperature reversals in the storage tank temperatures as explained earlier.

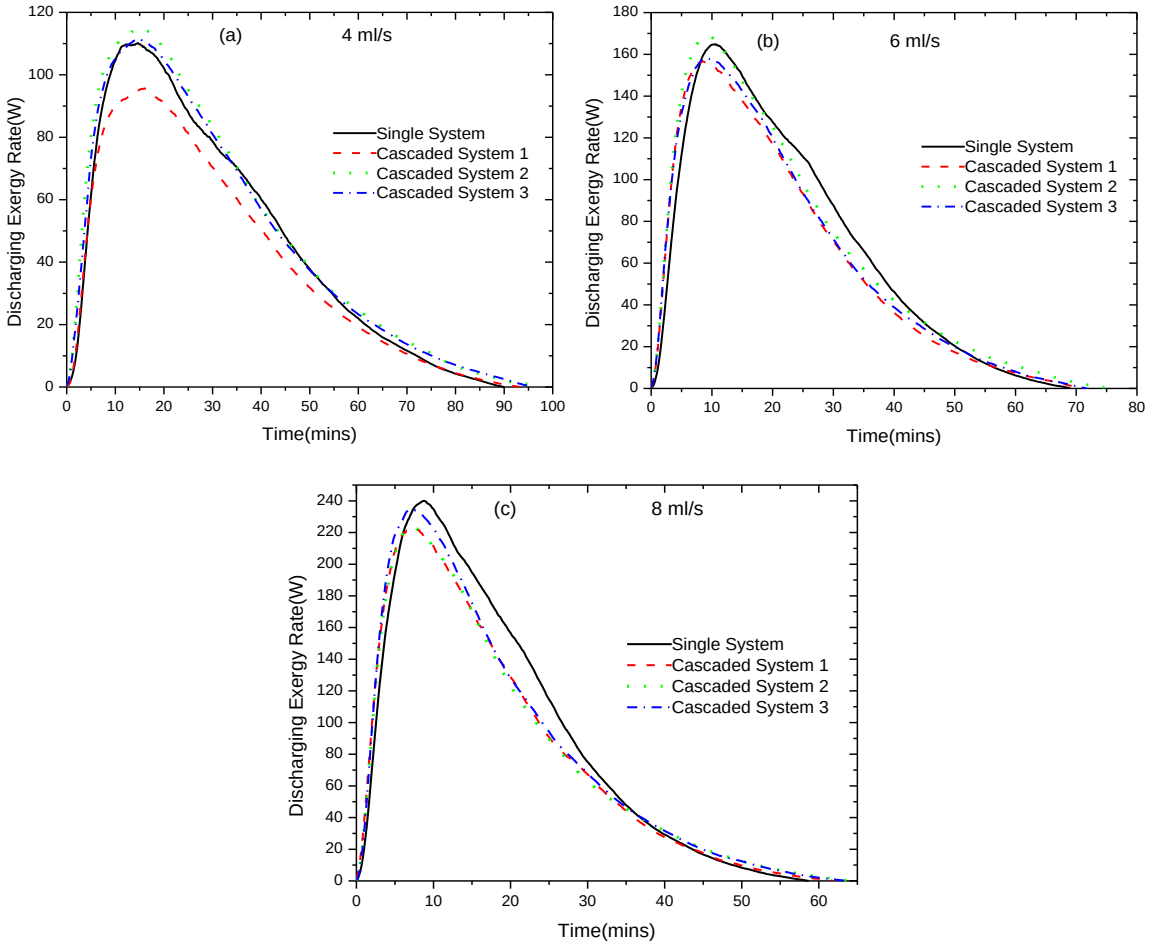

Figure 4.15**:** *Discharging exergy rate profiles at (a) low, (b) medium and (c) high flow rates for the four storage systems.*

Increasing the flow rate from 4 ml/s to 6 ml/s shows more or less the same trend as in the energy rate profiles, however, cascaded system 2 shows the highest peak value suggesting that it has best performance in terms of the initial stored exergy. As with the energy rate profiles, the single PCM system shows larger exergy rate values for most of the discharging process but its initial exergy rate rise is lower when compared to the other storage systems. This is possibly due to the higher initial exergy losses with slightly higher initial storage temperatures. A further increase in the flow rate from 6 ml/s to 8 ml/s results in comparable performances for three cascaded systems from 15 mins to the end of the discharging processes for similar reasons mentioned in the energy rate profiles. The single PCM shows

greater exergy rate values from 8 mins to around 35 mins, however, the initial rise to the peak value is also slower when compared to the cascaded systems

4.2.2 Effect of temperature

This section presents the profiles of the discharging temperature profiles of the TES systems after being charged at different set-heater temperatures to investigate the effect of the charging temperature on the discharging processes. The discharging flow rate used was 6 ml/s.

4.2.2.1 Profiles of discharging temperatures.

The discharging thermal profiles of the four TES systems after charging with a set-heater temperature of 260 ^{o}C at a set flow rate of 6 ml/s are presented in Figure 4.16. As in the case of the effect of flow rate, the discharging process commenced immediately after the charging cycle and was terminated when the inlet temperature was approximately equal to the outlet temperature. Cascaded systems show comparable discharging durations which are slightly longer than the single PCM system. However, cascaded system 2 shows a slightly longer discharging time, with the least axial thermal gradient at the end of discharging implying more effective discharging. This phenomenon also occurred in Figure 4.11 which can be explained by the effect of the lower initial temperature of the water of the discharging unit of cascaded system 2 creating a more pronounced temperature difference between the discharging unit and the storage medium thereby allowing more energy to be discharged. Another possible reason is the release of higher temperature latent heat from eutectic solder and adipic acid as compared to the other cascaded systems.

The single PCM system shows a slightly higher peak value of the inlet temperature of the discharging unit within 15 mins of the discharging process because of the higher initial temperature of the system before discharging. Cascaded systems with almost the same initial temperatures also show comparable peak values of the inlet charging temperatures. A steady drop of the $T_{Dischin}$ is observed in all the systems after the peak values as the stored energy is transferred to the water causing the water temperature to rise. The initial slow rise in the water temperature for the single PCM system has been explained earlier in the effect of the flow rate as an evidence of poor heat transfer during the initial stages.

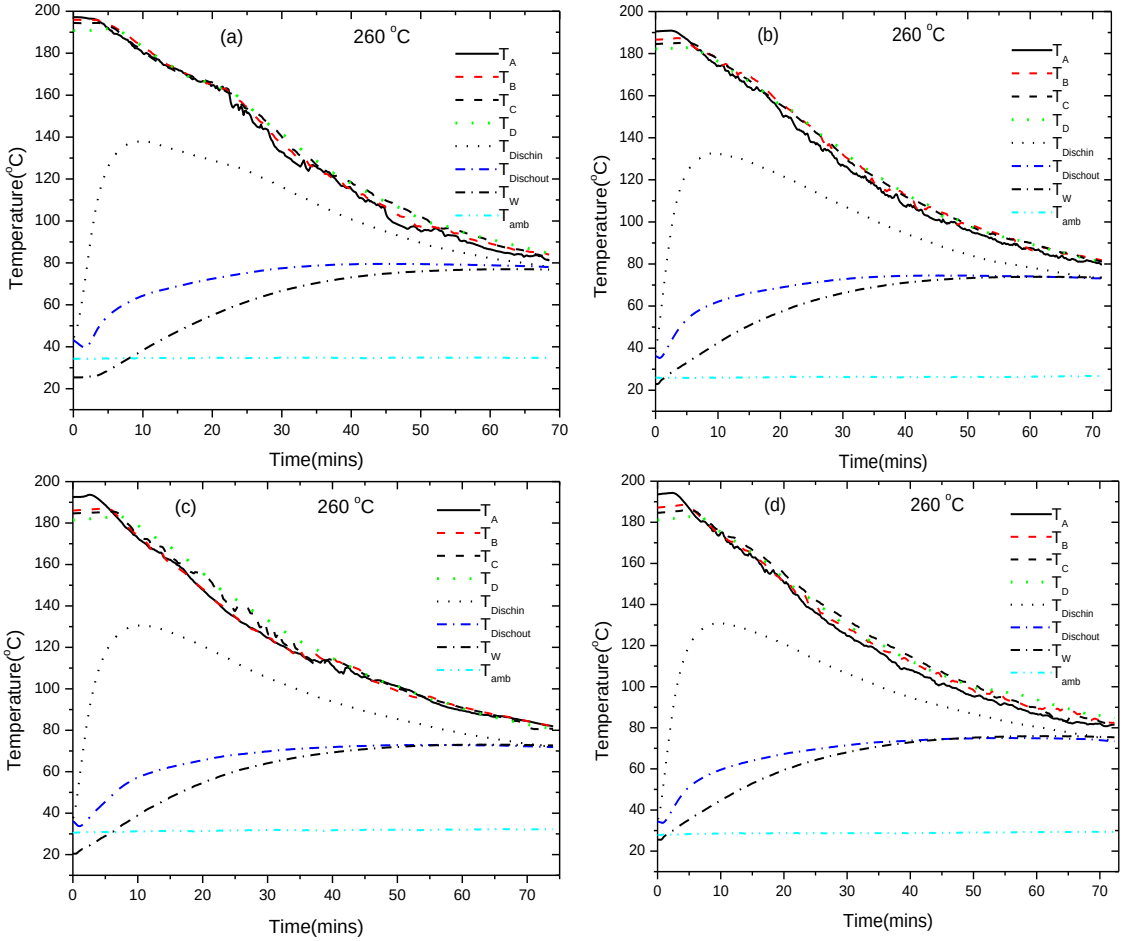

Figure 4.16: *Average discharging temperature profiles after charging with at a low set temperature for (a) the single PCM system, (b) cascaded system 1 (c), cascaded system 2 and (d) cascaded system 3.*

All the storage tank axial level temperatures (T_A-T_D) of all the systems initially rise within the first 10 mins of the discharging process with the lowest axial level temperatures (T_D) showing a more pronounced rise for a longer duration. A similar scenario was presented in the effect of the flow rate, and it was explained as the effect of the residing hot oil in the flow-line, which was first pumped down the storage tank before the oil passed through the discharging unit. As the discharging process progresses, all the storage tank temperatures for all the systems started to drop as the stored energy is used to heat up water in the discharging unit. The single PCM system shows a more pronounced phase change transition of the eutectic solder with the least thermal gradient after about 15 mins of the discharging process. This implies better initial heat transfer for the single PCM system. Cascaded system 3 shows the greatest

axial thermal gradient with the most pronounced temperature reversals compared to other systems implying that it has the poorest heat transfer characteristics. Cascaded system 2 shows the least axial thermal gradient from 40 mins to the end of discharging implying that it has a better heat transfer rate compared to other systems during this period.

Figure 4.17 presents the discharging thermal profiles of the four energy storage systems after charging with a 280 °C heater set temperature.

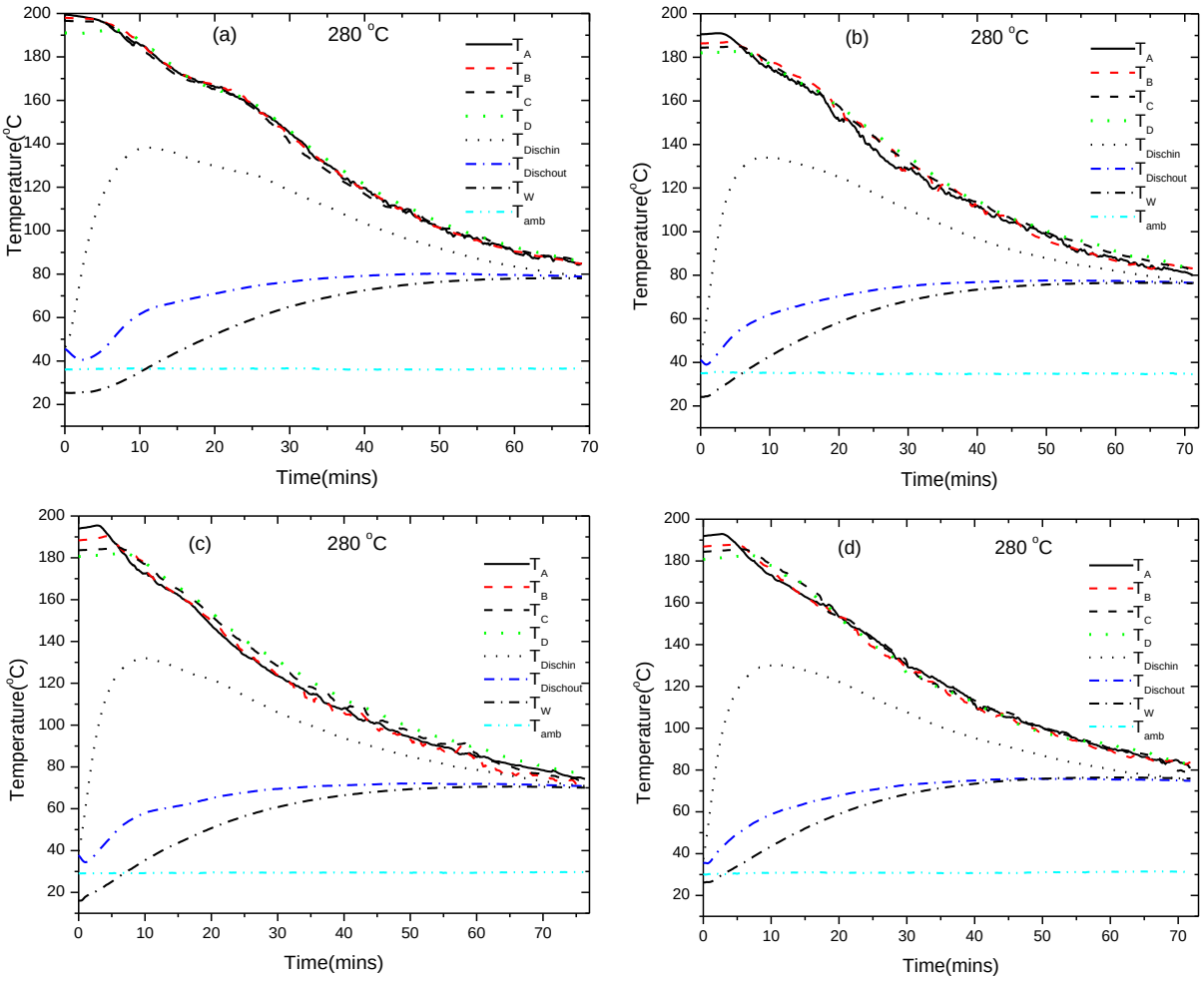

Figure 4.17: *Average discharging temperature profiles after charging with at a medium set temperature for (a) the single PCM system, (b) cascaded system 1, (c) cascaded system 2 and (d) cascaded system 3.*

The initial discharging temperatures are higher as compared to the 260 °C case. No significant change is observed in the discharging durations, the peak values of the discharging inlet temperatures and the water temperatures. Cascaded system 2 also shows the longer charging duration for reasons mentioned in the 260 °C case. The occurrence of the maximum values of

the discharging unit temperatures and the water temperatures is almost the same as for the 260 ^{o}C case, suggesting similar heat transfer characteristics with slightly higher TES temperatures since the same flow rate of 6 ml/s is used. It seems that the initial temperature of the storage tanks has a less significant effect as compared to the flow rate. The temperature profiles of the TES systems are affected by the initial TES temperatures. Lesser thermal gradients during discharging are shown with the single PCM system implying better nucleation and heater transfer after this storage tank has been charged with a medium temperature. This is further confirmed by the higher water temperature for the eutectic solder single PCM system. The best discharging characteristics with lesser gradients for the cascaded systems is seen with cascaded system 3 possibly due more effective phase change transitions in this 3 PCM at higher TES temperatures. Cascaded system 2 shows the greatest axial thermal gradients during discharging implying that it has the worst thermal performance as shown by the lowest water temperature at the end of discharging. This is a direct result of the slightly lower initial water temperature induced the lower initial ambient temperature. It also important to note that with an increase of the initial discharging temperatures, the temperature reversals are reduced when compared to the 260 ^{o}C case. The most probable reason is the more effective phase change transitions with higher temperatures.

The discharging thermal profiles of the systems after charging with a high heater set temperature (300 ^{o}C) are presented in Figure 4.18. The discharging durations are comparable with the other set temperatures. However, cascaded system 3 shows a slightly a longer discharging duration as compared to the other systems due to the lower initial water temperature during discharging. The initial storage temperatures during discharging are comparable to the 280 ^{o}C possibly due to the associated higher heat losses when charging with 300 ^{o}C. The single PCM shows a more pronounced phase change transition of eutectic solder and the least axial thermal gradients suggesting it has the best thermal performance. On the other hand, cascaded system 1 shows lower temperature differences and lower thermal gradients as compared to the other cascaded systems suggesting better discharging characteristics. It is important to note that the temperature gradients for cascaded system 2 and cascaded system 3 with adipic acid actually increase from 280 ^{o}C to 300 ^{o}C, suggesting a reduction in the thermal performance possibly due to more heat losses. Another plausible argument is that adipic acid with the slightly larger thermal conductivity as compared to

erythritol seems to induce more radial thermal heat loss effects to the walls of the storage tank resulting in larger axial thermal gradients.

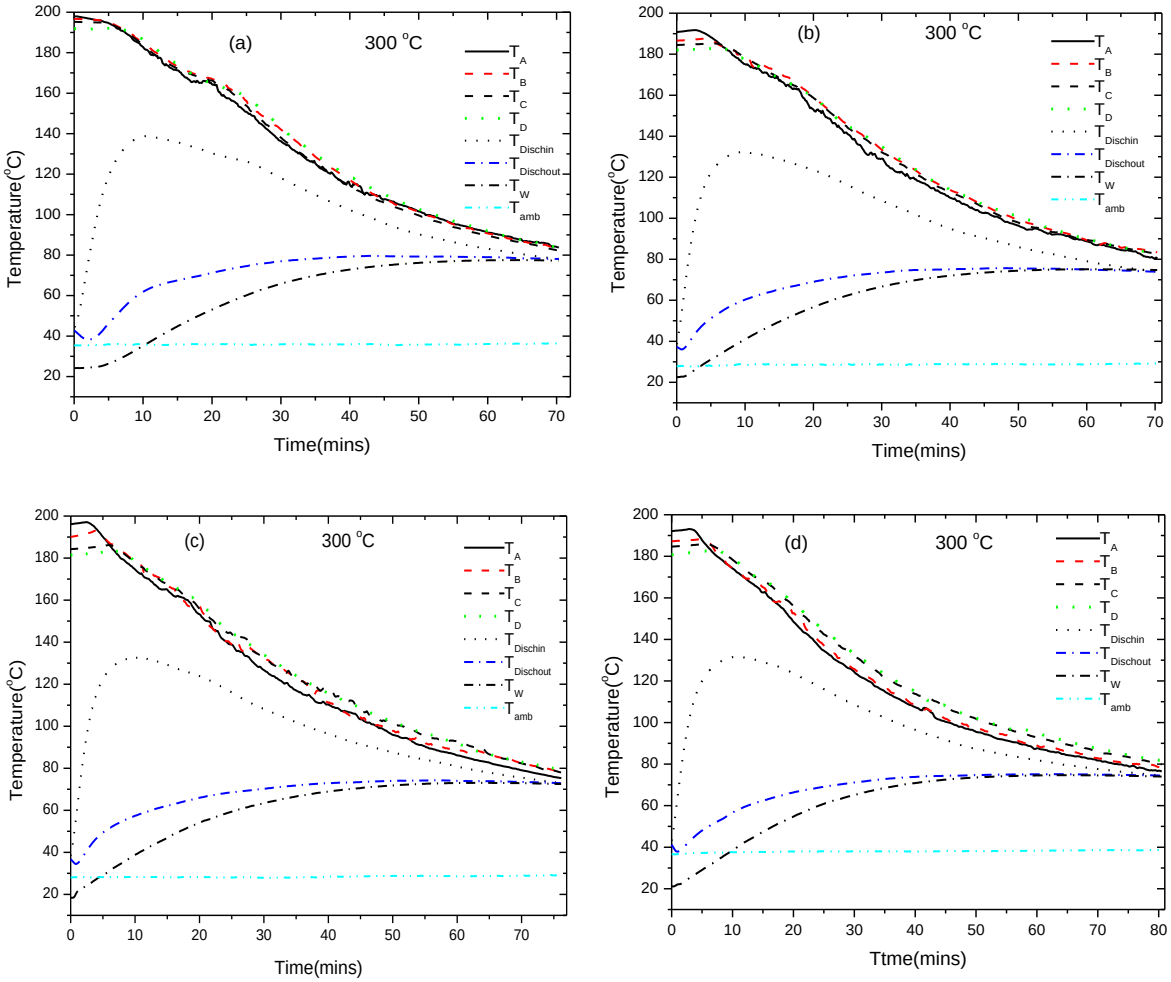

Figure 4.18: *Average discharging temperature profiles after charging with at a high set temperature for (a) the single PCM system, (b) cascaded system 1, (c) cascaded system 2 (d) and cascaded system 3*

4.2.2.2 Discharging energy and exergy rates

To evaluate the effect of charging heater set temperatures on the quantity and quality of energy discharged, energy and exergy rate profiles are presented in this section. The profiles of the discharging energy rates for the four thermal energy storage systems after charging with low (260 °C), medium (280 °C) and high (300 °C) set heater temperatures are presented in Figure 4.19.

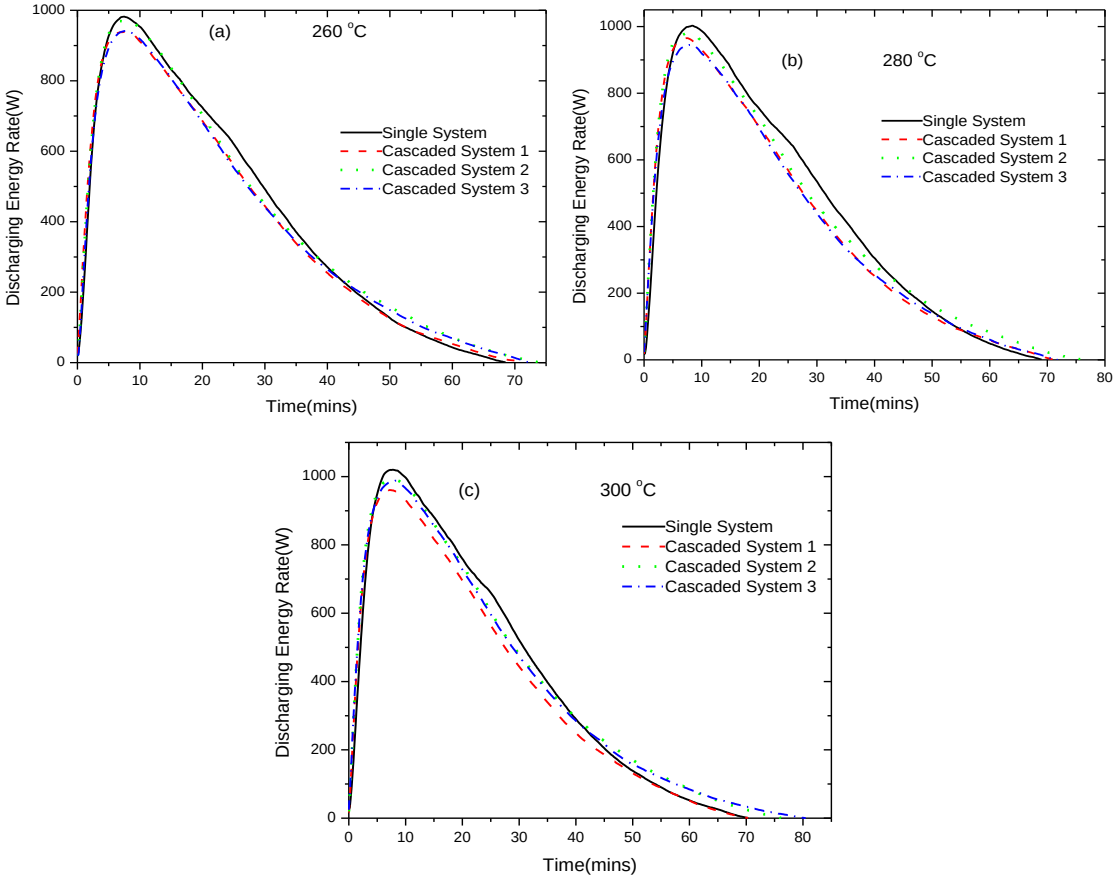

Figure 4.19: *Discharging energy rate profiles after charging with (a) low, (b) medium and (c) high set temperatures for the four storage systems.*

The single PCM shows the highest discharging energy rate peak values for the three heater set temperatures and higher energy rate values for most of the discharging time. This is as a result of its higher efficiency of discharging thermal energy with distinct phase change transitions, little axial thermal gradients and minimum temperature reversals as explained earlier in the effect of the flow rate. The charging set temperature, which affects the initial discharging temperature for the TES systems, seems to have minimal effect of the peak energy rates, and the time of occurrence of the peaks as with the case of the effect of the flow rate. The peak energy rate values only increase marginally with an increase in the set temperature. Discharging energy rates profiles for all cascaded TES systems are comparable. Figure 4.20 presents discharging exergy rate profiles of the four TES systems after charging with set temperatures of 260 ºC, 280 ºC and 300 ºC., respectively. Discharging exergy rate profiles are lower than discharging energy rate profiles presented in Figure 4.19 since they

account for heat losses. For the 260 ^{o}C case, the highest peak exergy rate value of around 175 W is shown with cascaded system 1 and the lowest with of around 160 W is shown with cascaded system 2. This is due to the least degree of thermal stratification of cascaded system 2 as compared to the other systems which implies better heat transfer but lower axial thermal gradients. Higher axial thermal gradients are essential in discharging more exergy from the storage systems. The ambient temperature of cascaded system 2 is higher as compared to cascaded system 1 suggesting more exergy losses from cascaded system 2 although the heat transfer rate is better. Cascaded system 3 and the single PCM with comparable discharging thermal profiles presented in Figure 4.16 show comparable exergy rate profiles. Unlike the energy rate profiles, the exergy rate profiles seem to evaluate the quality of discharged exergy more effectively since the thermal gradient and the ambient conditions are taken into consideration.

Plot (b) of Figure 4.20 shows the exergy rate profiles after charging with a set temperature of 280 ^{o}C. The peak exergy rate profiles are comparable with those obtained using 260 ^{o}C. Cascaded system 2 with the lowest ambient temperature and the highest thermal gradients during the discharging process show the highest peak exergy rate value which is comparable to the single PCM system. However, the single PCM shows higher exergy rate values as compared to cascaded system 2 from 20 mins to 45 mins which is attributed to its energy rate values despite of that the fact that its ambient temperature shows higher values. Cascaded system 1 and cascaded system 3 with comparable temperature profiles show almost identical exergy rate profiles.

For the set temperature of 280 ^{o}C, cascaded systems 1 and 3 show lower exergy rate values probably due to higher ambient temperatures during discharging implying more exergy losses. The exergy rate profiles for the other two systems are comparable, however, the single PCM system shows slightly higher values from 20 mins to 40 mins due to its higher energy rate content. It is important to note, unlike the effect of the flow rate on the exergy rate profiles which tends to increase the exergy rate values with an increase in the flow rate, the effect of the temperature shows marginal variations of the values of the exergy rate profiles. The exergy rate values are affected more by flow rate as compared to the set temperature.

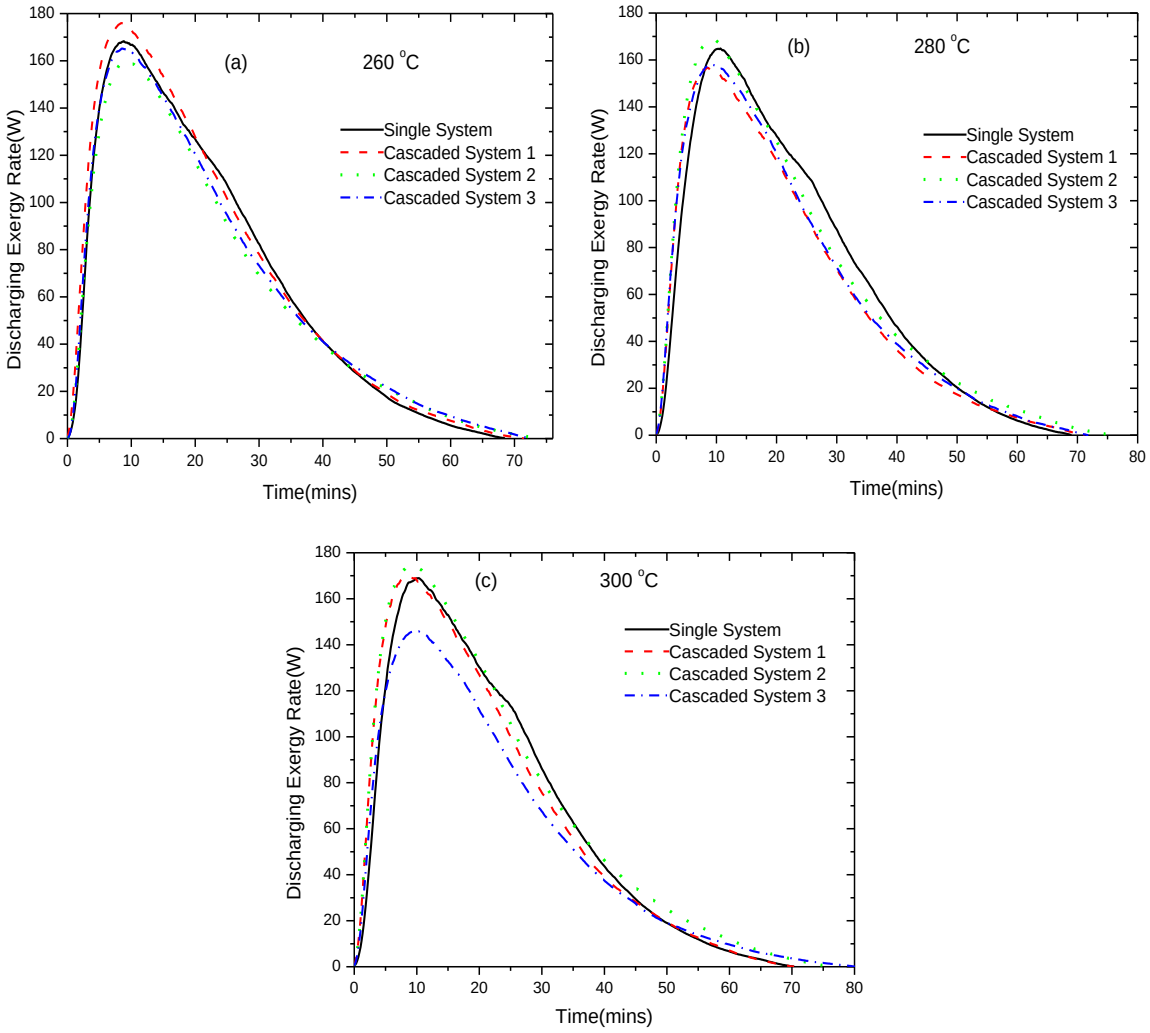

Figure 4.20: *Discharging exergy rate profiles after charging with (a) low, (b) medium and (c) high set temperatures for the four storage systems.*

4.3 Energy and exergy storage efficiencies

To evaluate the overall performances of the systems during charging and discharging cycles, energy and exergy storage efficiencies obtained at three different flow rates, and at three different set temperatures are presented in this section.

4.3.1 The effect of flow rate on energy and exergy efficiencies

Figure 4.21 presents the effects of low (4 ml/s), medium (6 ml/s) and high (8 ml/s) flow rates on the energy storage efficiencies of the storage systems.

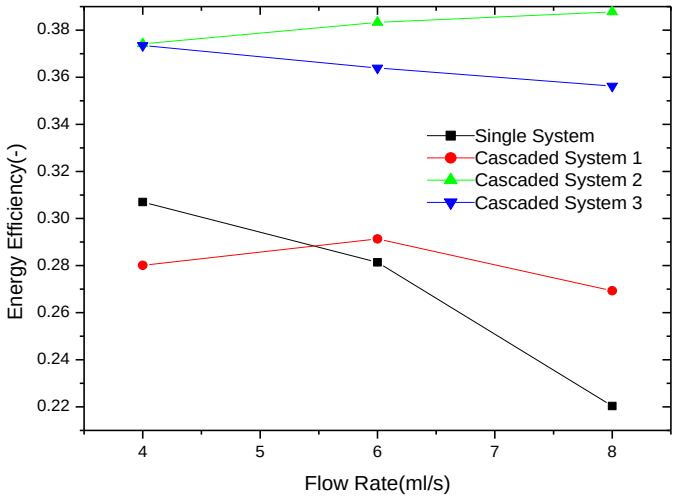

Figure 4.21: *The effect of the flow rate on the energy storage efficiencies for the four storage systems.*

Cascaded system 2 shows higher values of the energy storage efficiency for the higher flow rates (6 ml/s and 8 ml/s). It energy storage efficiency is comparable to cascaded system 3 for the lowest flow rate (4 ml/s). The reasons for the higher storage efficiencies for cascaded system 2 is the shorter charging duration of this system, the longer discharging duration and generally high energy rate values during charging and discharging. The storage efficiency is a measure of the total energy discharged to the total energy stored, thus a shorter charging duration and a longer discharging tends to increase this ratio if reasonably high charging and discharging rates are obtained. Cascaded system 2 almost shows a linear rise in the energy storage efficiency with an increase in the flow rate possibly because of more efficient charging and discharging with the higher melting point adipic acid at the bottom of the storage system which has a slightly higher thermal conductivity as compared to erythritol.

Cascaded system 3, the 3 PCM system shows better storage efficiencies as compared to cascaded system 1 and the single PCM. This is a direct result of the shorter and more efficient charging duration of this system as compared to cascaded system 1 and the single PCM system. The energy storage efficiencies of cascaded system 3 tends to decrease slightly with an increase in the flow rate. This is possibly due to the effect of the lower melting temperature and slightly lower thermal conductivity erythritol at the bottom which tends to reduce the energy discharging rates with an increase in the flow rate. The charging and discharging

energy rate profiles for cascaded system 2 and cascaded system 3 are comparable with the lowest flow rate of 4 ml/s, thus the two systems show the same energy storage efficiencies for this flow rate.

Cascaded system 1 shows a lower energy storage efficiency with the lowest flow rate when compared to the single PCM although it releases latent heat in two phase change transitions. This is because of the lower values of the discharging energy rate for this flow rate induced by a lower rise of the discharging inlet temperature. Cascaded system 1 shows higher energy storage efficiencies when compared to the single PCM system for the flow rates of 6 ml/s and 8 ml/s, respectively which ensured that the bottom PCM melted. These lower energy storage efficiencies are evident despite of higher quantity of energy stored and discharged by the single PCM as compared to cascaded system 1. The energy storage efficiencies of the single PCM reduce with an increase in the flow rate most likely due to the associated increase in the charging time, and the decrease in the discharging time.

The effect of the flow rate on the exergy efficiency is shown in Figure 4.22 for the assessment of the quality of energy stored. Exergy storage efficiency values are lower compared to energy storage efficiency values because heat losses are accounted for in the exergy efficiency calculations. Cascaded system 2 shows higher exergy storage efficiencies as compared to the other systems as in the case of the energy storage efficiencies depicted in Figure 4.21. This is due to the reasons mentioned earlier in the energy storage efficiency plots. However, the exergy storage efficiency of cascaded system 3 is lower than that of cascaded system 2 for the 6 ml/s case due to the slightly shorter charging time of cascaded system 3. It is important to note that the rise in the exergy efficiency with the flow rate for cascaded system 2 is more pronounced as compared to the rise in the energy efficiency. This is because of comparable charging exergy rate values for the three flow rates whereas the discharging exergy rate values tend to increase with the increase in the flow rate. This has an effect of increasing the exergy storage efficiency with an increase in the flow rate.

Cascaded system 3 shows higher exergy storage efficiencies when compared to cascaded system 1 and the single PCM system for possible reasons mentioned earlier in the energy storage efficiencies. Unlike the energy storage efficiencies for cascaded system 3, the exergy storage efficiencies increase with flow rate from 4 ml/s to 6 ml/s since the discharging exergy rate values increase with the flow rate whereas the charging exergy rate values are almost

comparable. For an increase from 6 ml/s to 8 ml/s the exergy storage efficiency remains almost constant for cascaded system 2 suggesting 6 ml/s is a limiting value for this storage system where the performance cannot increase anymore possibly due to increased heat losses. Cascaded system 2 and cascaded system 3 show higher and comparable exergy storage efficiencies due to their short charging times as compared to the single PCM system and cascaded system 1.

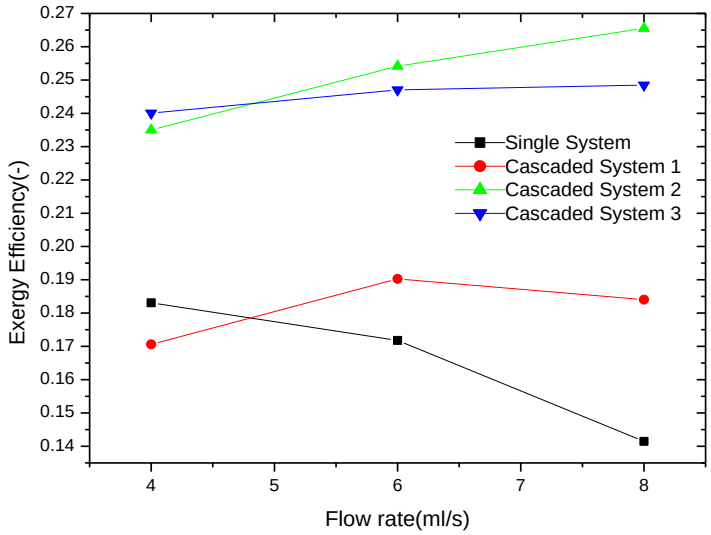

Figure 4.22: *The effect of the flow rate on the exergy storage efficiencies for the four storage systems.*

With the lowest flow rate, the exergy storage efficiency of the single PCM system is slightly greater than that of cascaded system 1 due to the lower discharging exergy rate shown by this system. However, due to the shorter charging durations for the flow rates of 6 ml/s and 8 ml/s, cascaded system 1 shows higher exergy storage efficiencies when compared to the single PCM system. The limiting flow rate for the best exergy storage efficiency is also 6 ml/s for cascaded system 1 since its exergy storage efficiency slightly decreases from 6 ml/s to 8 ml/s. The single PCM although showing higher charging and discharging exergy rates, the exergy storage efficiencies are lower as compared to the other storage systems due to a combined effect of the longer charging durations and the shorter charging durations. In contrast to the other systems, the exergy storage efficiencies decrease with an increase in the

flow rate, and it seems the lowest flow rate which maintains thermal stratification within the single PCM system is more appropriate for efficient exergy storage.

4.3.2 The effect of temperature on energy and exergy efficiencies

Low (260 °C), medium (280 °C) and high (300 °C) charging set temperature effects on the energy storage efficiencies for the four storage systems are presented in Figure 4.23.

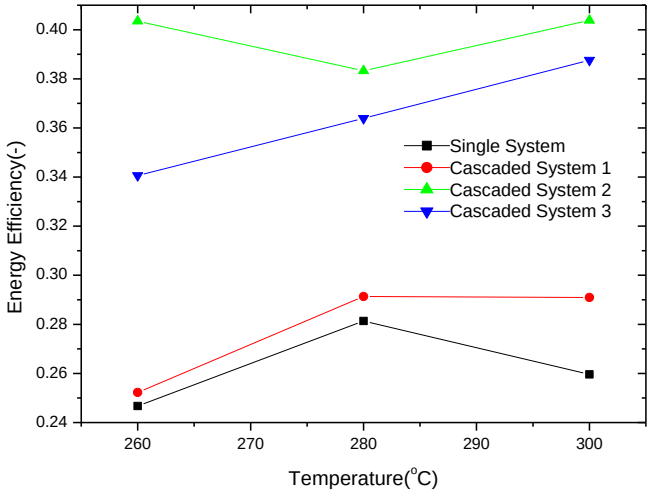

Figure 4.23: *The effect of the temperature on the energy storage efficiencies for the four storage systems.*

Cascaded system 2 shows the highest values of energy storage efficiency for all the set temperatures considered with an up and down trend of comparable energy storage efficiencies. For a set temperature increment from 260 °C to 280 °C, the energy storage efficiency drops, whereas for a set temperature increment from 280 °C to 300 °C, it increases. The possible reason of the drop at 280 °C is the drop in the charging energy rate using 280 °C. However, even with this drop, the energy storage efficiencies seem to be quite comparable for the three set temperatures. The higher energy storage efficiencies achieved by cascaded system 2 is probably due to the slightly shorter charging times and longer discharging times when compared to other systems as a result of the better heat transfer characteristics of adipic acid at the bottom this system.

Cascaded system 3 shows a continuous rise in the energy storage efficiencies from low to high heater set temperatures due to the increase in the charging temperature, which increases

the rate of heat transfer during the charging cycles thereby shortening the charging time. The results of cascaded system 3 shows that an increase in the heater set temperature will increase the energy storage efficiency of the system, and its energy storage efficiencies are higher as compared to cascaded system 1 and the single PCM as a result of the shorter charging durations induced by better heat transfer.

Cascaded system 1 shows slightly higher energy storage efficiencies with an increase in the set charging temperature of the heater as compared to the single PCM due its shorter charging durations. For a temperature increase from 280 ^{o}C to 300 ^{o}C, cascaded system 1 shows no change in the energy storage efficiency suggesting a limiting charging temperature for efficient storage of energy. This is due to the insignificant change in the charging and discharging times with the increase in the temperature. The results of cascaded system 1 suggest that the best charging temperature for that storage system is 280 ^{o}C since increasing the temperature tends to produce no increment in the energy storage efficiency.

The single PCM system shows lower energy storage efficiency values as compared to the other systems due to a combined effect of lower energy charging rates, longer charging durations and slightly shorter discharging durations. The energy storage efficiencies for the 260 ^{o}C and the 280 ^{o}C are comparable to those of cascaded system 1. However, unlike the cascaded systems, the single PCM system shows a more pronounced drop in the energy storage efficiency from 280 ^{o}C to 300 ^{o}C due to the longer charging time as compared to 280 ^{o}C case. The results of the single PCM system also suggest a best charging temperature of 280 ^{o}C as the case with cascaded system 1.

Figure 4.24 presents the effects of low (260 ^{o}C), medium (280 ^{o}C) and high (300 ^{o}C) charging heater set temperatures on the energy storage efficiencies of the storage systems. As in the case of the effect flow rate, exergy storage efficiencies are lower as compared to the energy storage efficiencies since heat losses are accounted for. Cascaded system 2 shows higher exergy storage efficiencies with a similar variation to the energy storage efficiencies due to the combined factors of the slightly longer discharging durations, shorter charging durations and relatively higher peak exergy rate values as compared to the other cascaded systems. Cascaded system 3 shows higher exergy storage efficiencies as compared to the single PCM system and cascaded system 1 due to shorter charging durations. The exergy storage efficiency rises slightly for a set temperature increment of 260 ^{o}C to 280 ^{o}C, and it drops

slightly from 280 °C from 300 °C. The drop is a result of the higher initial ambient temperature of the system during the discharging process using 300 °C which reduces the discharging exergy rate as explained earlier. This higher initial ambient temperature encourages more heat losses thus it lowers the discharging exergy rate making the exergy storage efficiency to drop. The best charging temperature of 280 °C is suggested by the results of the exergy storage efficiency for cascaded system 3.

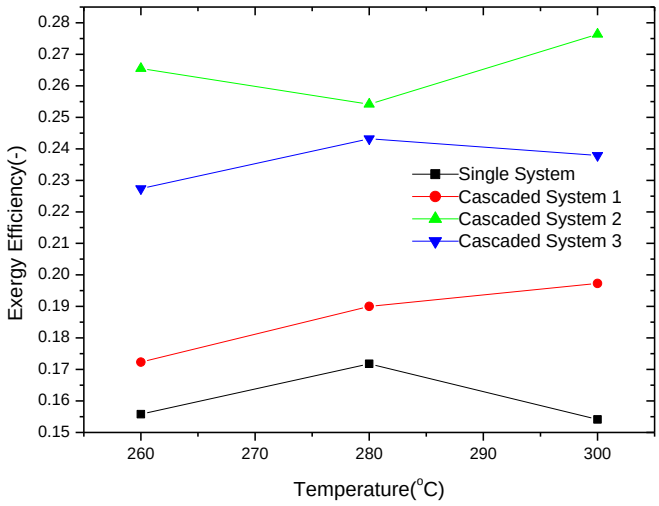

Figure 4.24: *The effect of the temperature on the exergy storage efficiencies for the four storage systems.*

Cascaded system 1 shows better exergy storage efficiencies for all the set charging temperatures as compared to single PCM due to its shorter charging times. The exergy storage efficiency increases with an increase in the charging temperature suggesting that higher charging temperatures result in better storage of exergy for cascaded system 1. The single PCM system shows the poorest exergy storage efficiencies despite of its high thermal conductivity due the longer durations of its charging processes which ensured that the bottom PCM melted. The variation of its exergy storage efficiency shows a similar trend to the energy storage efficiency and the best charging temperature is seen to be 280 °C.

4.4 Summary of the chapter

This chapter presented the experimental thermal performance comparison results of four latent heat thermal energy storage systems during both charging and discharging cycles. Cascaded system 3, the 3-PCM showed the best thermal performance characteristics during charging cycles when compared to the other systems due to its shorter charging duration and higher charging energy and exergy rates. Cascaded system 2 showed the second best performance in the experimental charging tests. Cascaded system 1 generally showed better performance than the single PCM system during charging, however, its performance deteriorated after melting of the bottom PCM as it showed lower energy and exergy rate values as compared to the single PCM system. The effect of the charging flow rate was more pronounced than the effect of the heater set charging temperature. For discharging cycles, the effect of the flow rate was more pronounced that the effect of the temperature. The single PCM system showed the best discharging characteristics with the least widening of the thermal gradient as compared to other systems. Cascaded system 2 and cascaded system 3 showed comparable thermal performances during discharging, while cascaded system 1 showed the worst thermal performance, which was comparable to the performance of the other cascaded systems in some cases. Cascaded system 2 showed the highest energy and exergy storage efficiencies. Cascaded system 3 showed the second best energy and exergy storage efficiencies which were comparable to those of cascaded system 2. The energy and exergy storage efficiency of the single PCM was the worst. The overall storage efficiency results also suggested that the performance of a cascaded system may depend on the thermal properties of the PCM irrespective of the number of stages since the two PCM system with a higher bottom melting temperature (Cascaded system 2 with adipic acid at the bottom) showed better overall performance compared to a three PCM system (Cascaded system 3 with erythritol at the bottom).

4.5 References

1. Davis, D.D. and Kemp, D.R., 2000. Adipic acid. *Kirk-Othmer Encyclopedia of Chemical Technology*.
2. Morando, C., Fornaro, O., Garbellini, O. and Palacio, H., 2014. Thermal properties of Sn-based solder alloys. *Journal of Materials Science: Materials in Electronics 25,* 3440-3447.

3. Mawire A., Lentswe K.A. and Shobo, A.B., 2019. Performance comparison of four spherically encapsulated phase change materials for medium temperature domestic applications. *Journal of Energy Storage 23,* 469-479.
4. Mawire, A., Lefenya, T.M., Ekwomadu, C.S., Lentswe, K.A. and Shobo, A.B., 2020. Performance comparison of medium temperature domestic packed bed latent heat storage systems. *Renewable Energy 146*, 1897-1906.
5. Lugolole, R., Mawire, A., Lentswe, K.A., Okello, D. and Nyeinga, K., 2018. Thermal performance comparison of three sensible heat thermal energy storage systems during charging cycles. *Sustainable Energy Technologies and Assessments 30*, 37-51.

5. CONCLUSIONS AND RECOMMENDATIONS FOR FUTURE WORK

5.1 Conclusions

The thermal performances of four different configurations of latent heat thermal energy storage systems were compared experimentally during charging and discharging cycles for medium temperature applications. The charging and discharging thermal performances of three packed bed cascaded latent heat thermal energy storage (LHTES) systems were experimentally evaluated and compared to a single PCM packed bed LHTES of eutectic solder capsules. Cascaded system 1 was composed of eutectic solder PCM capsules at the top, and erythritol PCM capsules at the bottom in equal storage volumes. Cascaded system 2 consisted of eutectic solder PCM capsules at the top and adipic acid PCM capsules at the bottom in equal storage volumes. Cascaded system 3 consisted of three PCM capsule layers of eutectic solder at the top, adipic acid in the middle, and erythritol at the bottom in equal storage volumes. From this study, the following conclusions were made:

1. An increase in the flow rate increased the heat transfer rate in all the storage systems such that the peak energy and exergy rates were obtained earlier. The charging time also increased with an increase in the flow rate due to the inlet temperature reducing as a result of more pronounced cooling of the charging heater with higher flow rates and the shorter interaction of the fluid with the heating coil at higher flow rates. This made the bottom experimental limiting temperatures to be approached at later times resulting in longer charging durations with the higher flow rates.
2. Cascaded system 3, the 3 PCM cascaded system showed higher energy and exergy charging rates with the three charging flow rates because of the release of latent heat in 3 phase change transitions. Its thermal performance was, however, comparable to cascaded system 2 with adipic acid at the bottom of the storage tank. The charging times for cascaded system 2 and cascaded system 3 were also shorter as compared to the other storage systems suggesting that the higher melting point PCM, adipic acid at the bottom and the middle sections of cascaded system 2 and cascaded system 3, respectively, tended to improve the charging performance. Another plausible reason for the shorter charging time for the storage systems with adipic acid is the slightly higher thermal conductivity of

adipic acid in the liquid phase when compared to erythritol. The longest charging duration was shown with single PCM eutectic solder due to its larger thermal mass as a result of its higher density. Cascaded system 1 generally showed better performance than the single PCM system, however, its performance deteriorated after melting of the bottom PCM, and it showed lower energy and exergy rate values as compared to the single PCM system. Although the eutectic solder showed the worst performance in terms of the charging exergy rates, its exergy rates values improved with an increase in the charging flow rate. Secondary peaks in the energy and exergy rate profiles were qualitatively used to identify the time when the phase change processes were occurring at the bottom of the cascaded systems.

3. An increase in the set heater charging temperature slightly reduced the charging times for the cascaded systems, but the exergy rate values were comparable for all the cascaded systems. There was no clear relationship between the charging temperature and the charging time for the eutectic solder single PCM system. Cascaded system 3 with the 3 PCMs showed the best thermal performance with generally higher energy and exergy rates as compared to the other storage systems. Cascaded system 2 showed the second best thermal performance which was comparable to that of cascaded system 3 in some instances. The effect of the set temperature was less pronounced as compared to the effect of the flow rate.
4. During discharging, the increase in flow rate increased the rate of heat transfer which caused the energy rate, exergy rate, and discharging inlet temperature peak-values to occur earlier with increasing peak values. The discharging time also decreased due to the increase in the flow rate. The performances of the systems generally increased with an increase in the discharging flow rate. The single PCM system showed the best discharging characteristics with the least widening of the thermal gradient as compared to other systems. This was an evidence of good heat transfer in the single PCM system. Cascaded system 2 and cascaded system 3 show comparable thermal performances during discharging, while cascaded system 1 showed slightly worse thermal performance with greater temperature reversals in the storage tank. In some cases, the discharging thermal performance characteristics for cascaded system 1 were comparable to those of the other cascaded systems. The final charging temperature showed an insignificant influence on

the discharging performance and the more significant effects were seen with the discharging flow rate.

5. The overall storage performance was evaluated in terms of the energy and exergy storage efficiencies. Cascaded system 2 showed the highest energy and exergy storage efficiencies, which seemed to increase with an increase in flow rate. However, the energy and exergy storage efficiencies of cascaded system 3 and cascaded system 2 were comparable. The energy and exergy efficiency of the single PCM was the worst, possibly due to the longer charging time and the uniform release and storage of latent heat. The higher energy and exergy efficiencies of cascaded system 2 in almost all the experiments when compared to cascaded system 3 were possibly due to a greater volume of adipic acid in cascaded system 2. Adipic acid had a slightly higher thermal conductivity and a higher melting temperature as compared to erythritol at the bottom of cascaded system 1. The overall thermal performance results also suggested that the performance of a cascaded system may depend on the PCM properties irrespective of the number of stages since a two PCM system with a higher bottom melting temperature (Cascaded system 2 with adipic acid at the bottom) showed a better overall performance than the three PCM system (Cascaded system 3 with erythritol at the bottom). Cascaded system 1 showed lower energy and exergy storage efficiencies as compared to the other two cascaded systems.

5.2 Recommendations for possible future work

For both charging and discharging cycles, the flow direction was from the top to the bottom of the TES tank which was not really efficient for the discharging cycle. Discharging from the bottom to the top will result in more thermodynamically efficient discharging since hot oil will be extracted from the top. New pipes and valves need to be accommodated in the storage system to cater for this design change. Heat losses in the system need to be calculated and reduced to increase the overall energy and exergy storage efficiency. The current experimental results will be used to evaluate the heat losses as a follow up study. The heat loss evaluations will also be done with the use of a numerical heat loss model that needs to be developed.

Generally, cascaded systems with higher melting point PCMs performed better as compared to the one with the lower melting point PCM suggesting that higher temperature PCMs should be used in oil based medium temperature cascaded systems. More investigations need to be carried out with suitable organic or metallic PCMs with melting temperatures greater than 160 ^{o}C but less than the melting temperature of the eutectic solder. The issue of using higher thermal conductivity bottom level PCMs needs to be investigated in the future to reduce the charging time. To reduce the amount of expensive PCMs in the system, a combined storage system with alternate layers of PCM and sensible heat storage materials needs to be investigated both numerically and experimentally. A numerical model for parametric studies on different PCM/fluid/sensible combinations needs to be developed for performance comparison and optimisation. This model will be validated with the experimental studies presented in this dissertation. An optimal storage system is to be scaled up and used for a real life application like solar cooking that combines the storage system with a solar collector which uses solar energy to charge up the storage system. Different heat utilization devices using the stored heat also need to be developed and tested experimentally and numerically.

A techno-economic analysis also needs to be carried out to find out the viability of the proposed TES system in real life solar process heat applications. The economic analysis will highlight the advantages and disadvantages in terms of the costs and payback periods.